

國立交通大學

材料科學與工程研究所

博士論文

銅電鍍與電解拋光於銅鑲嵌金屬連導線應用之研究

**Copper Electroplating and Electropolishing for the
Application of Cu Damascene Interconnects**



研究生：劉書宏

指導教授：陳智 博士

謝嘉民博士

中華民國九十五年七月

銅電鍍與電解拋光於銅鑲嵌金屬連導線應用之研究

Copper Electroplating and Electropolishing for the

Application of Cu Damascene Interconnects

研究生：劉書宏

Student : Sue-Hong Liu

指導教授：陳 智

Advisor : Chih Chen

Jia-Min Shieh

國立交通大學

材料科學與工程學研究所

博士論文



A Dissertation

Submitted to Department of Materials Science and Engineering

College of Engineering

National Chiao Tung University

in Partial Fulfillment of the Requirements

for the Degree of Doctor of Philosophy

in

Materials Science and Engineering

July 2006

Hsinchu, Taiwan, Republic of China

中華民國九十五年七月

銅電鍍與電解拋光於銅鑲嵌金屬導線應用之研究

研究生：劉書宏

指導教授：陳智 博士

謝嘉民博士

國立交通大學 材料科學與工程學系

摘要

本論文含有三個部分，第一部份介紹銅電鍍液中抑制劑 PEG 與加速劑 SPS 經由電流驅使的衰敗對填孔能力的影響。第二部分則研究具有氫氧基的醇類與有機酸添加劑加入電解液後對銅電解拋光的影響。第三部分則是因為考量到成本與許多製程風險的影響，所以提出一種電化學方法將電鍍與電解拋光整合於同一電解液並利用電腦程式的控制能將填孔與平坦化以一個程序完成。

首先，我們研究了經過一段長時間或多次電鍍後，鍍液中添加劑 PEG 與 SPS 的衰敗對填孔能力與表面形貌的影響。當同一溶液中只具有 PEG 時，多次電鍍與高電流密度將使得高分子類的 PEG 產生裂解。PEG 的裂解不但會降低 PEG 的電流抑制效果，而且會使得許多短鏈 PEG 與銅的錯合物產生在溶液擴散層中。因此，經過越多次的電鍍，越不佳的填孔能力與越粗糙的銅膜表面將會呈現。我們利用即時觀測電鍍時鍍液電壓突然升高的現象來推測 PEG 在銅表面的吸附脫附行為能力與銅離子的還原速度。電壓突然升高的程度與電化學陰極交流阻抗分析將可推測 PEG 的劣化程度與電鍍液的可靠度。

除此之外，我們證明了兩種加速劑 SPS 在經過多次電鍍後所可能劣化的原因。第一、一個 SPS 會經由電流驅使分裂成為兩個 MPS，MPS 比 SPS 更具有去極化的效果。當電鍍進行時，越來越多的 MPS 將會使得電鍍液的填孔能力喪失。第二、SPS 會經由空氣氧化或電流驅使在一段時間後生成不再具有加速效

果的硫化物 (S-product)。

本論文第二部份，我們發展了一種雙添加劑系統的電解拋光溶液來達到銅鑲嵌構造拋光後大小線寬(1-50 μm)皆達到高度平坦化的效果。這種電解液含有具有氫氧基的醇類與有機酸，再加上原本的主體溶液磷酸。在銅表面上有高潤濕能力的醇類能加強保護溝渠 (Trench 底部) 的效果。而因為醇類吸附銅表面也會增加表面黏度更能抑制銅的拋光速度。這個對銅 Trench 底部卓越的保護能力使得此雙添加劑成為銅電解拋光後階段性高低差 (Step-height) 能快速平坦的原因。

另外，我們還研究了含醇電解拋光液中有機酸加速拋光劑對銅溶解的影響。我們建立的有機酸雙添加劑系統為醋酸、檸檬酸、Citrazinic 酸以及苯甲酸。在溝渠的底部，被證明酯化反應有效的生成一層抵抗電解拋光的黏膜且降低了局部區域的酸度。因此在 Trench 外部，銅的溶解速率由電解液中的酸度主導。而在 Trench 底部，則由此生成的高黏度的電阻值主導。對於弱酸系統例如醋酸來說，比較高濃度的添加劑量較能維持較低的酸度與緻密的酯化層，所以能在 Trench 底部抑制銅的溶解。所以能得知為何此含有醋酸加上醇類的電解液能在電解拋光後得到最高的銅平坦化效率。

論文第三部份，我們提出了一種方法：銅雙重模式電鍍，寄望能使得銅電鍍與電解拋光能在一個電解槽完成。最重要的參數除了為電解液的選用外，還包含電化學程式的最佳化。目前為止，我們發展了幾種有效的電解液配方與電脈衝頻率來促進銅雙重電鍍模式的效能。目前發現有效的電解液中，包含了銅標準電鍍液、抑制劑、平整劑以及電解拋光的必備磷酸。對於小線寬銅線，已經有特定參數能達到電鍍後的表面平整與高度填孔能力。對於大線寬銅線，則在良率 60% 的情形下達到階段性高低差的減少。

Copper Electroplating and Electropolishing for the Application of Cu Damascene Interconnects

Student: Sue-Hong Liu

Advisor: Dr. Chih Chen

Dr. Jia-Min Sjieh

Department of Materials Science and Engineering

National Chiao Tung University

Abstract

There are three parts in this study. The first introduces aging influence of polyethylene glycol (PEG) and PEG- bis-3-sodiumsulfopropyl disulfide (SPS) containing bath on gaps filling during Cu electrodeposition. The second part introduces the role of alcohols and organic acids additives in electrolyte of damascene Cu electropolishing. In order to save many risks and cost at the back end of the interconnect fabrication, third part demonstrates a method that can integrate Cu electrodeposition and electropolishing in one electrolyte and electrochemical tank. The developing method can be called dual-mode plating.

First part, we investigate how the degradation of poly (ethylene glycol) (PEG) additives-containing and PEG-bis-(3-sodiumsulfopropyl disulfide) (SPS)-containing Cu electroplating electrolytes influences the gaps filling of damascene features and the roughness of plated surfaces. For only PEG-containing bath, the cleavage of PEG whose reaction is enhanced by a high bias current and more plating cycles, not only diminishes the inhibition effect of the electrolytes, but also enables the formation of enormous complexes of short-chain PEG–Cu far from the reacting surfaces. Hence, the more plating cycles performed, the worse the gaps filling characteristic and the rougher the plated surfaces. Furthermore, an overshoot phenomenon on the transient

cells voltage for PEG-containing electrolytes is observed and explained well by a dynamic equilibrium between PEG absorption ability and Cu reduction speed. Accordingly, the change in overshoot shape is closely related to PEG aging and this fact is employed to examine the reliability of electrolytes.

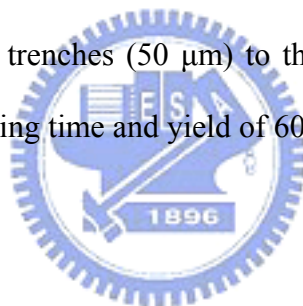
Moreover, we verify the two possible mechanisms of degradation of SPS. First explanation: SPS will crack into two MPS driven by the overpotential of plating, and MPS is more active depolarization than SPS. Moreover, the more and more existed MPS will make the electrolyte more ineffective for filling capability during aging process. Second explanation is SPS will lose all the accelerating ability after becoming S product which is some kinds of derivatives of SPS.

Second part, we demonstrate a two-additive electropolishing (EP) electrolytes that exhibit an extremely high planarization-efficiency in Cu damascene schemes, independent of pattern sizes (1-50 μm). This electrolyte is displayed by adding alcohols and organic acids to the H_3PO_4 electrolyte. The high wetting ability of alcohols allows such additives to easily access the damascene bottom. This mechanism, assisted by the reduced polishing rate associated with the high surface viscosity caused by alcohol additives, greatly passivates the damascene bottom from electropolishing. Accordingly, the superpolishing functionality of the two-additive electrolyte outperforms additive-free and one-additive electrolyte.

Furthermore, this study also explores how the dissolution of damascene Cu depends on accelerators of organic acids in alcohol-containing H_3PO_4 electropolishing electrolytes. Four two-additive electrolytes that contain different accelerators, acetic, citric, citrazinic, and benzoic acids, are evaluated. At the bottom of damascene features, an esterification reaction between alcohols and organic acids efficiently forms a highly resistive layer and reduces the acidity of the solution. Accordingly, outside the damascene features, the rate of removal of Cu is dominated by the acidity

of electrolytes but, inside the features, it is also determined by the resistance of the viscous layer. For a weak acidic additive, acetic acid, an extremely high additive concentration is introduced to sustain the moderate acidity of the solution to initiate intense esterification. Therefore, how acetic-acid-based two-additive electrolytes exhibit excellent Cu planarization capability is realized.

In third part, an effective technology (Cu dual-mode plating) containing two functions of Cu film depositing and polishing in one-step electrochemical process in one tank has been developed. We have identified chemical additives and processing parameters in dual-mode plating. By mixing inhibitors, leveler, and phosphoric acid with standard copper electroplating solution, we are able to obtain similar planarization and gap-filling performance in narrow trenches (350nm) and step-height reduction in wide trenches (50 μm) to those of standard electroplating solution with identical processing time and yield of 60%.



誌謝

首先我要感謝我的指導教授陳智老師在研生活這六年來不厭其煩的給予我指導與協助，並且在生活與人生觀念上給予許多的啟發與鼓勵。有幸成為老師回國指導的第一批研究所學生，在此我要對陳智老師致上我最高的謝意。感謝國家奈米元件實驗室謝嘉民博士在研究上給於我的辛勤訓練以及工程技術上的指導，使我在學術觀念上進步快速。也感謝眾口試委員在畢業口試中給於我的指教。

實驗室裡要感謝的人名實在太多，無法一一列名感謝。交通大學六年，有酸甜苦辣，有歡笑，有淚水，有感動也有不捨的回憶。學長、學姐、學弟、學妹、同學們，不論你們是否已經畢業正在進行你們的另一段精彩人生還是還在學校裡當一位努力的研究生。我都千言萬語以一句感謝來代替，感謝！

最後我要感謝父母親這三十年的栽培與弟弟的加油打氣還有女友如婷的一路陪伴。很幸運，有你們無私的支持才能順利完成學業。



List of Contents

Abstract in Chinese.....	I
Abstract in English.....	III
Acknowledgements.....	IX
Lists of Contents.....	IX
Lists of Tables.....	IX
Lists of Figures.....	IX

Chapter 1: Review of Electrochemical Deposition (ECD) in Multilevel Interconnection and Experimental Procedure

1.1 Motivation.....	1
1.2 Introduction of Cu Electroplating Bath.....	3
1.2.1 Basic solution of Cu Electrodeposition.....	3
1.2.2 Organic Additives in Plating Baths.....	3
1.2.3 Relationship between PEG and SPS.....	4
1.2.4 Filling Model of Cu Line/Via.....	7
1.2.5 Aging influence of Electrodeposition Bath for Gaps Filling (Degradation of Electrodeposition Bath).....	9

Chapter 2: Aging Influence of Organic additives (PEG and PEG-SPS containing) of Cu Electrolytes on Gaps Filling

2.1 Introduction.....	13
2.2 Experimental.....	14
2.3 Aging Influence of PEG Suppressors of Cu Electrolytes on Gaps Filling.....	15

2.4 Aging Influence of PEG-SPS-containing Cu Electrolytes on Gaps Filling.....	24
2.4.1 Degradation Trends of Different SPS Concentrations.....	24
2.4.2 Electrochemical Analyses of Aged PEG-SPS-containing Cu Plating Electrolytes.....	29

Chapter 3: Introduction of Cu Electropolishing and Experimental Details

3.1 Cu Planarization in Damascene process.....	31
3.2 Background and Microleveling Mechanism of Cu EP.....	34
3.3 Factors Affecting the Limiting Current on Cu Surface of Electropolishing.....	35
3.4 Recent work of Cu Electropolishing Applying in Interconnect Metallization and Behavior of Chemical Additives in Cu Electropolishing.....	37
3.5 Experimental Procedure of Cu Electropolishing.....	39



Chapter 4: Role of Alcohols in Two-Additive System for Cu Damascene Copper Electropolishing

4.1 Superplanarization for Damascene Cu metals.....	42
4.2 Reduction of Etching Pits on Cu Surface by Additives.....	48

Chapter 5: Role of Organic Acids in Two-additive System for Cu Damascene Copper Electropolishing

5.1 Introduction of Accelerator and Inhibitor in Cu Electropolishing.....	50
5.2 Results and Discussions.....	50

**Chapter 6: Integration of Electroplating and Electropolishing of Cu
Damascene Process: Dual-mode Cu Plating**

6.1 Motivation of Dual-Mode Cu plating.....64
6.2 Experimental set up of Dual-Mode plating.....65
6.3 Results and Discussions.....65

Chapter 7: Conclusions and Future Works

7.1 Conclusions.....72
7.2 Future Work and Pulse Cu-Electropolishing.....74

Reference.....77

Lists of Publications.....84



List of Tables

Table I . Relative information to SPS and MPS.....	7
Table II . Optimal recipes for various EP electrolytes with best PE and fundamental performance of polished Cu metals using those electrolytes.....	48
Table III : Optimal parameters associated with two-additive electrolytes in this study.....	51



List of Figures

Chapter 1: Review of Electrochemical Deposition (ECD) in Multilevel

Interconnection and Experimental Procedural

Fig.1-1. Procedural for Cu Damascene process.....	2
Fig.1-2 Schematic Diagram of a electrodeposition cell.....	2
Fig.1-3 Evolution of v-t curves of PEG bath and SPS bath during ECD.....	6
Fig.1-4 Illustration of the slow adsorption/desorption mechanism.....	6
Fig.1-5. Scheme of the mechanism of the overfilling.....	8
Fig.1-6. The HPLC scan of electrolytes before and after aged respectively. The carrier component reduced after aging process.....	10
Fig.1-7. Schematic of assumed mechanisms for different filling aspects between MPS and SPS/aged MPS.....	11
Fig.1-8. Comparison of the effect of ambient on the accelerator decomposition rate.....	11
Fig.1-9. Possible Chemical formula of S-products.....	12

Chapter 2: Aging Influence of Organic additives (PEG and PEG-SPS containing) of Cu Electrolytes on Gaps Filling

Fig.2-1. Side-view and cross-sectional SEM images for 0.35 μ m trenches electroplated with PEG (PEG4000) electrolytes undergoing various aging stages with various bias currents.....	16
Fig.2-2. Gaps filling yields in trenches electroplated with PEG400-containing electrolytes operated at various bias currents as functions of (a) number of plating cycles, and (b) trench width.....	17
Fig.2-3. Decay rates of gaps filling yield for PEG-containing electrolytes operated at	

various bias currents, as function of trench width.....	18
Fig.2-4.Nyquist plots for standard, (a) PEG200-containing and (b) PEG4000-containing (100 and 200 ppm) baths undergoing one and five plating cycles.....	20
Fig.2-5. Potentialdynamic curves for standard and PEG4000-containing (100 and 200 ppm) baths undergoing one and five plating cycles.....	21
Fig.2-6. Evolutions of cells voltage vs transient time (V-t) for PEG4000-containing electrolytes galvanostatically performed and controlled at various currents.....	23
Fig.2-7. Extracted fall-times of overshoot shape of transient cell-voltage for PEG4000-containing electrolytes undergoing various plating cycles and performed using different bias currents.....	23
Fig.2-8. Evolutions of the v-t curves of various SPS-concentrated baths.....	26
Fig.2-9. Evolutions of the v-t curves at various currents.....	26
Fig.2-10. Gaps filling yields in trenches electroplated with SPS-PEG-containing electrolytes operated at (a) various concentrations of SPS (b) higher applied current and pre-aged conditions. Trench width: 350nm.....	27
Fig.2-11. Side-view and cross-sectional SEM images for 0.35 μm trenches electroplated with SPS-PEG-containing electrolytes undergoing various aging stages with various concentration of SPS.....	28
Fig.2-12. Side-view and cross-sectional SEM images for 0.35 μm trenches electroplated with SPS-PEG-containing electrolytes undergoing various aging stages with various bias currents.....	28
Fig.2-13. Evolutions of the v-t curves at various pretreatment durations, the applied current density is $3.3 \times 10^{-3} \text{ A/cm}^2$	29
Fig.2-14. AC scans of the fresh and aged baths containing SPS (a) 6ppm, (b) 1ppm.....	30

Chapter 3: Introduction of Cu Electropolishing and Experimental Details

Fig.3-1. Common CMP processing problems resulting from the different polishing rates of copper, barrier, and ILD.....32

Fig.3-2. A schematic diagram of Electrochemical Mechanical Deposition (ECMD).....33

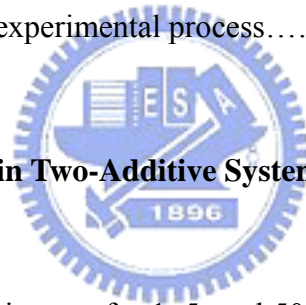
Fig.3-3. Microleveling effect of Cu electropolishing.....35

Fig.3-4. Potentialdynamic curve of Cu EP in the 85% (vol.) H₃PO₄ solution.....37

Fig.3-5. Evolutions of PE and EP rates inside and outside of 1- μ m-wide trenches at various applied voltages.....39

Fig.3-6. SEM cross-sectional profiles: (a) Before EP, (b) After EP at the applied voltage of 1.75 V for 3 min.....39

Fig.3-7. Flow chart of Cu-EP experimental process.....41



Chapter 4: Role of Alcohols in Two-Additive System for Cu Damascene Copper Electropolishing

Fig.4-1. Cross-sectional SEM images for 1, 5, and 50 μ m damascene patterns filled with electroplating Cu metals before and after electropolishing at 1.75 V using one-additive (acetic acid) and two-additive (acetic acid + glycerol) EP electrolytes.....44

Fig.4-2. PE for additive-free, one-additive (acetic acid), and two-additive (alcohols + acetic or citric acids) as a function of feature size. EP was conducted at 1.75 V...45

Fig.4-3. Polishing rate for alcohol-containing or acetic acid-containing one-additive EP electrolytes as a function of additive concentrations. EP was conducted at 1.75 V.....45

Fig.4-4. Proposed model of step-reduction mechanism by adding organic acid into H₃PO₄ electrolyte in Cu-EP.....46

Fig.4-5. The extracted Cu removal rate gradient for two-additive (alcohols + acetic acid), and one-additive (acetic acid) EP electrolytes. EP was conducted at 1.75 V.....46

Fig.4-6. (a) Measured contact angle for pure phosphoric acid, phosphoric acid electrolytes containing pure glycerol, pure glycerol, pure methanol and pure ethanol on Cu substrate. (b) OM image capture form in-situ measurement.....47

Fig.4-7. AFM images of Cu surfaces polished at 2.0 V using (a) additive-free, (b) one-additive (acetic acid), (c) and two-additive (glycerol + acetic acid) EP electrolytes.....49

Chapter 5: Role of Organic Acids in Two-additive System for Cu Damascene Copper Electropolishing

Fig.5-1. Cross-sectional SEM images for 50 μm damascene patterns filled with electroplating Cu metals before and after electropolishing at 1.75 V using (a) additive-free and (b)–(e) four two-additive (various organic acids + glycerol) EP electrolytes. (f) A schematic illustration of two-additive-assisted EP within damascene features shown.....52

Fig.5-2. PE for additive-free, one-additive (glycerol), and four two-additive (glycerol + various organic acids) EP electrolytes as a function of feature size. EP was conducted at 1.75 V.....53

Fig.5-3. Polishing rates outside and inside the features for four two-additive, glycerol-containing one-additive and additive-free. EP electrolytes: (a) obtained with 1 μm width patterned substrates; (b) obtained with 50 μm width patterned substrates; and (c) extracted with blanket substrates. EP was conducted at 1.75 V.....54

Fig.5-4. The extracted Cu removal rate gradient for four two-additive EP electrolytes. EP was conducted at 1.75 V.....55

Fig.5-5. (a): Extracted acidity, and (b) extracted viscous layer resistance (calculated from Nyquist plots shown in Fig. 5-6) outside and inside the features for four two-additive, and additive-free EP electrolytes. EP was conducted at 1.75 V. For evaluating the impact of applied voltage on esterification, EP using acetic acid-containing two-additive electrolytes was also conducted at 1.5, 1.6, and 1.9 V, respectively.....58

Fig.5-6. Nyquist plots for four two-additive EP electrolytes using (a) optimal, and (b) diluted additive concentrations. For comparison, the plot for additive-free electrolytes was also shown. EP was conducted at 1.75 V.....59

Fig.5-7. XPS spectra for Cu metals polished using four two-additive, and additive-free EP electrolytes.....60

Fig.5-8. Raman spectra for Cu metals polished using four two-additive EP electrolytes that comprise diluted additives with concentrations that are 10 times less than the optimal additive concentrations. The inset shows the spectra associated with glycerol-containing, and acetic acid-containing one-additive EP electrolytes.....61

Chapter 6: Integration of Electroplating and Electropolishing of Cu Damascene Process: Dual-mode Cu Plating

Fig.6-1. Schematic diagram of Cu dual mode plating.....67

Fig.6-2. In-situ typical recorded current and voltage on electrode surface during Cu dual-mode plating.....67

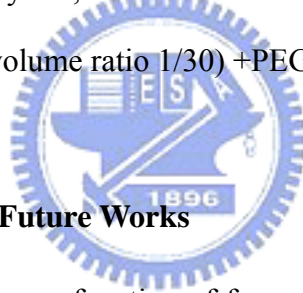
Fig.6-3. The dependence of electric conductivity with the amount of phosphate acid in various dual-mode electroplating solution.....68

Fig.6-4. Surface morphology of Cu film after dual-mode electroplating in H_3PO_4 /electrolytes = 1/30, 1/10 and 1/3 volume ratio trench at the same pulse-frequency. Pulse condition: ECD 30sec + EP 6sec, 30 cycles.....68

Fig.6-5 (a) Comparison diagram showing pore filling capability with different chemical condition processing parameters at the same pulse-frequency of narrow trenches (trench width: 350nm) (b) SEM image of A, B and F are corresponded to the data in (a).....69

Fig.6-6. (a) Comparison diagram showing pore filling capability with different pulse-time processing parameters at optimized chemical condition of narrow trenches (trench width: 350nm) (b) SEM image of A, C and E are corresponded to the data in (a).....70

Fig.6-7. Step height of wide trench after Cu plating and under various dual-mode conditions. A: Standard plating for 15min, B: (ECD 10sec + EP 3sec) 90 cycles, C: (ECD 20sec + EP 3sec) 45 cycles, D: dual-mode at (ECD 30sec + EP 6sec) 30 cycles. Additives are H₃PO₄ (volume ratio 1/30) +PEG 100 ppm.....71.



Chapter 7: Conclusions and Future Works

Fig.7-1. PE of pulse-polishing as a function of frequency for various trench widths. The positive voltage is 1.75V, and the negative voltage is 1.3V. The chemical recipe is H₃PO₄ + CH₃COOH 10000ppm + Glycerol1/100.....76

Fig.7-2. PE of constant voltage polishing and Pulse Cu-EP as function of line width. The pulse frequency is 0.033 and duty cycle is 75%.....76

Chapter 1: Review of Electrochemical Deposition (ECD) in Multilevel Interconnection and Experimental Procedure

1.1 Motivation

Cu has been adopted in deep submicron ULSI metallization due to its lower resistivity and better electromigration performance compared to conventional Al alloys,¹⁻² as shown in Fig.1-1. Recently, the challenge of Damascene processing is thus considered and has been studied for several years; this integration approach requires Cu to be deposited void-free in trench and via structures with high aspect ratios recently. Electrochemical deposition (ECD) is an important technology for constructing damascene Cu schemes for interconnects³⁻⁴ or even for three-dimensional metal photonic crystals⁵. The performances of organic additives (suppressors, accelerators, levelers) in electrolytes have effect on gap-filling ability, uniformity of plated surface. Many groups demonstrated their research results about these additives.

Cu electrodeposition usually takes place at atmospheric pressure, room temperature and in the presence of an aqueous electrolyte in a non-conducting cell. Figure 1-2 display a schematic diagram of a electroplating cell.⁶ In the cell, the wafer, which has a thin copper conductive layer (seed layer) deposited by either chemical vapor deposition (CVD) or physical vapor deposition (PVD), acts as a cathode. A consumable Cu anode at the another side of the cell completes the electrochemical circuit.⁶

However, it would be of interest to examine depletion of various organic additives after aging of plating bath now. Very little literature has been published about the aging influence of these additives. In this study, we concentrate on the depletion of suppressors (wetting agents) and accelerators after aging.

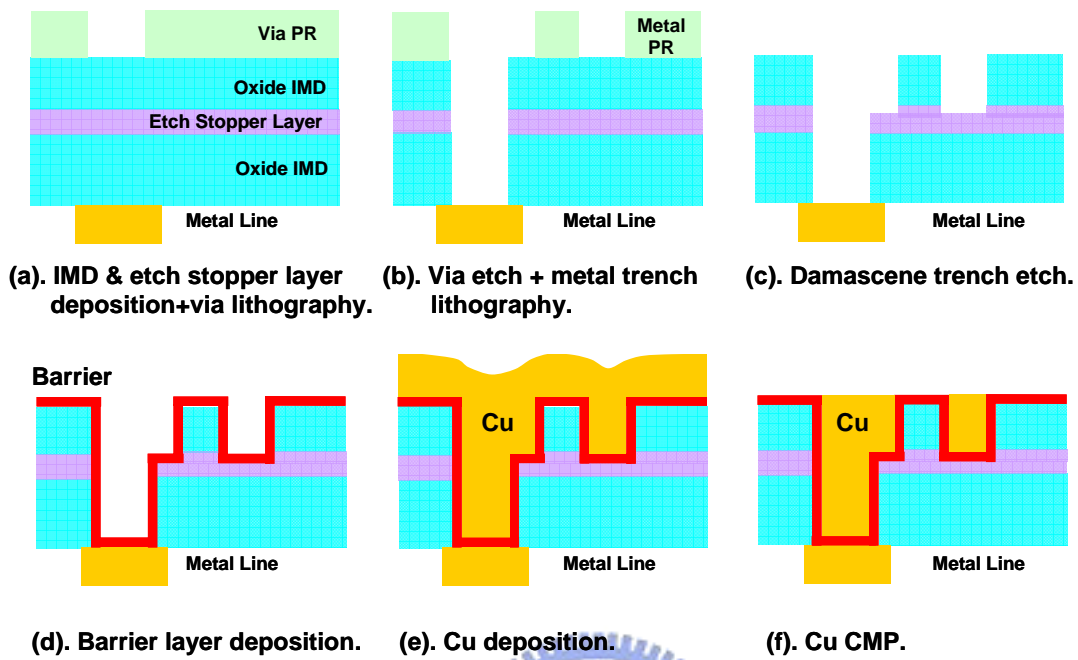


Fig. 1-1. Procedure for Cu Damascene process

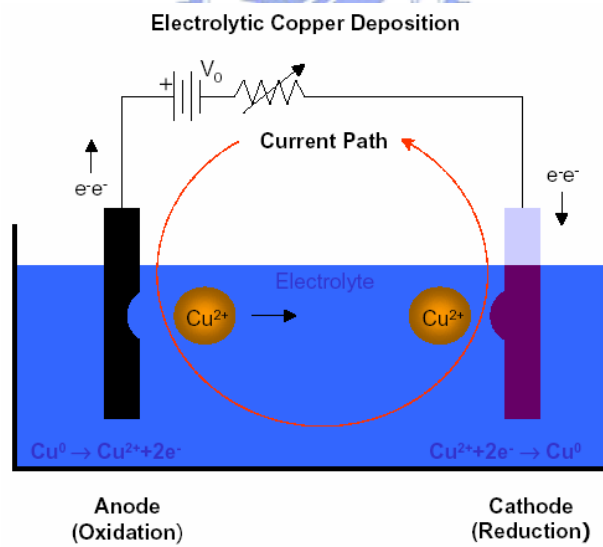


Fig. 1-2. Schematic Diagram of an electrodeposition cell ⁶

1.2 Introduction of Cu Electroplating Bath

1.2.1 Basic solution of Cu Electrodeposition

Cu ECD baths are normally formulated using a highly stable acid electrolyte solution containing copper sulfate and sulfuric acid. The basic kinetics and properties of these solutions have been investigated for more than 80 years and well understood ⁷.

In integrated circuit damascene applications, the unique important criterion for copper sulfate concentration is to avoid the depletion of cupric ion during gap-filling in features processes. Typical cupric ion concentrations in use are in the range of 17.5-60 g/L and sulfuric acid is usually added into the ECD electrolyte (45-325 g/L) to maintain solution conductivity and improve wetting or oxide dissolution on seed surfaces. Generally, more conductivity solutions result in a system where plating thickness distribution is less dependent on plating cell geometry, while low acid electrolytes result in a system with less dependence on seed layer resistivity.

1.2.2 Organic Additives of Plating Baths

Copper Electroplating can provide bottom-up filling or superfilling behavior by adding chemical additives such as poly (ethylene glycol) (PEG) suppressors together with chloride ions, inhibitors, and accelerators, into H₂SO₄-based electrolytes thus resulting in the void-free or super filling of narrow Cu trenches and vias in damascene process ⁸⁻⁹. This is commonly assigned to the action of organic additives and chlorides ions added in small amounts to the electrodeposition (ECD) bath¹⁰. The mechanisms by which these additives lead to super-fill have been proposed in many investigations. The basic solution and followed by the additives will be introduced in next section.

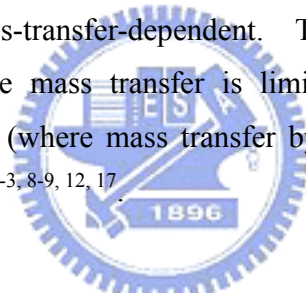
At present, organic additives added to the electrolyte of Cu ECD lead to three basic categories.

Accelerator which can be called brightener or anti-suppressor, catalyzes and accelerates the conformal overfilling of vias and trenches by locally accelerating current at a given voltage where they are adsorbed. It contains sulfur-containing molecules, typically sulfonic acid groups or disulfides such as SPS (Bis- (sodium

sulfopropyl)-disulfide) with the chemical formula of $\text{NaSO}_3(\text{CH}_2)_3\text{S-S}(\text{CH}_2)_3\text{SO}_3\text{Na}$. Accelerators are usually adopted in the plating bath in the concentration range of 1-25ppm^{8-9, 11-12}.

Suppressors is a kind of surfactant or wetting agent which can be called the carrier, that suppresses Cu growth at the top edges of vias and trenches, thus slowing the deposition rate by competing with copper for electron transfer sites or crystal lattice sites on the metal surface. Surfactants containing long chain polymers such as polyethylene glycol (PEG) or co-polymers of polyoxyethylene and polyoxypropylene have average molecular weights more than 1000.¹³⁻¹⁷

Levelers (also called a grain refiner or over-plate inhibitor) are usually high-molecular weight polymers with amine (-NH₃) or amide (-NH₂) functional groups. They are second class of current-suppressing molecules, which are usually added to the plating bath at a low concentration. Hence, unlike suppressors, the concentration of levelers at the interface is mass-transfer-dependent. Therefore, isolated locations such as the inside of a via (where mass transfer is limited) are less suppressed, while protruding surfaces or corners (where mass transfer by diffusion or migration is more efficient) are more suppressed^{2-3, 8-9, 12, 17}.



1.2.3 Relationship between PEG and SPS

Many researchers suggested one reaction equations for the (PEG, SPS)-containing baths to achieve void-free filling.^{9,15, 18-21}

In the statement of Moffat et al, the I-V curves revealed that the competition between the effects of PEG and MPS during electrodeposition²¹. The linear sweep voltammetry (LSV) indicates the competition between inhibition provided by Cl-PEG-Cu²⁺/Cu⁺/Cu interaction and the catalytic effects of Cl-MPS-Cu²⁺/Cu⁺/Cu interaction. A possible reason of the LSV effect entails the following sequence of events. Potential-driven desorption or disruption of the blocking Cl-PEG-based layer allows thiolate, or a derivative thereof, then to adsorb on the surface. This further disrupts the inhibiting function of the Cl-PEG-based monolayer. N. Kovarsky et. al agreed with this mechanism that SPS adsorb on the site of surface in place of the originally adsorbed PEG²².

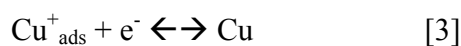
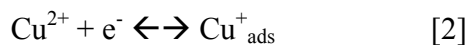
Furthermore, M. Tan proposed that a transition time of the system to reach steady state was observed under both galvanostatic and potentiostatic conditions and found to be a strong function of SPS concentration ⁸. These experimental results provide evidence for slow adsorption and desorption of the accelerator and SPS incorporation into the deposit. Linear sweep voltammetry (LSV) indicates that behavior of the accelerator is potential dependent.

In the respect for the interaction of SPS in plating bath, the reaction was established in the system containing SPS only ¹⁹



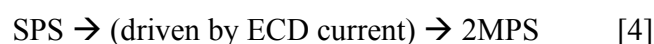
In conclusively of the mentioned above, we would like to introduce the kinetics in SPS system to our two-component-additive system, in agreement with the assumption from Moffat.

The both effects of PEG and SPS on the deposition of Cu from dilute acid sulphate solutions have been studied for several years. When were PEG added alone in the plating bath, a polymer film adsorbed at a metal surface is expected to slow down deposition currents by imposing a dense barrier at the surface and thus lowering the concentration of cupric ion at inner Helmholtz plane. Cupric ions compete with adsorbed PEG and adsorbed cuprous ions for free adsorption site, the adsorbed PEG molecules do not further affect electrode kinetics. The proposed mechanism is :¹³



Where Cu_{ads}^+ denotes an adsorbed cuprous ion, which competes with PEG_{ads} on Cu substrate.

When PEG-containing bath combine with SPS, the v-t curves will be different, as shown in Fig.1-3. During copper ECD, PEGs immediately adsorb on the interface in the potential range and then SPS gradually substitutes the sites of PEGs on the Cu surface. ^{18-19, 23} Ultimately, equilibrium between the adsorption of these two additives is accomplished. Possible reactions are:



Thus the complex Cu(I)MPSs gradually replace the adsorbed PEGs, and then reduce the inhibition as well as enhances depolarization. This model is called slow adsorption/desorption mechanism. A schematic diagram is shown below in the Fig. 1-4. The relative information to SPS and MPS¹⁷ are listed in Table I .

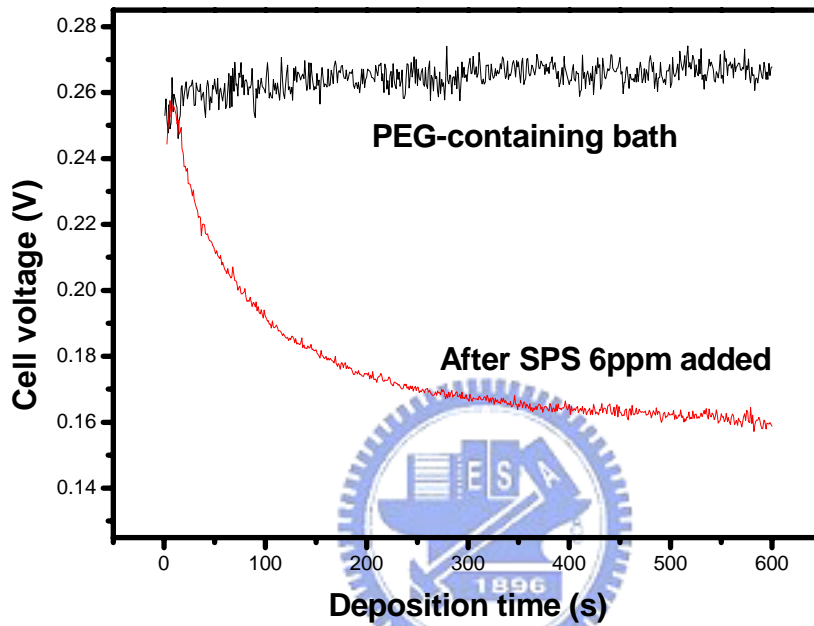


Fig.1-3. Evolution of v-t curves of PEG bath and SPS bath during ECD, respectively.

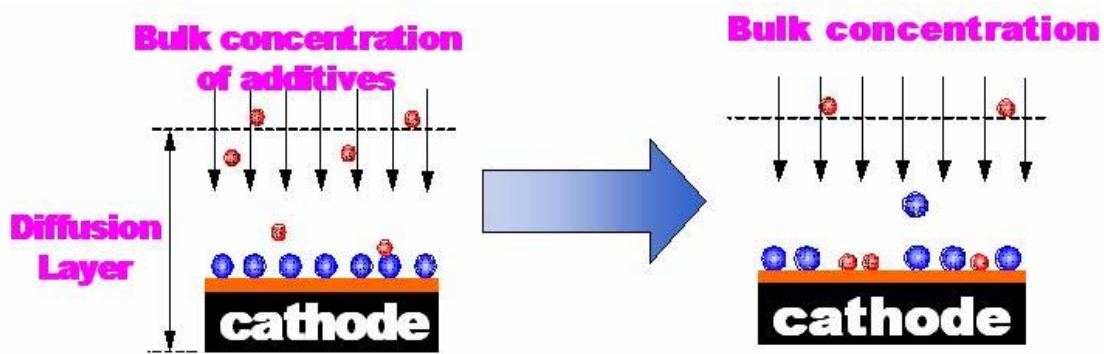


Fig.1-4. Illustration of the slow adsorption/desorption mechanism¹⁷

Name	abbreviation	Chemical formula
bis-(3-sodiumsulfopropyl disulfide), or sulfopropyl sulfonate	SPS	$^{-}\text{SO}_3(\text{CH}_2)_3\text{S-S}(\text{CH}_2)_3\text{SO}_3^{-}$
3,3'-dipropansulfonic acid disulfide	DDDS / DTODSA	$[\text{HSO}_3(\text{CH}_2)_3\text{S}]_2$
3-mercapto-1-propanesulfonate	MPS	$^{-}\text{SO}_3(\text{CH}_2)_3\text{SH}$
3-mercapto-1-propane sulfonic acid, or mercaptopropyl sulfonic acid	MPSA	$\text{HSO}_3(\text{CH}_2)_3\text{SH}$

Table I . Relative information to SPS and MPS

1.2.4 Filling Model of Cu Line/Via

Accelerated bottom-up deposition has been explained by a local accumulation of the accelerator species at the deep of a feature, as the surface area within the feature decreases during deposition process^{11, 24}. Recently, the bottom-up gap filling of Cu ECD with plating additives has been clarified by growth-accelerator species such as SPS and its byproduct such as MPS at the bottom of small features and slow diffusion of free MPS out of these features. The reduction of SPS to MPS provides a possible catalytic path for copper deposition through the formation of cuprous thiolate¹⁰. The model of overfilling is described step-by-step in Fig. 1-5¹⁰. As current flow was applied in electrolyte, it is assumed that all additive species have reached an equilibrium level on all surfaces of the wafer. In the initial stage, applied currents should be expected are approximately equivalent on all surfaces. This effect is corresponded with the observing relatively small amount of bottom-up growth seen in the initial 5-10 sec of a filling process.

After a period of plating time, two effects might begin to contribute filling. First, the accumulation of accelerating mercapto species (or their more accelerating derivatives) within the features takes place on the surfaces. This accumulation results in surface area within feature and sidewall decreases and adsorbed mercapto species (which are neither

incorporated in the deposit nor desorbed into solution) are thereby increased. Current increases in the areas of geometric concentration (bottom's corners) as chloride and suppressing polymer is displaced.

Too much accelerator in plating bath disrupts filling because the accumulation of accelerating species also take place outside the feature, and differentiation of the deposition rate from the via base is lost. The accumulation of catalytic species on the growing surfaces within features is strongly supported by the continued Cu growth above features in the absence of leveler. Discontinuing current flow to allow polymer re-equilibration does not interrupt this behavior. However, this is disrupted by reversal of interfacial potential to a value causing oxidation or desorption of the adsorbed catalytic material, or by addition of a leveling additive that suppresses current at protruding geometries.^{10, 17, 24}

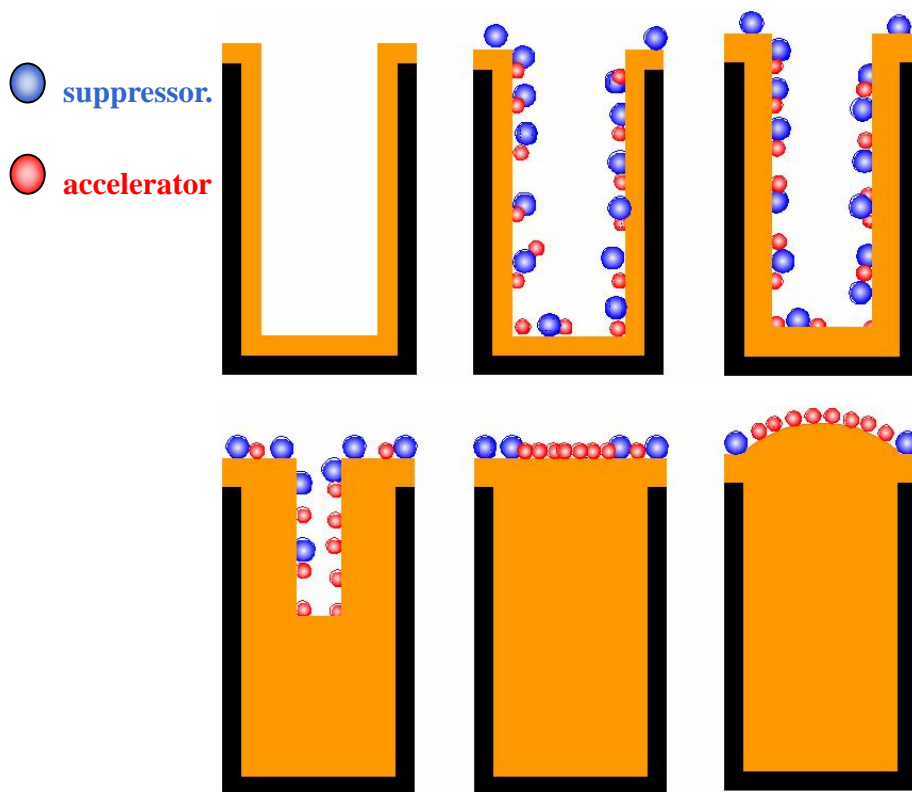


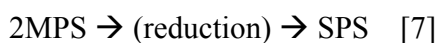
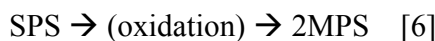
Fig.1-5. Scheme of the mechanism of the overfilling.¹⁷

1.2.5 Aging Influence of Electrodeposition Bath for Gaps Filling (Degradation of Electrodeposition Bath)

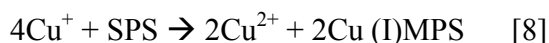
K.H. Dietz proposed that PEG is quite stable in acidic solution¹². However, it is interesting to learn that these organic additive or organic-copper complexes degrading in acid Cu plating baths. Once the kind of polyglycol chain is cleaved, thus can yielding shorter chain polyglycol fractions. A solvent extract of a fresh plating bath gives a high performance liquid chromatography (HPLC) scan with a narrow peak indicating a narrow molecular weight distribution of the poly (ethyleneglycol), as shown in Fig.1-6. After a couple of time, the original peak gets smaller, and wide distributions of lower molecular weight PEG species appears in the HPLC of the extract.²⁵

However, Koh et al. found that a large MW PEG polymer cleaved randomly into smaller molecules is activated by catalyzed oxidation or hydrolysis²⁵.

On the other hand, the following is a summary of the proposed mechanism about the effect of SPS in ECD bath. Accelerator SPS will crack into two MPS when driven by the overpotential of plating, and MPS is more active depolarization than SPS.^{19, 26} Moreover, the more and more existed MPS will make the electrolyte more ineffective for filling capability during aging process. As illustrated in Fig.1-7, after aging of plating cycle, it can be assumed that the entire reaction between the MPS/SPS and $\text{Cu}^{2+}/\text{Cu}^+$ are circulating and autocatalytic reaction systems, where the reaction products involve the initial reaction again and the reaction rate is slow initially.^{19, 26-27} In other words, two molecular MPS tend to oxidize to one SPS after more aging periods of plating, thus the relationship are listed below^{18-19, 26}:

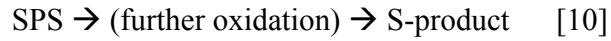


Furthermore, detail reactions with Cu ions involved is shown as followed



Therefore, the key depolarization effect of SPS is the oxidation of MPS, and then accelerate the cupric ions reduce to cuprous ions. The interfacial-adsorbed cuprous-thiolate complex allowed to move by surface diffusion, and also to break apart

into an adsorbed cuprous ion and an adsorbed disulfide product, and thus acted to accelerate the rate-limiting step⁹. However, T.O. Drews et al. provided another destructive oxidation reaction of SPS.



The electrolyte will lose all the accelerating ability after SPS become S product which is some forms of derivatives of aged SPS. Koh confirmed the dissolved-oxygen damage to SPS and observed a similar phenomenon to the above results²⁵, as shown in Fig. 1-8. The effect of accelerator will be depleted at atmosphere. We suggest that the most amounts of SPS in electrolyte will be decomposed to S-product and loss depolarization ability after many plating cycles faster at atmosphere.

Furthermore, K.H. Dietz also described the possible chemical formulas for that two reactions, as shown in Fig. 1-9. Since the formed compounds contains no divalent sulfur, the oxidation will result in a loss of depolarization.¹²

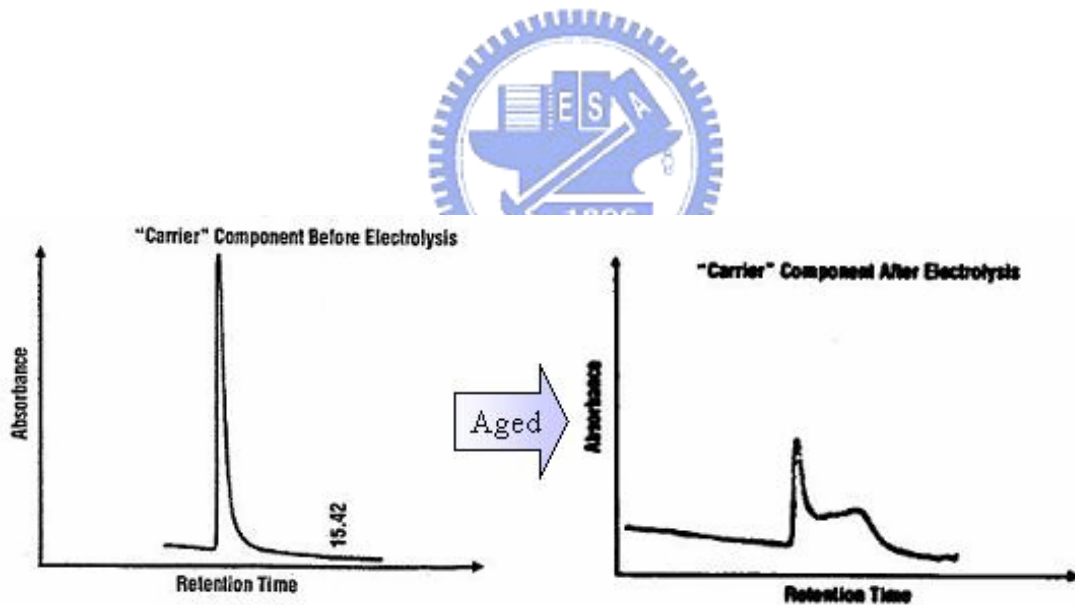


Fig.1-6. The HPLC scan of electrolytes before and after aged respectively. The carrier component reduced after aging process.²⁵

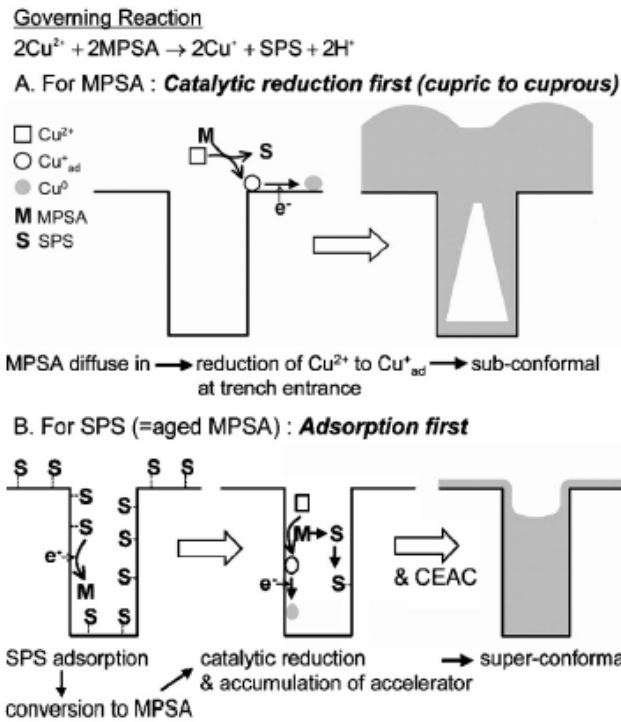


Fig.1-7. Schematic of assumed mechanisms for different filling aspects between MPS and SPS/aged MPS. (stoichiometry is ignored in this illustration).²⁷

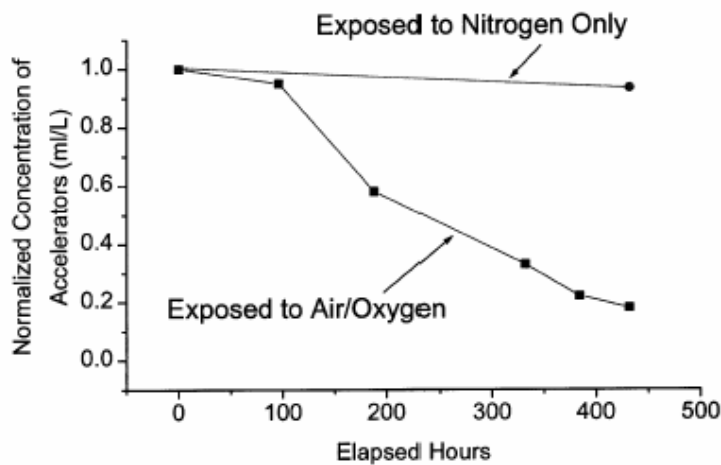
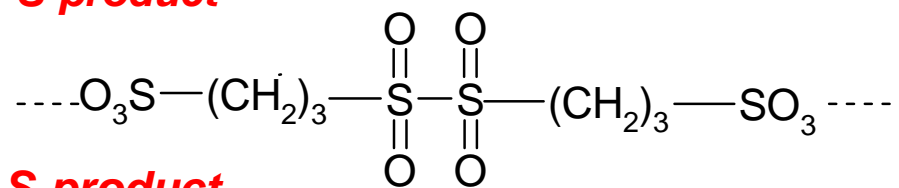


Fig.1-8. Comparison of the effect of ambient on the accelerator decomposition rate.²⁵

S-product



S-product

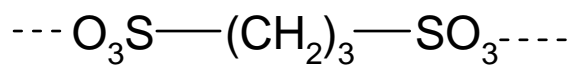


Fig.1-9. Possible Chemical formula of S-products ¹⁷



Chapter 2: Aging Influence of Organic additives (PEG and PEG-SPS containing) of Cu Electrolytes on Gaps Filling

2.1 Introduction

Several investigators have used an electrochemical method to study the inhibition effect of PEGs on electroplating¹⁻⁴. Kelly and West indicated that PEGs react with metal ions on cathodic surfaces, forming complex agents of PEG-Cl-Cu composites¹⁻². Material characteristics determined by atomic force microscopy (AFM), surface-enhanced Raman spectroscopy (SERS) and secondary ion mass spectroscopy (SIMS)⁵⁻⁷ also verify the presence of a monolayer of PEG-Cu-Cl film. This composite adsorbed on reacting surfaces constructs a diffusion barrier against the accumulation of cupric ions at the inner Helmholtz plane, thus reducing the number of Cu ions. Moreover, Stoychev and Tsvetanov proposed that the inhibition effect of PEG originates not only from the formation of PEG-Cl-Cu (requiring the presence of chloride ions) on Cu surfaces, but also from the complexation of Cu ions and PEG in electrolytes⁸ with Cl ions not participating. The latter mechanism impedes the overall ionic transport in bulk electrolyte. In general, both reactions reduce Cu deposition rate.

In addition to the Cu ECD rate and morphology of plated surfaces, PEG-related composites also influence the effectiveness of both inhibitors and accelerators in superfilling. In particular, for PEG-containing electrolytes free of inhibitors and accelerators, gaps filling ability is only governed by the combination of PEG additives of different molecular weights (MWs)⁹. In general, all or some PEG additives introduced to electrolytes should have high MWs to provide sufficient inhibition of electroplating¹⁰. The smaller-molecular-weight PEG with higher diffusion ability can enhance cupric ions migrating into deep features and be used to achieve bottom-up filling. The larger-molecular-weight PEG can provide enough inhibition effect of surface current to obtain denser and small-grained Cu deposition thus enhance the filling capability.

The effects of PEG and SPS on the deposition of copper from dilute acid sulphate solutions have been studied for several years¹¹⁻¹³. When electrolyte involves with accelerator (SPS), v-t curves change dramatically, i.e., a depolarization effect also occurs.

Therefore, by applying ECD into integrated circuits process, SPS plays can enhance diffusivity of ions in gap-filling ability.

However, few studies have addressed the impact of PEG and PEG-SPS aging on gap-filling. In this study, the gap-filling ability of PEG-containing electrolytes was investigated in relation to various aging stages with a fixed Cl^- concentration for various feature sizes. Real-time cell voltage transient and electrochemical analyses were performed to explore the degradation mechanism.

2.2 Experimental

(A) Sample preparation: Wafers were prepared by sputtering a 50-nm-thick Ta diffusion barrier and a 50-nm-thick Cu seed layer on SiO_2/Si substrates or patterned substrates with regular trenches (0.5 μm in depth and 0.35-1 μm in width).

(B) Apparatus of Cu ECD: The experiments on Cu ECD were carried out in a tank of non-conducting material. The counter electrode was a Cu plate with a size of 6 \times 6 cm^2 and the working electrode was a wafer with a size of 1 \times 3 cm^2 . The distance from counter electrode to working electrode was about 10 cm. Contact to the electrode was implemented outside of the electrolyte with an alligator clip. Agitation air was introduced into the solution from a compressor. In Cu ECP processes, the standard electrolyte was composed of $\text{CuSO}_4 \cdot 5\text{H}_2\text{O}$ (purity > 99%), 30 g/l, H_2SO_4 (97%): 50 g/l, chloride ions: 66 ppm, and deionized water ($\sim 18 \text{ M}\Omega$). It was additive-free. All organic additives (PEG and SPS) used in this work were purchased from Fluka. The films were deposited under galvanostatic control at room temperature. The direct current power supply utilized in this study was Keithley model 2400, while cell v-t curves are in-situ recorded by PC via GBIP protocol.

(C) Electrochemical analyses: All D.C. and A.C. electrochemical polarization studies were made in three-electrode cells using a computer-controlled EG&G model 273A potentiostat. Potentiodynamic (PD) polarization curves were employed to analyze electrochemical behavior of Cu ECP. The counter electrode was platinum (Pt) and the working electrode was Cu with a constant surface area of 0.5 cm^2 . Before each experiment the working electrode was first mechanically ground and cleaned with deionized (DI) water. All potentials were reported relative to an Ag/AgCl electrode,

which was used as the reference electrode.

2.3 Aging Influence of PEG Suppressors of Cu Electrolytes on Gaps Filling

Cross-sectional SEM images in Fig. 2-1 show 0.35 μm patterns filled with ECD Cu using single-PEG (PEG4000) electrolytes undergoing numbers of electroplating cycles (1 and 5 cycles), and using bias currents of 6 mA (2×10^{-3} A/cm²), 15 mA (5×10^{-3} A/cm²) and 30 mA (1×10^{-2} A/cm²). With a low plating current of 2×10^{-3} mA/cm², the filling quality for the damascene features and roughness of plated Cu surfaces are almost independent of the number of electroplating cycles. With a higher plating current of 5×10^{-3} A/cm², worse gaps filling and rougher surfaces were obtained with aged electrolytes than those obtained with fresh electrolytes. This deterioration phenomenon with electroplating cycles becomes more significant with increasing plating current, as confirmed by SEM images for the plating current of 1×10^{-2} A/cm². Examining STD electrolytes using the same tests applied to PEG-containing electrolytes revealed that plating cycles have a negligible influence on the gaps filling capability and field, and roughness of plated surfaces (results not shown here). Hence, PEGs in electrolytes are expected to be the predominant constituents degraded during plating cycles. Notably, fresh STD electrolytes have the worst performance in gaps filling and surface smoothening among the three electrolytes discussed.

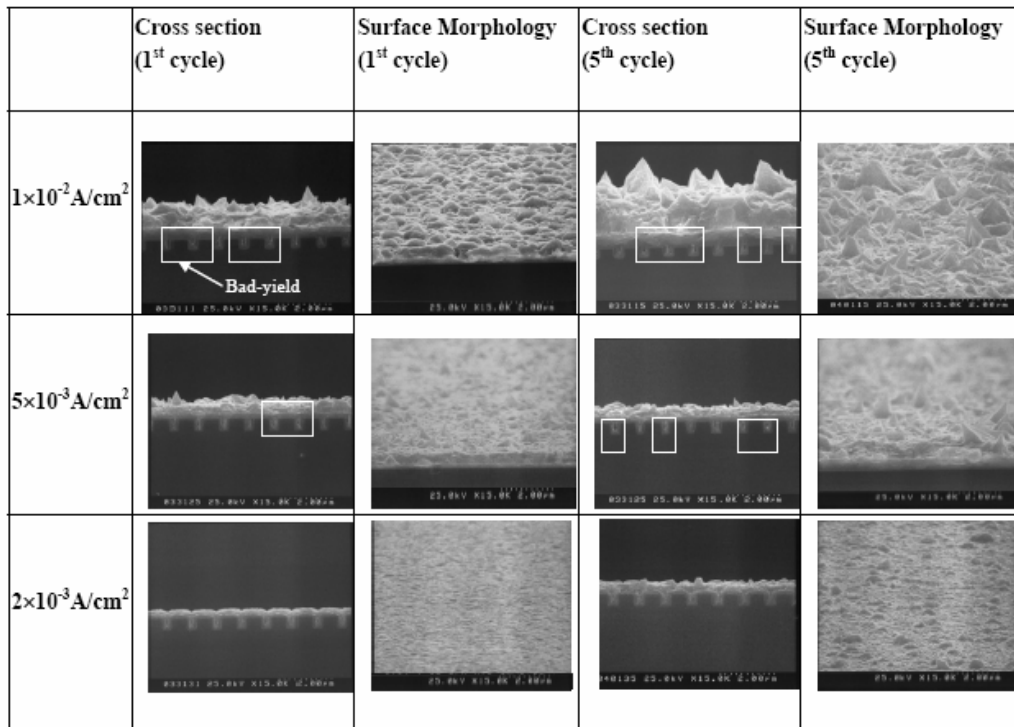


Fig.2-1. Side-view and cross-sectional SEM images for $0.35 \mu\text{m}$ trenches electroplated with PEG (PEG4000) electrolytes undergoing various aging stages with various bias currents.

To investigate gap-filling yield with different plating cycles under various conditions, hundreds of trenches, with sizes ranging from 0.35 to $1 \mu\text{m}$, plated with PEG-containing electrolytes were analyzed. Figure 2-2 (a) shows plots of gap-filling yield, Y_G , as functions of plating cycles for the three current densities. Gaps filling yield decreases as the number of plating cycles increase, and was higher at higher current densities. In addition, the gaps filling yield increases with trench width for the three current densities, and a higher current density gives a higher yield. To examine the aging-induced gaps filling degradation, the decay rate of gaps filling ability $\Delta Y_G / \Delta n$, which is defined as the change in gaps filling yield during specific cycles and obtained by analyzing the data in Fig. 2-2, is plotted in Fig. 2-3.

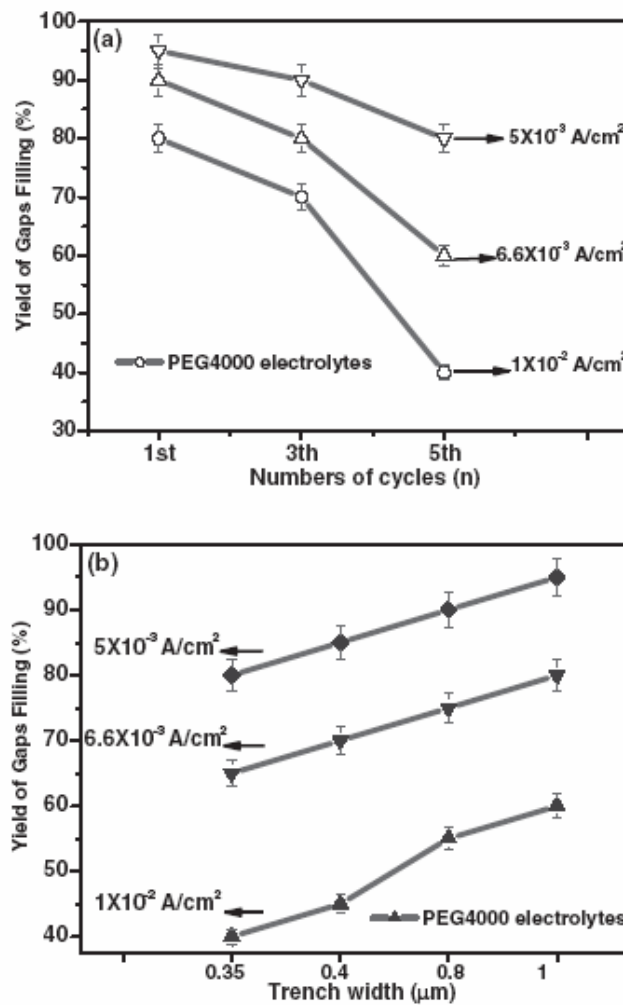


Fig.2-2. Gaps filling yields in trenches electroplated with PEG400-containing electrolytes operated at various bias currents as functions of (a) number of plating cycles, and (b) trench width.

Therefore, a higher $\Delta Y_G / \Delta n$ means a higher level of more serious gaps filling decay. Figure 2-3 reveals one interesting trend: gaps filling decay for narrower trenches is at a higher level than that for wider trenches. Moreover, excellent gap-filling in wide trenches is possibly obtained with electrolytes without additives, and hence gap-filling is not affected by the alteration (or decay) of additives in electrolytes. Nevertheless, Figure 2-3 reveals clearly that the decay rate of gap-filling increases with the bias current employed regardless of the electrolyte used or trench width considered.

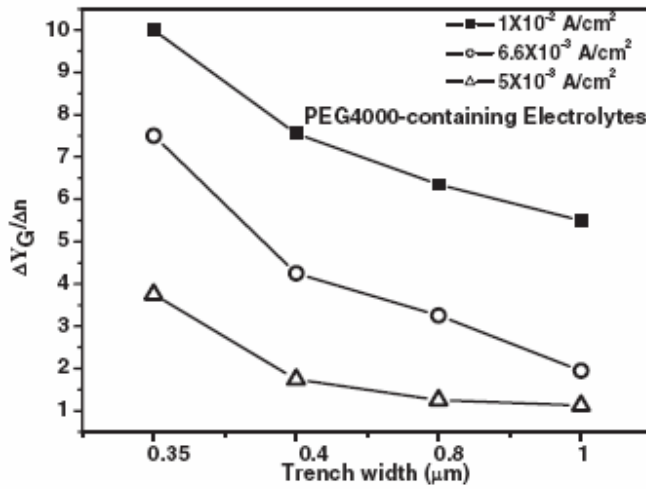


Fig.2-3. Decay rates of gaps filling yield for PEG-containing electrolytes operated at various bias currents, as function of trench width.

Next, we will correlate aging-induced electrochemical reactions with gaps filling degradations. To date, two possible degradation mechanisms for PEGs during ECD have been proposed by Stoychev and Tsvetanov, and Dietz^{8, 14}: (1) the cracking of long-chain PEGs, and (2) increasing numbers of small clusters of Cu ions complexing with $-(CH_2)-$ bonds of PEGs formed outside the double-layer region. Because electroplating systems can be modeled as an equivalent circuit, Nyquist plots resolve impedances that originate from various reactions in ECD^{2,11,15}. For verifying our assumption, the electrochemical behavior of low-MW/short-chain PEG on a Cu surface should be analyzed. Nyquist plots in Fig. 2-4(a) depict a higher diffusion layer resistance of 4Ω (calculated from the second semicircle of the curves) but a similar charge-transfer resistance of 2Ω (first semicircle) for the fresh PEG200-containing electrolyte in comparison with the STD electrolyte with associated resistances of 2.5 and 2Ω , respectively. This implies that low-MW/short-chain PEG complexes preferentially with Cu ions outside the double-layer region but has a negligible absorption effect (or a polarization effect). Figure 2-4(b) shows that the addition of high-MW PEG4000 to STD electrolytes enhances significantly the polarization effect by increasing the charge-transfer resistance from 2Ω (STD) to 15.5Ω (STD+PEG4000) but has less influence on the diffusion layer resistance (3.5Ω) than the addition of low-MW PEG200.

Figure 2-5 displays PD curves for the electrolytes shown in Fig. 2-4(b). As can be seen, the polarization effects of PEG-containing electrolytes increase with MW⁹. Unstable complexing between long-chain PEG and Cu ions, which is caused by the steric block effect of long-chain polymers in the diffusion layer⁸, and the MW-dependent polarization effect on PEG¹⁴⁻¹⁵ explain well the above observations.

After five plating cycles, the charge-transfer resistance of the aged PEG4000-containing bath (12.5 Ω) is lower than that of the fresh PEG4000-containing bath (15.5 Ω), but their diffusion layer resistances are almost the same. On the other hand, for low-MW PEG200, aging influences diffusion layer resistance rather than double-layer resistance (or charge-transfer resistance). Because short-chain PEG200 is difficult to crack⁸, the consumption of these short-chain PEGs via complexing with Cu ions in each plating cycle is a possible reason for the reduced diffusion layer resistance of aged PEG200-containing electrolytes. Moreover, short-chain PEGs have a negligible polarization effect, as observed in Fig. 2-4(a), resulting in double-layer resistance for PEG200-containing electrolytes while STD electrolytes are independent of PEG-related aging. In contrast to low-MW PEG200, the cleavage of high-MW PEG4000 during ECD also occurs and result in short-chain PEG, which is prone to complex with Cu ions in the diffusion layer. Although the continuous consumption and cleavage of PEG4000 worsens PEG4000-related polarization effects and diffusion layer resistance, the formation of increasing numbers of short-chain PEG-Cu complexes in the diffusion layer causes the diffusion layer resistance to remain unchanged. Although the consumption of these short-chain PEGs via complexing with Cu ions during each plating cycle may reduce the resistance of the diffusion layer, uncracked or unadsorbed long-chain/high-MW PEG and transient long-chain PEG-Cu complexes still occupy most of the space in the diffusion layer.⁸ Therefore, the long-chain PEG may still dominate the resistance of the diffusion layer and thus the measured resistance in the diffusion layer remained almost unchanged. In addition, the formation of more and more short-chain PEG-Cu complexes in the diffusion layer replenishes the consumption of PEGs, which are incorporated into Cu film during plating.

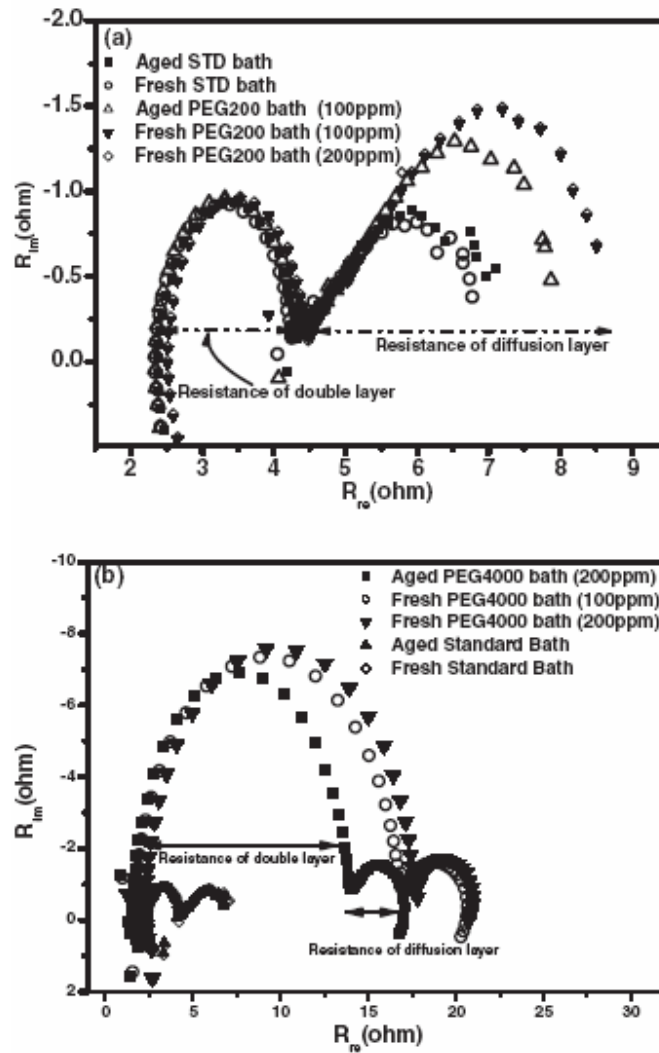


Fig.2-4. Nyquist plots for standard, (a) PEG200-containing and (b) PEG4000-containing (100 and 200 ppm) baths undergoing one and five plating cycles.

The cleavage of long-chain PEG into short-chain PEG is driven by bias current or dissolved oxygen^{8,16}. Because short-chain PEGs have low polarization resistances and thus weak suppression abilities, the electroplated Cu would have a rough surface when PEG200 is presented owing to the cleavage of PEG4000 during plating. In addition, the presence of the short-chain PEGs may also degrade the inhibitive ability of the electrolyte and this may be the reason why the partials filling of the trench was observed more frequently with an increasing number of plating cycles⁹, as shown in Fig. 2-1. These explain the bias current dependence of gaps filling degradation caused by aged PEGs, as

shown in Fig. 2-3. Figure 2-5 shows the PD curves for the STD, fresh 100-ppm and 200-ppm PEG4000, and aged 200-ppm PEG400. It can be seen that the inhibitive ability of PEG4000 decreased after aging. Therefore, the charge-transfer resistance (Fig. 2-4) or polarization effect (Fig. 2-5) is insensitive to a variation in PEG concentration of 50 %, which is in agreement with the results reported by Reid and David.¹¹ Suppressors are usually distributed in the plating bath at high concentrations (200-2000ppm) so that their concentration at the interface is not strongly dependent on their rate of mass transfer or diffusion to the surface^{1-2, 9-10}.

This means that the reduction of the polarization effect or the degradation of gaps filling ability caused by aging-induced PEG consumption and the cracking of PEG400 is quite serious. Thus, studying transient PEG adsorption ability or real-time aging-related reactions in relation to bias currents and plating cycles is instructive.

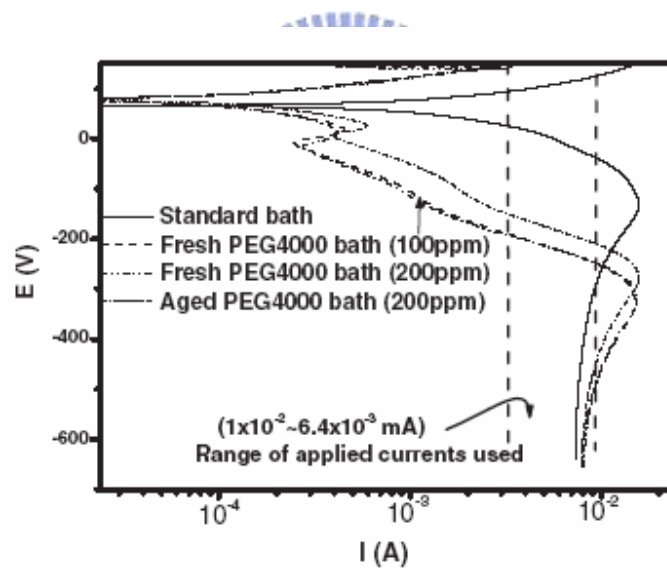


Fig.2-5. Potentialdynamic curves for standard and PEG4000-containing (100 and 200ppm) baths undergoing one and five plating cycles.

Figure 2-6 shows transient V-t curves for fresh and aged electrolytes operated at various bias currents. Observing the initial stage of the transient V-t curves for fresh PEG4000-containing electrolytes operated at bias currents higher than $3.3 \times 10^{-3} \text{ A/cm}^2$ reveals that cell-voltage increases abruptly and then drops to a stable value. According to Healy, PEG additives adsorb initially on the cathodic surface, forming a blockage layer of PEG-based polymer consisting of accumulated and adsorbed PEGs on reacting surfaces¹⁹ in response to rising cell-voltage. Moreover, both the adsorption/desorption of PEGs and the reduction of Cu ions on plated surfaces occur simultaneously and a dynamic equilibrium between these two reactions determines the shape of the overshoot or falls time (t_F) of cell-voltage on V-t curves. Figure 2-7 shows the falls time of different numbers of plating cycles for the three current densities. The falls time was obtained by fitting the overshoot fall-time using an exponential curve as shown in the inset in Fig.2-6. Undergoing plating cycles, effective PEGs (or large MW PEGs) on reactive surfaces decrease in number, making numerous adsorption sites available for the reduction of Cu ions, and hence, the dynamic equilibrium is reached more quickly (or a shorter falls time is obtained). For the same plating cycles, faster fall is obtained with a higher bias current. This can be attributed to the extremely high charge-transfer rate or the high Cu reduction rate caused by the high current density, which enables Cu ions to occupy efficiently the adsorption/re-adsorption sites of PEGs, thus weakening the PEG-dominated polarization effect or shortening the falls time of the initial cell-voltage. Therefore, this method has potential applications in the in-situ checking of the long-term reliability of electrolytes.

So far, the influences of aging poly PEG-Cl-containing electrolytes on Cu's gap-filling ability are studied. The polymeric additive, PEGs, cracked continuously in electrolytes undergoing a sequence of galvanostatic plating and was confirmed by in-situ cells voltage-time measurements and electrochemical analyses, forming numerous PEG-based complexes outside the double layer but fewer high-MW PEGs adsorbed on the reacting surface. This is regarded as the predominant mechanism causing reduced polarization effects (or low inhibition effects) and the subsequent decay in gap-filling ability for aged electrolytes.

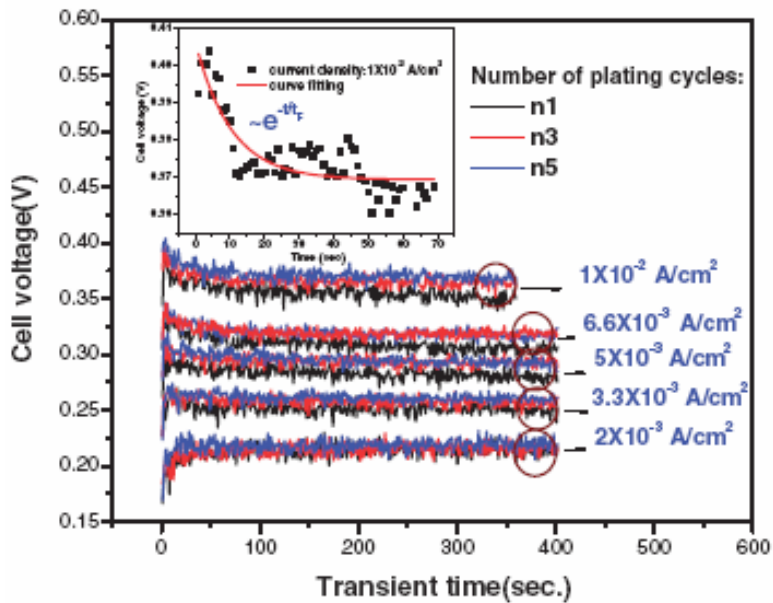


Fig.2-6. Evolutions of cells voltage vs transient time (V-t) for PEG4000-containing electrolytes galvanostatically performed and controlled at various currents.

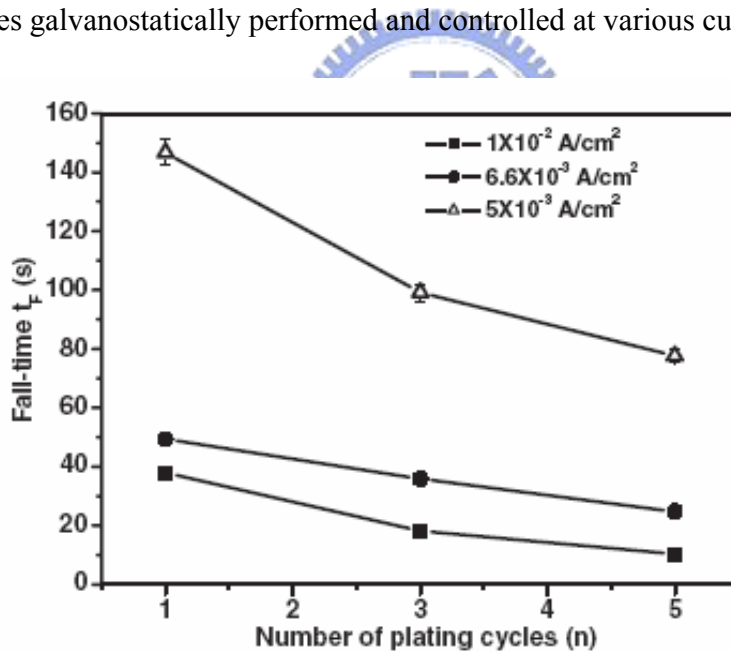


Fig.2-7. Extracted fall-times of overshoot shape of transient cell-voltage for PEG4000-containing electrolytes undergoing various plating cycles and performed using different bias currents.

2.4 Aging Influence of PEG-SPS-containing Cu Electrolytes on Gaps Filling

2.4.1 Degradation Trends of Different SPS Concentrations

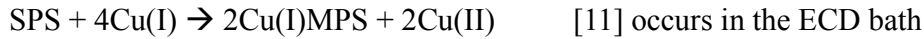
When various concentrations of SPS are doped, different slopes as well as amplitude of the voltage drop were obtained, as seen in Fig.2-8. Based on the slow adsorption/desorption model, the rate of faster replacement in the higher concentrations leads to the sharper decreasing of the voltage, while the amplitude of voltage drop is larger due to the higher SPS equilibrium concentration (cathodic surface sites occupied ratio of SPS to PEG) on the as-deposited surface.

Figure 2-9 shows v-t curves at various applied currents. As the higher current applied, the sharper drop of voltage corresponds to the fast substitution for PEG by Cu(I)MPS, which could be explained by our model. Besides, the amplitude of voltage drop is larger at higher current, in agreement with the high equilibrium concentration of Cu(I)MPS in the cathodic surface.

Similar scan that performed in PEG-containing bath was used to examine the yield of gap-filling in the (PEG, SPS)-containing bath, as shown in Fig.2-10. In this Figure, three concentration of SPS of (PEG, SPS)-containing baths were aged in ECD process and obtained the static gaps filling. For bath of higher concentration SPS (above 6ppm), as shown in Fig. 2-10 (b), decreasing trend of gaps filling as a function of plating cycles is observed obviously. The filling capability can not recover with the increase of plating cycle when the electrolyte contains high concentration of SPS (above 3ppm). However, for the concentration of 1 ppm-SPS bath, as shown in Fig. 2-10 (a), the gaps filling degraded after 5 cycles but rose at 7th cycle. It is very interesting. The corresponded SEM image is also shown in Fig.2-11 and 2-12.

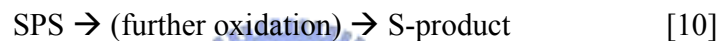
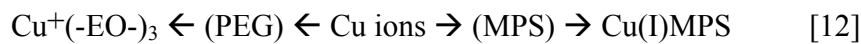
Three possible mechanisms may be responsible for the degradation of (PEG, SPS)-containing bath. We suggest one possible mechanism for the low concentration of SPS during plating. From the above section, in which the depolarization occurs in the interface between the bath and the cathodic surface, Healy et al. suggested an alternative

mechanism for the decomposition of SPS into MPS, which occurs in electroplating baths. Again, it involved the formation of a stable Cu^+ complex, Cu(I)MPS ¹⁷.



Therefore, more active MPS in the bath accelerate the ECD rate gradually. However, the more and more existed MPS will make the electrolyte more ineffective for filling capability during aging process because the most reduction of Cu^{2+} to Cu^+_{ad} occurs at the trench entrance.¹⁸ Most part of accelerator can not diffuse into bottom of trench after the aging of electrolyte. However, after 7th cycles, some MPS tend to transferred back to SPS because of the reaction as described in Eq.9.

Therefore, in the degradation of the gap-filling ability of SPS, two possible mechanisms are proposed.



After plenty of plating cycles, both accelerator SPS and suppressors PEG degrade due to the cracking behavior and oxidation. Meanwhile, the filling capability of the additive-degrading electrolyte reduced. As shown in Fig.2-10 (b), higher plating current densities and pre-aged at room temperature will accelerate the degradation of filling capability of SPS-PEG-containing electrolyte. It verify that cleave of SPS comes from current driven and oxidation. If the amount of SPS in electrolyte is excess, the degradation of most SPS will be dominant so the MPS will be excess after many palting cycles.

At first, as combined above last chapter, both PEGs and SPSs tend to form complexes with Cu ions. Koh et al suggested that the decrease of cuprous thiolate complexes is due to consumption of cuprous ions by chelating with PEGs. Thus the accelerator degradation rate decreases when PEGs suppressing species are added into the solution¹⁶. As a result, Cu ions are less trapped by MPSs due to the increasing of short-chain PEGs, and thus their acceleration ability is reduced. On the other hand, as the ECD process is sparging with air (atmosphere), the SPS could be possibly oxidized to S-product.^{17, 19}

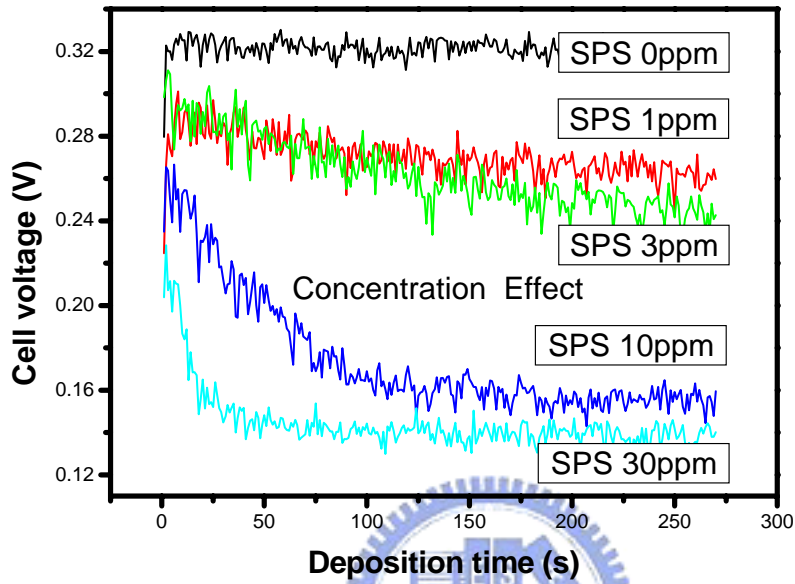


Fig.2-8. Evolutions of the v-t curves of various SPS-concentrated baths

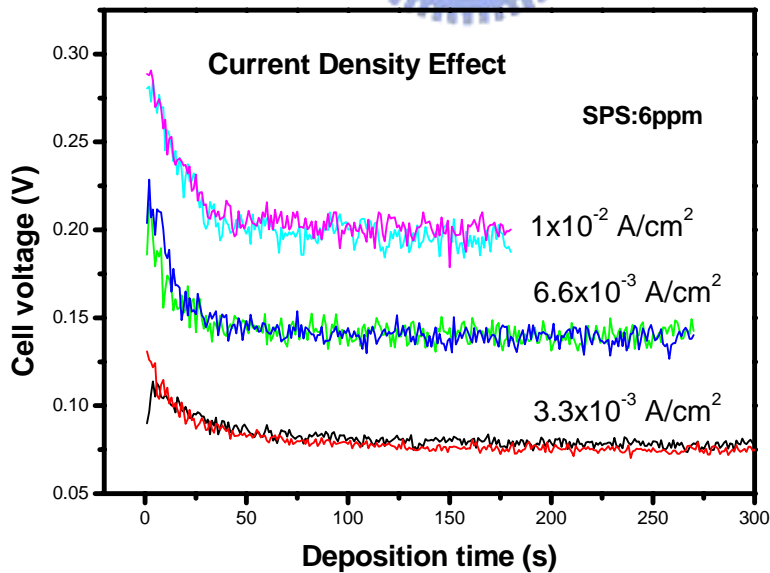


Fig.2-9. Evolutions of the v-t curves at various currents

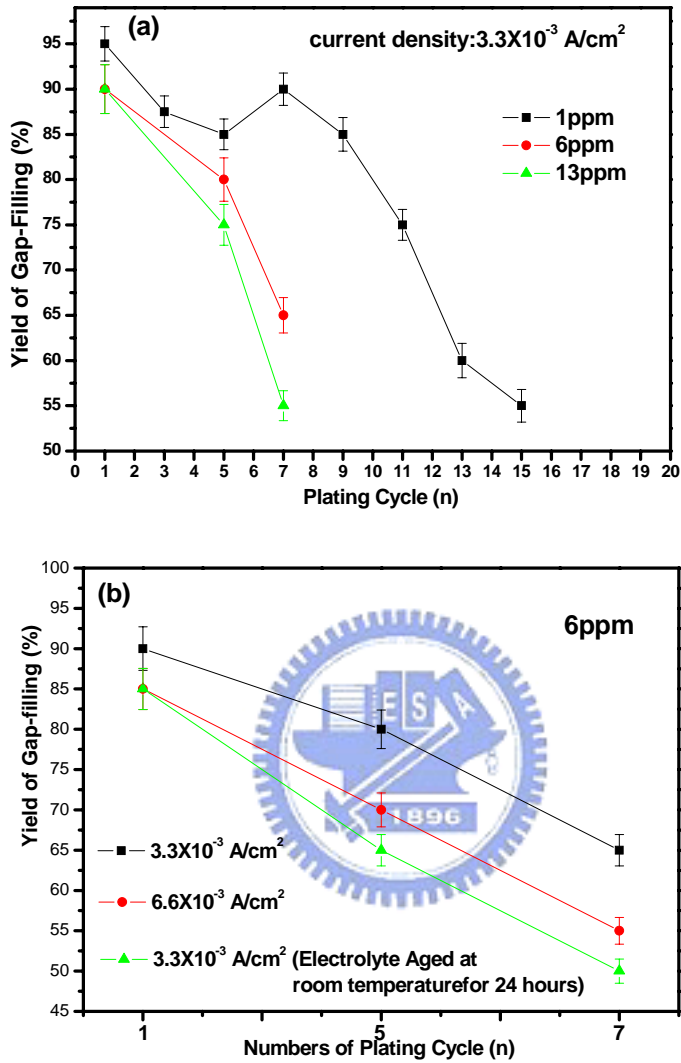


Fig.2-10. Gaps filling yields in trenches electroplated with SPS-PEG-containing electrolytes operated at (a) various concentrations of SPS (b) higher applied current and pre-aged conditions. Trench width: 350nm.

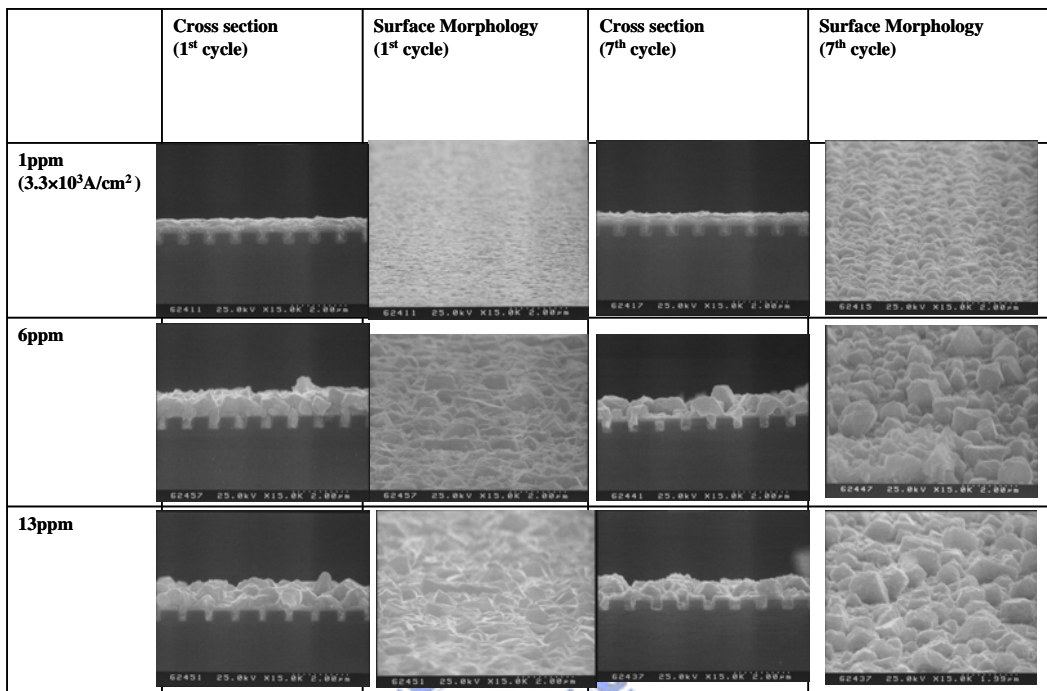


Fig.2-11. Side-view and cross-sectional SEM images for $0.35 \mu\text{m}$ trenches electroplated with SPS-PEG-containing electrolytes undergoing various aging stages with various concentration of SPS.

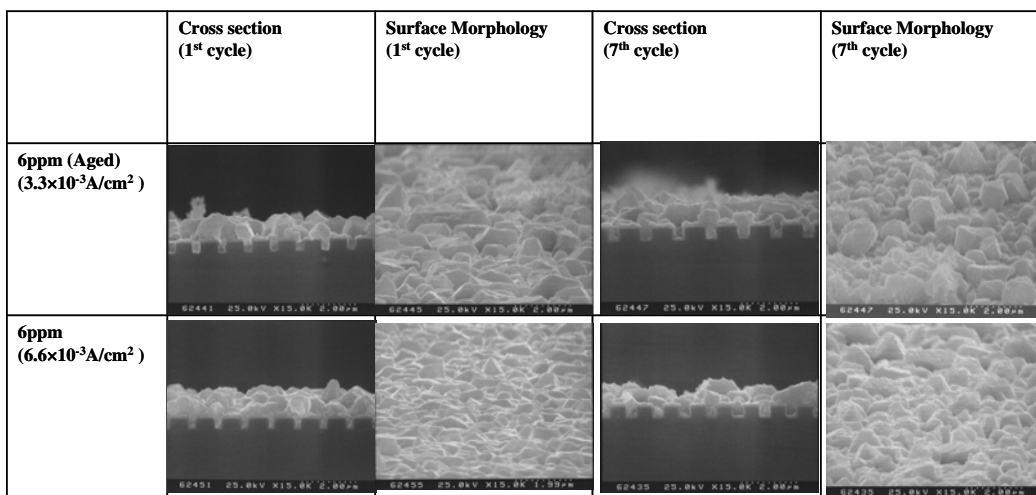


Fig.2-12. Side-view and cross-sectional SEM images for $0.35 \mu\text{m}$ trenches electroplated with SPS-PEG-containing electrolytes undergoing various aging stages with various bias currents.

As discussed above, one SPS can be cleaved into two MPSs by applied current. On the other hand, as seen in Fig. 2-13, depolarization could also occur when no current was applied; this is similar to the results of Tan's¹³. Before plating, samples are immersed into the electrolyte for various periods; the immersed time is respectively 0 min, 4 min, and 8min without sparging. Some enhanced depolarization occurs during the pretreatment period. The cell voltage is decreased as the pretreatment time increased. For comparison, the sample pretreated with 8-min immersion with sparging results in dissolution of seed layer, and thus a highly rough v-t curve is observed as seen in the “gray” curve in Fig.2-13.

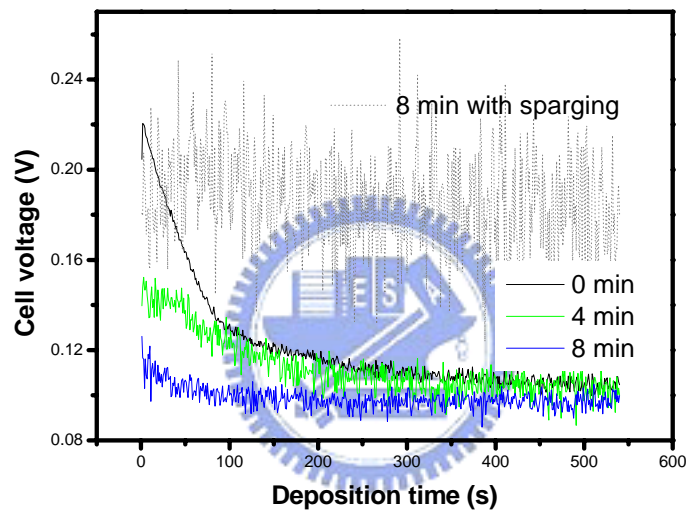


Fig.2-13. Evolutions of the v-t curves at various pretreatment durations, the applied current density is $3.3 \times 10^{-3} \text{ A/cm}^2$.

2.4.2 Electrochemical Analyses of Aged PEG-SPS-containing Cu Plating Electrolytes

The AC-impedance scans were performed to verify the above assumptions. Both fresh and aged baths are analyzed, as seen in Fig. 2-14 (a) and (b). When SPS was doped into the PEG-containing bath, the inhibition dramatically decrease, i.e., the depolarization occurs. After aging of plating cycle increases, the depolarization behavior of electrolyte containing high concentration of SPS is almost diminished, and a result of nearly pure PEG-containing bath is observed. The effect of organic additives in electrolyte decayed obviously. The However, for low concentration of SPS in Fig.2-14 (b), the acceleration

ability restore due to the back transient transfer of MPS to SPS. This is in accordance with our experimental results. After aging for 17 cycles, it is suggested that SPSs were almost consumed and PEG were decayed almost completely during ECD process concurrently.

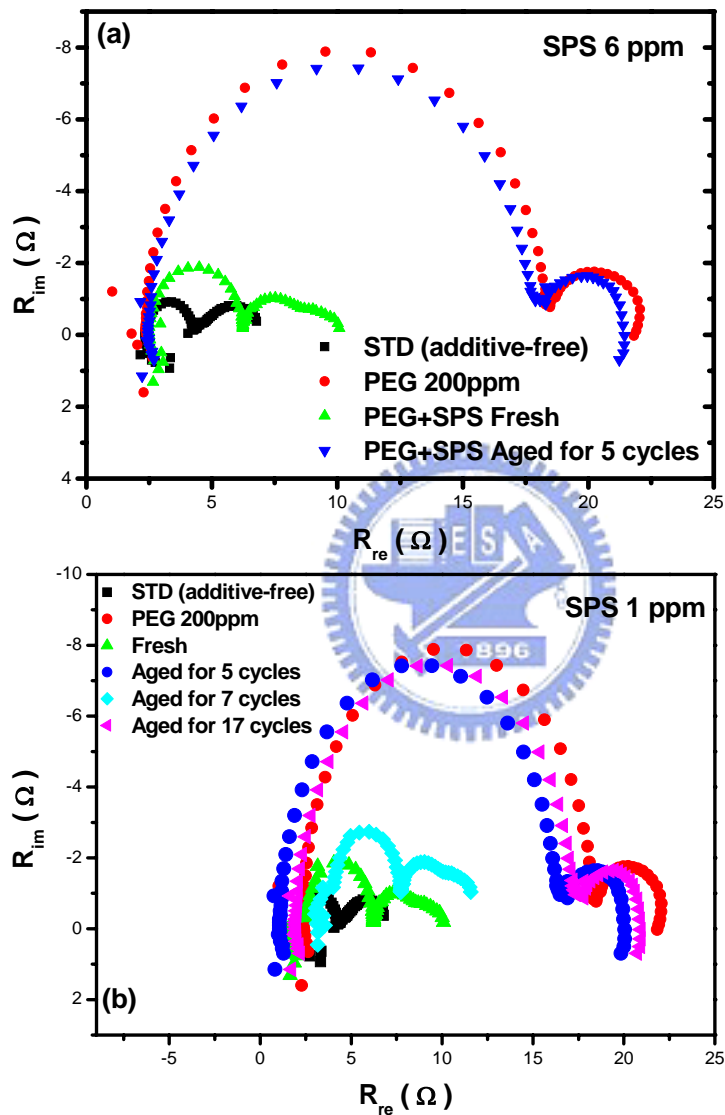


Fig.2-14. AC scans of the fresh and aged baths containing SPS (a) 6ppm, (b) 1ppm.

Chapter 3 Introduction of Cu Electropolishing and Experimental Details

3.1 Cu Planarization in Damascene Process

Cu damascene schemes continue to dominate the next generation of interconnect preparation in the integrated circuit (IC) industry as feature sizes are scaled down below several tens of nm. In conventional damascene processes, Cu electrodeposition will produce step-height on/between various trench widths of features. In general, anywhere from sub-micrometer to several micrometer of metal needs to be planarized. Chemical mechanical polishing (CMP) of copper and barrier metals is the current method for defining a planarized interconnection area.¹⁻³

As shown in Fig. 1-1, excess Cu on patterned area should be removed by using CMP process which contains a chemical interaction of slurry with polishing substrate and mechanical friction to this substrate. However, conventional CMP for dissolution of such large quantities of metal requires a long polishing time and consumes a large quantity of slurries, adding in materials costs. Meanwhile, CMP process accompanies some disadvantages for damascene process, including remaining particles on Cu surface of abrasive, erosion and dishing for the final production yield, costly equipment Cu corrosion⁴, poor uniformity, and difficult end-point measurement for industrial work. Also, mechanical hard abrasives in slurries or breaking diamond tips embedded in the polishing pad usually causes scratches on Cu surface during the pad polishing. These scratches may degrade the reliability of follow-up processes integration. These points are described in Fig.3-1. Furthermore, a tremendous challenge of post-CMP cleaning is the critical issue for contamination-free CMP. Recently, an introduction of low-k films (such as porous dielectrics) as inter-metal dielectrics (IMD) has been developed, this low-k dielectric films have much lower mechanical properties than silicon oxide. Therefore, how to minimize the mechanical components from the Cu-CMP becomes more important.

In addition to the review of Cu CMP process, slurry chemistry is a key issue in Cu planarization for both present manufacturing and future applications and cost over 50% of entire process.⁴⁻⁵ The chemical parameters involved in the slurry chemical formulations should be consisted of complexing agents, inhibitors, and solutions which can tune pH values. The other compositions in slurry are silica and alumina abrasives. Each additive in slurry has its special function to enhance the significant effect of CMP. Thus, very high Cu polish rates can be obtained by formulating slurries at low pH in the absence of corrosion inhibitors.⁶ However, the cost of slurry in CMP could not be reduced easily in a short period of time. Therefore, the optimization of chemical slurry's recipe and abrasive-less CMP become future trend of CMP.

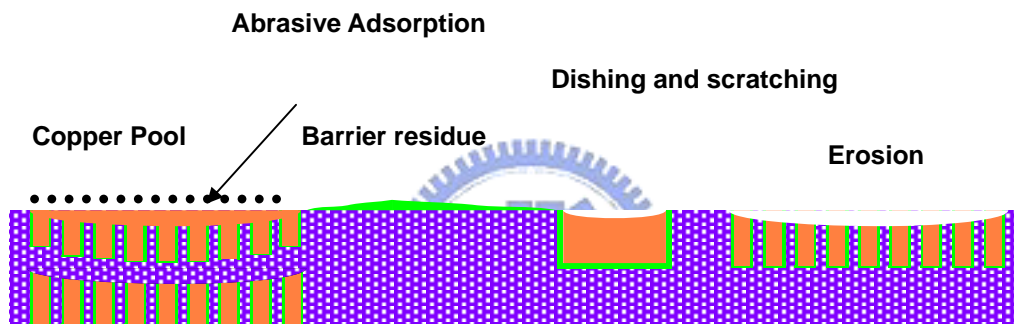


Fig.3-1. Common CMP processing problems resulting from the different polishing rates of copper, barrier, and ILD. Orange–copper; green–TaN; purple–ILD. The “copper pool” defect is caused by erosion in the previous underlying metal layer.⁴

Therefore, low-stress planarization techniques such as electrochemical mechanical deposition (ECMD),⁵ Abrasive-free mechanical polishing (AFP),⁷ and additive-assisted electropolishing (EP), have been demonstrated to be feasible for solvent in reduction of mechanical component for planarization of porous dielectric/Cu damascene metallization.

Electrochemical mechanical deposition (ECMD) was studied by industrial work and presented very good superfilling ability and planarized step-height for low-aspect-ratio trenches for Cu damascene filling process. Electrochemical Mechanical Deposition (ECMD)⁵ as shown in Fig. 3-2, involves copper electroplating with externally applied stress to achieve copper film growth with better uniformity and finer structure. On the

other hand, the plating electrolyte for the period of Cu filling in ECMD contained high acid sulfate, chloride ions, and other organic additives. This method provides a concept that makes cost down of necessary Cu planarization equipments

Similar technologies under intensive development include abrasive-free polishing⁷⁻⁹ as well as novel electropolishing basing on function-specific chemical additives. Among them, electropolishing of copper, in particular, bears strong resemblance to electrodeposition of copper as both are performed in a single electrochemical bath.

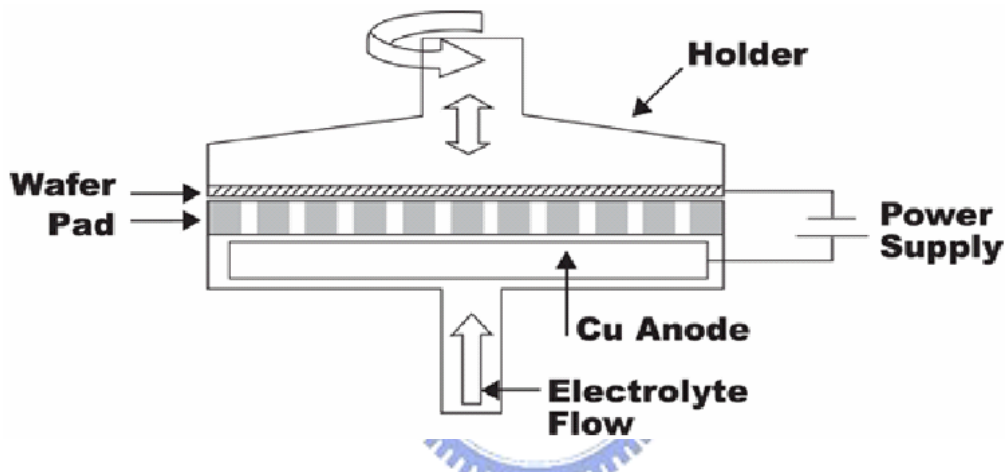


Fig.3-2. A schematic diagram of Electrochemical Mechanical Deposition (ECMD). It is based on modification of typical copper electroplating setup in which one electrode is used for electroplating while the other electrode is covered with abrasive overlayer to facilitate the planarization of the as-deposited copper film.⁵

In a Cu-CMP process, abrasives of chemical slurry often bring mechanical damages such as micro-scratch on Cu surface. Cu abrasive-free mechanical polishing (AFP) is technology is developed as an alternative method to avoid mechanical abrasion on metal surface.^{1, 7-9} Cu AFP can produce a scratch-free surface because of the reduction of mechanical force. In other words, the force pressured on polished surface would be significantly reduced in-situ during AFP so that can enhance the integration with porous low-K materials in dielectric layers. However, the removal rate of Cu-AFP is too low for use in a manufacturing environment (about 150 nm/min in Kondo et al.'s study).¹

Cu Electropolishing (EP) technology is recently explored as a replacement of Cu-CMP.¹⁰⁻¹⁵ An applied electric field is substituted for the mechanical force component in CMP to remove excess Cu layers. The stress-free characteristic of Cu EP can handle low-k dielectrics. Furthermore, Cu EP has advantages of high polishing rate, low waste stream, no abrasive and no scratching. This stress-free process can produce a clean and scratch-free Cu surface. However, very few research of enhancing planarization efficiency of Cu EP by chemical additives in damascene processing was reported. The mechanisms and application of chemical additives in Cu EP will be discussed in later chapter.

3.2 Background and Microleveling Mechanism of Cu EP

Electropolishing is an important surface treatment technology and can be operated at or above the current density at which the dissolution rate could be controlled on metal surface. Furthermore, the equipment of electropolishing is compatible with electrodeposition. The electrode to be electropolished is immersed in an electrolyte and subject to an electrical current as an anode. Traditional mechanical finishing techniques can be replaced by these electrochemistry and the fundamental principles of electrolysis (Faraday's Law). During metal EP, the object is maintained anodic, with the cathodic connection being made to a nearby metal conductor.^{10, 12, 15}

This dissolution rate is depended on the formed limiting current density and may be a function of viscosity and conductivity of the electrolyte, diffusion coefficient of the reactant in electrolyte and the rotating speed of polishing electrode.^{10-11, 15-16} Figure 3-3 displays simple schematic of Cu-EP. During electropolishing, microlevelling effect occurs at interface of electrolyte/electrode and then the convex of metal can be dissolved more quickly.

When Cu surface was anodized at specific range of potentials (the plateau region), accelerated dissolution occurred initially. As the fixed potential applied continuously, a viscous layer started to form at the anode/electrolyte interface and then a diffusion-limited region existed within this range where Cu-EP behavior usually took place. When the viscous layer continues to grow and achieve steady state, the polishing current on sliced wafer maintained at a range of steady value. Consequently, the

polishing rate is not accelerated and the ion transport of anode/viscous layer/electrolyte interface maintain at a dynamic equilibrium.^{10, 15}

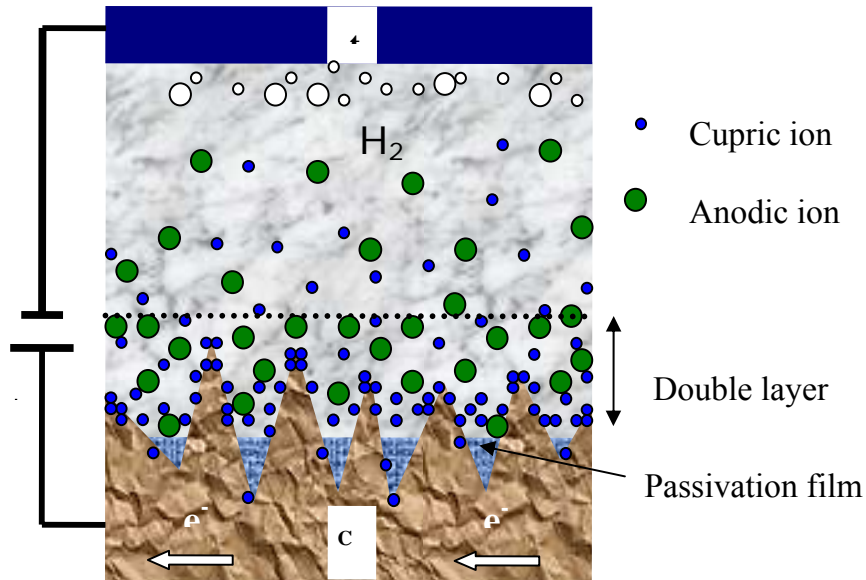


Fig.3-3. Microleveling effect of Cu electropolishing.¹²

3.3 Factors Affecting the Limiting Current on Cu Surface of Electropolishing

Anodic limiting currents play an important role in Cu-EP.^{4, 10, 17} Many researchers reported that EP is a diffusion-controlled process taking place at the limiting current. When the state of current on Cu surface reach limiting current, the diffusion layer becomes saturated with Cu^{2+} then dissolved in electrolyte. Therefore, the value of the limiting current which determines the Cu dissolution rate depends on the rate of mass transfer of Cu ions from the double layer to the bulk of solution. Figure 3-4 depicts the potentialdynamic curve of Cu EP in the 85% H_3PO_4 solution.^{4, 11} In the initial stage, in the AB region, positive polarization induces anodic current that increases with applied potentials. Dissolution in this region is a charge-transfer-controlled reaction and produces a pitting surface. When the potential increases from point B into the BC region, a viscous layer (passivation effect) starts to form on the anodic surface. In this

region, which can be called plateau region, the current becomes insensitive to the applied potentials and where EP usually takes place. In plateau region, a smooth surface could be obtained because the rate-limiting step is mass-transfer controlled. That is to say, the existence of passivity electrode/electrolyte layer is very crucial for attaining electropolishing.^{10-12, 14-16}

Most theories that explain the mechanism of limiting-current plateau, but how the mass-transfer limitation exists still not clear at present. D. Padhi et. al reported that this limiting value depends on the solubility of the dissolving species in the particular electrolyte, the concentration, the temperature and the diffusion coefficient.¹⁰ However, in an acceptor mechanism, it is assumed that the dissolved ions remain adsorbed on the electrode surface until they are complexed by acceptors, which are normally taken to be either anions or water molecules.^{10, 14, 16} The EP rate is controlled by mass transfer of acceptors to the electrode surface.

Du and Suni proposed that limiting current distributed on Cu/electrolyte interface could be affected by the varieties and concentrations of additives in phosphoric-based solution and obtained by using Levich analysis.¹⁴ Meanwhile, the variations of kinematic viscosity of electrolytes are also depended on the varieties of additives. This is an excellent research for analyzing the limiting current under various conditions on Cu surface during Cu-EP.

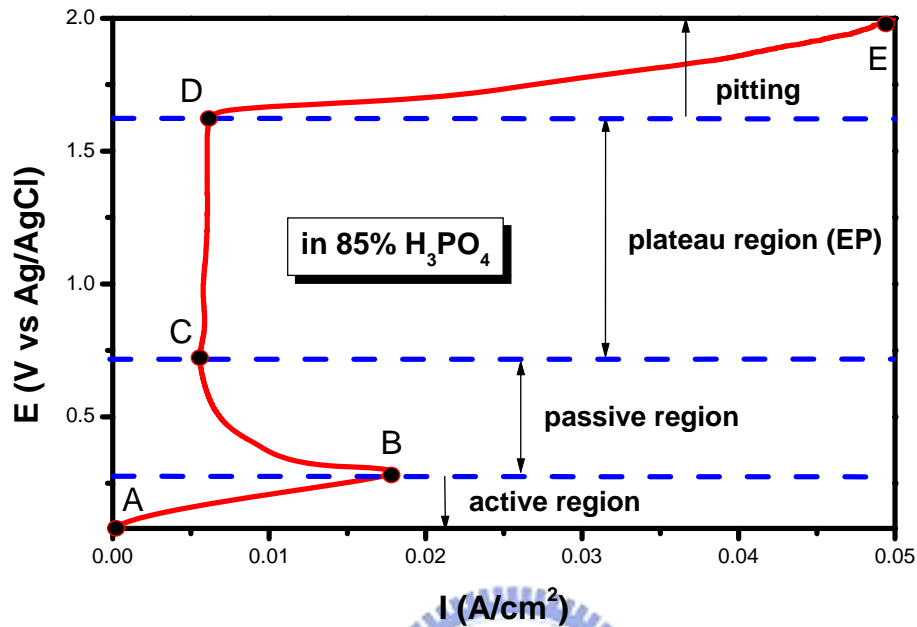


Fig.3-4. Potentialdynamic curve of Cu EP in the 85% (vol.) H_3PO_4 solution.¹¹

3.4 Recent work of Cu Electropolishing Applying in Interconnect

Metallization and Behavior of Chemical Additives in Cu EP

In the applications to multilevel interconnects, Contolini et al. have integrated Cu EP with barrier wet-etching technology to be a novel planarization process.¹⁸⁻¹⁹ For industrial application, Taiwan semiconductor manufactured company (TSMC) has proposed CMP-Free and CMP-Less approaches by integration of Cu EP and Cu contact-plating in 2003.²⁰ On the other hand, SONY company has also demonstrated a 25- μ m-wide feature formed by soft polishing technology.²¹ This soft polishing technology emphasis on the pit-free and low roughness Cu surface. Moreover, the Applied Materials Incorporated showed that efficient Cu EP can be achieved under galvanostatic conditions (constant current between the Cu and counter electrode). That is an crucial information because the effects of changes in current density and rotation

speed of wafer on the extent of planarization could be demonstrated.¹⁰ However, very limited information of Cu EP was reported for damascene processing. In this chapter, the mechanism and application of Cu EP in Cu damascene processing will be discussed.

For academic research, many studies have reported the feasibility of Cu-EP for planarizing Cu in interconnect metallization.^{10-16, 22-23} The effects of applied voltages, pattern size and density on planarization efficiency (PE) of Cu-EP were investigated.¹² It was reported that the initial polishing rate and the formation time of a passivation layer associated with applied voltage were crucial for the PE. The best PE of Cu-EP could be optimized in various sizes of pattern by controlling the applied voltage in the additive-free H₃PO₄, as shown in Fig.3-5 and Fig. 3-6.²²

However, Cu-EP of damascene processing confronts additional challenges in the industrial field, such as end-point detection, uniformity, dishing, residual copper, and etch pits. Therefore, there should be many topics about Cu-EP for researching in damascene process in the near future.

Improving the properties of electrolytes in Cu-EP is the event for this research. Our group also demonstrated a one-additive (organic acid species) EP electrolyte, a so-called superpolishing electrolyte, which can improve the planarization-efficiency (PE) of Cu-EP.¹⁵ This one-additive EP electrolyte provides the functionality of a selective Cu dissolution rate within damascene features. However, the PE of superpolished Cu still depends on the feature size; the best value is about 34% for 50 mm patterns. With reference to two or three-additive electroplating electrolytes,²⁴⁻²⁵ the introduction of different EP functionalities from the various additives is a possible solution. Wetting additives for Cu electroplating, like polyethylene glycols (PEG), alcohols were found to access easily the reacting surfaces in EP.²⁶⁻²⁷ Moreover, the Cu surface viscosity for alcohol-containing electrolytes is higher than for alcohol-free electrolytes.¹⁶ Undoubtedly, the addition of additives into electrolytes can influence the surface chemical reaction and polishing rate. Because Cu dissolution is suppressed by increased solution viscosity near polished interfaces and the reduced solution conductivity, using alcohol-containing EP electrolytes for planarizing damascene features leads to numerous alcohol additives at the damascene bottom, thus passivating that area from EP. These additives are proposed inhibitor, assisted by the superpolishing functionality.

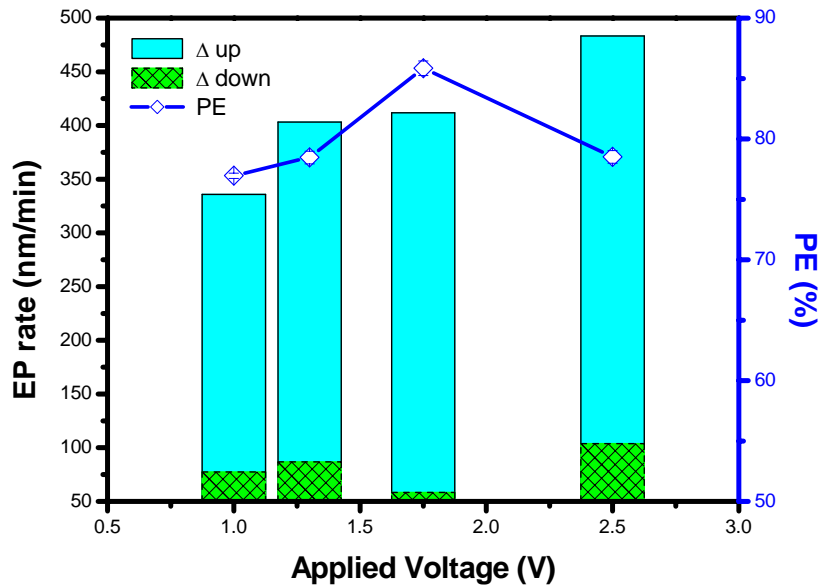


Fig.3-5. Evolutions of PE and EP rates inside and outside of 1- μm -wide trenches at various applied voltages.²³

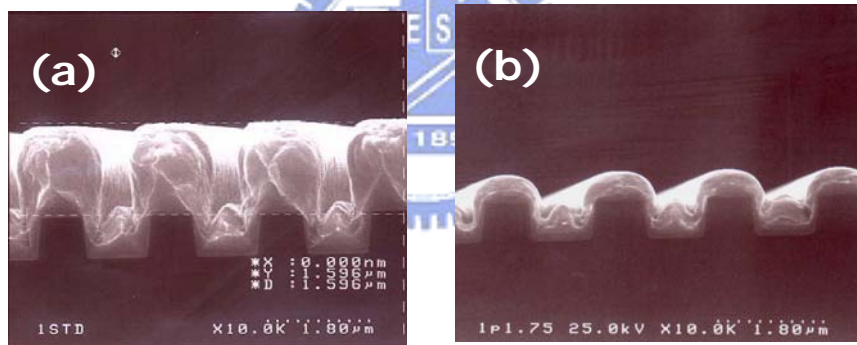


Fig.3-6. SEM cross-sectional profiles: (a) Before EP, (b) After EP at the applied voltage of 1.75 V for 3 min.²²

3.5 Experimental Procedure of Cu Electropolishing

(A) Sample preparation: For Cu electropolishing, a blanket wafer was prepared by depositing a 50-nm sputtered Ta diffusion barrier and a 1.7- μm sputtered or electroplated Cu conduction layer on a SiO_2/Si substrate. The patterned wafer was composed of a 50-nm-thick sputtered-Ta layer as the diffusion barrier and a 1.7- μm -thick sputtered or electroplated-Cu film as the conductive layer, deposited into trenches with various widths

(1-100 μm) and depth of 1 μm .

(B) Apparatus of Cu electropolishing and electroplating: The experiments on Cu electroplating and EP were carried out in a tank of non-conducting material. The counter electrode was a platinum plate with a size of 6 \times 6 cm^2 and the working electrode was a wafer with a size of 2 \times 3 cm^2 . The electropolishing electrolyte was phosphoric acid (~85% H_3PO_4 , purchased from BASF Electronic Materials) and the films were plated and polished at room temperature. For Cu electroplating, contact to the electrode was implemented outside of the electrolyte with an alligator clip. The electrolytes of plating include copper sulfate, sulfuric acid, chloride ions, and filling promoters. Furthermore, the electropolishing rate associated with various electrolytes was measured on Cu blanket wafers. The pH values and conductivities for each electrolytic system during Cu-EP were measured using a pH meter and a conductivity meter while the wafer was polished in-situ.

(C) Electrochemical analyses: All potentiodynamic (PD) and alternating current (AC) impedance electrochemical measurements were carried out on an EG&G potentiostatic/galvanostatic (model 273A) and an EG&G frequency response detector (model 1025A), with a personal computer. PD and AC (Nyquist-plot) polarization curves were employed to analyze electrochemical behavior of Cu EP on Cu surface. During measurement of electrochemical behavior, the counter electrode was platinum and the working electrode was Cu with a constant surface area of 1 cm^2 . This Cu electrode was surrounded by the teflon material. All potentials recorded by computer were reported relative to the Ag/AgCl electrode, which was used as the reference electrode. Besides, in-situ PD and current-time curves were measured by Labview software with a laptop computer.

(D) Measurements of film properties and morphology: Cross-sectional profiles of Cu films before and after EP were examined using a field emission scanning electron microscope (FESEM). Therefore, thickness of Cu removal by Cu-EP can be measured precisely by SEM. Surface roughness was measured using an atomic force microscope (AFM). Moreover, the sheet resistance of polished Cu was measured by the four-point probe technique. In this study, the pH values for each electrolytic system during Cu-EP were measured using a pH meter while the wafer was polished in-situ. Raman

spectroscopy (type: JASCO Ventuno-21), and electron spectroscopy for chemical analysis (ESCA) (type: VG-Micro lab) were adopted to characterize the adsorbed species on polished Cu surface. Furthermore, this study applied contact angle measurement to observe wetting ability of electrolytes with various ratio of useful additives on Cu surface. The contact angle between unpolished Cu surface and various electrolytes results from the balance of liquid/gas or solid, and gas/solid surface tension. The wetting ability of various electrolytes on Cu surface can affect the Cu dissolution rate apparently, and this effect will be discussed in later chapter.

In short, the detail flow chart of all experimental and analytical process is shown in Fig.3-7.

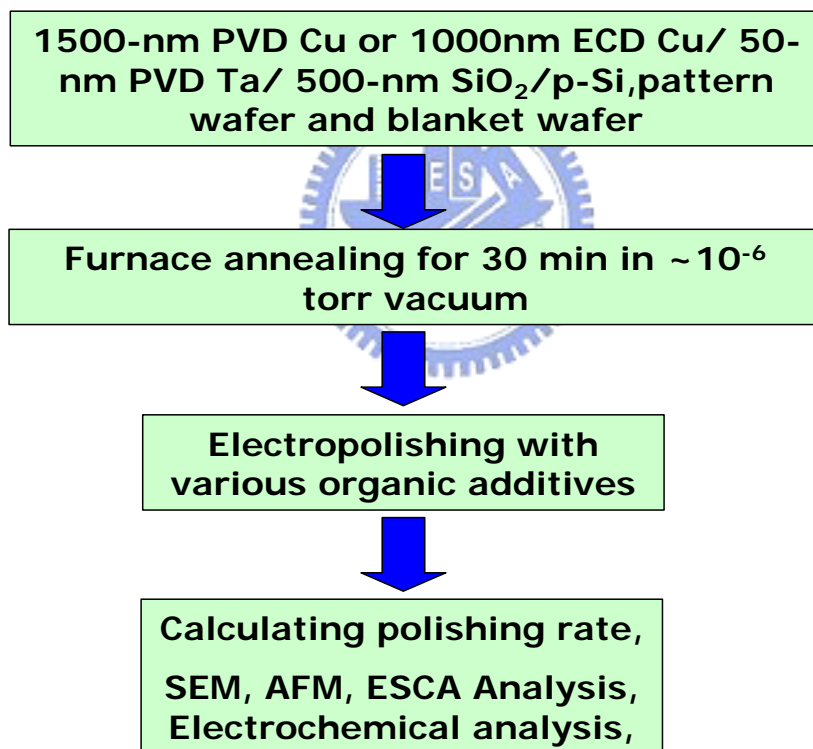


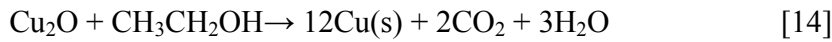
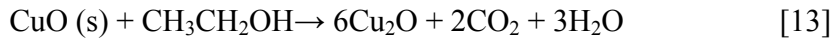
Fig.3-7. Flow chart of Cu-EP experimental process

Chapter 4: Role of Alcohols in Two-Additive System for Cu Damascene Copper Electropolishing

4.1 Superplanarization for Damascene Cu metals

Cross-sectional SEM images in Fig. 4-1 (a) and (b) show 1 μm patterns before, and after EP using one-additive electrolytes (10000ppm acetic acid). This result shows that the one-additive (organic acids) superpolishing electrolytes can form a significant gradient of Cu dissolution rate between the damascene bottom and opening, enabling the elimination of step-height Cu morphologies and thus the planarization of damascene Cu metals. The PE for such an electrolyte can be calculated according to the definition of Ref. 1 and 2, and is plotted in Fig. 4-2. However, pictures Fig. 4-1 (d) and (e) and Fig. 4-1 (g) and (h) reveal that the planarization capability for such electrolytes is pattern-size dependent; and the calculated PE value is below 50% when the trench-size is wider than 2 μm , as depicted in Fig. 4-2. This PE deterioration phenomenon is greatly improved by adding other kinds of additives, alcohols, to the one-additive electrolytes, as shown in pictures Fig. 4-1 (c), (f), and (i). The two-additive electrolyte used herein consists of 10000 ppm acetic acid, and glycerol/ H_3PO_4 = 1/100 (volume ratio). The PE for this two-additive electrolyte retains an extremely high value of 98%, almost independent of pattern size, as revealed in Fig. 4-2. The data in Fig. 4-1 and 4-2 clearly reveal the high effectiveness of two-additive EP electrolytes in planarizing damascene patterns.

Figure 4-3 shows that the EP rate of alcohol-containing one-additive EP electrolytes decreases with the additive concentration. The role of alcohols in two-additive EP electrolytes is thus as an inhibitor and is expected to passivate the damascene bottom from EP or to inhibit Cu dissolution at that area, leading to the improvement of the superpolishing functionality generated by organic acids. In Satta et al.'s report, alcohols which contains OH functional group can be used as the reducing agent to inhibit the formation of Cu oxide, as shown in the equation below.³ Therefore, we assume that this surface reaction by alcohols additives could inhibit Cu oxidation (releasing electron) thus reduce the Cu dissolution rate during electropolishing.



A similar usage is the addition of accelerating agents to form three-additive electroplating electrolytes. Accelerators provide the functionality of increasing the Cu electroplating rate at the damascene bottom even though leveling additives already generate a superfilling action with a capability of selective Cu deposition. It is suggested that the organic can release hydrogen ion (H^+) into the H_3PO_4 electrolyte and increase the acidity and conductivity of the solution. For example, adding citric acid into H_3PO_4 can enhance polishing rate of Cu EP.² On the other hand, acetic acid or Citric acid has usually been employed as a Cu oxide etchant in manufacturing PCB for Cu plating and in metal finishing industries.³⁻⁴ The planarized profile of polished damascene patterns attributes to organic additives in polishing electrolytes and depends on their concentrations. Because of the mass-transfer-limited transportation of organic acid in the electrolyte, the Cu dissolution rate on the outside of features with more organic acid is higher than that on the inside of features with less organic acid. Therefore, a dissolution gradient forms and reduces the step height of features. The proposed “super-polishing” model is shown in Fig 4-4.²

Since the selective Cu dissolution rate within features is difficult to obtain experimentally, alternative methods should be proposed. According to the study of multi-additive electroplating electrolytes,⁵⁻⁶ the change of additive concentrations of EP electrolytes within features is reasonably assumed to be in the range of 5-100 times. The diluted additive concentration is a critical parameter. The valid of test results is based on a proper diluted additive concentration. Therefore, applying electrolytes with various additive concentrations to electropolishing Cu metals and analyzing the associated polishing rates (partial results shown in Fig. 4-3) can extract the Cu removal rate gradient, $(R_{\text{up}}-R_{\text{down}})/R_{\text{up}}$. Herein, R_{up} represents the Cu removal rate at the damascene opening and is obtained with the two-additive EP electrolytes with optimal additive concentrations. Moreover, R_{down} represents the Cu removal rate at the damascene bottom and is obtained with the electrolytes with the diluted additive concentrations. Table II lists the optimal

parameters associated with one-additive or two-additive EP electrolytes. The extracted Cu removal rate gradient for glycerol-containing two-additive EP electrolytes, shown in Fig. 4-5, is actually larger than for acetic acid-containing one-additive EP electrolytes. The inhibition mechanism caused by alcohols, thus responds to the superpolishing functionality in the two-additive electrolyte better than in the one-additive electrolyte, as shown in Fig. 4-1 and 4-2. Comparing the polishing rate and wettability for H_3PO_4 electrolytes containing the different alcohols (glycerol, methanol, and ethanol), is instructive. Measured contact angles for these three alcohol-containing one-additive EP electrolytes show that the glycerol-containing electrolytes with a minimum value of 19.4° , as shown in Fig. 4-6. The results imply that glycerol additives more readily access the reacting interfaces or inhibit the Cu dissolution at the damascene bottom than the other two additives, as shown in Fig. 4-2. Accordingly, the glycerol-containing two-additive EP electrolyte has the highest $(R_{up}-R_{down})/R_{up}$ and the best PE among the three alcohol-containing two-additive electrolytes, as shown in Fig. 4-2 and 4-3.



	Initial pattern	Planarized pattern using one-additive electrolytes	Planarized pattern using two-additive electrolytes
1 μ m pattern	(a)	(b)	(c)
5 μ m pattern	(d)	(e)	(f)
50 μ m pattern	(g)	(h)	(i)

Fig.4-1. Cross-sectional SEM images for 1, 5, and 50 mm damascene patterns filled with electroplating Cu metals before and after electropolishing at 1.75 V using one-additive (acetic acid) and two-additive (acetic acid + glycerol) EP electrolytes.

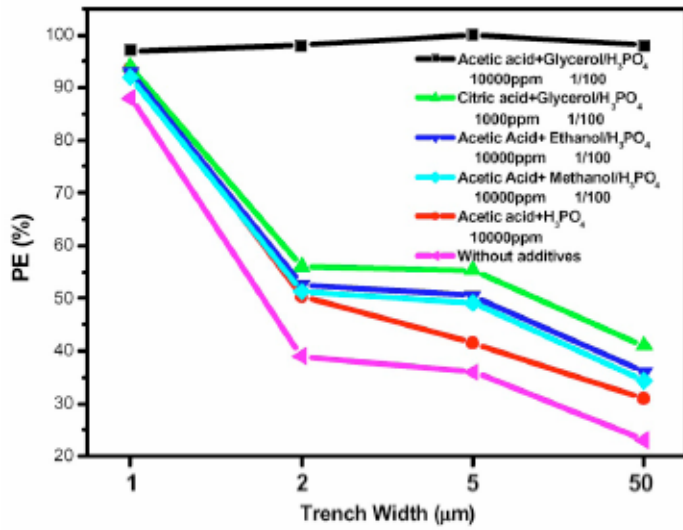


Fig.4-2. PE for additive-free, one-additive (acetic acid), and two-additive (alcohols + acetic or citric acids) as a function of feature size. EP was conducted at 1.75 V. (PE = $[1 - (\Delta_{\text{down}}/\Delta_{\text{up}}) \times 100\%]$, where Δ_{down} , and Δ_{up} are schematically illustrated in Fig. 4-1 (d) and (e). The recipes for the EP electrolytes are listed in Table II.

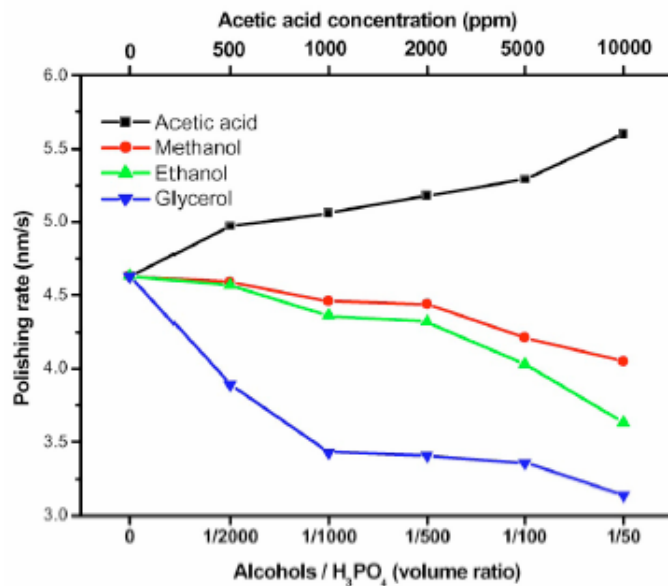


Fig.4-3. Polishing rate for alcohol-containing or acetic acid-containing one-additive EP electrolytes as a function of additive concentrations. EP was conducted at 1.75 V.

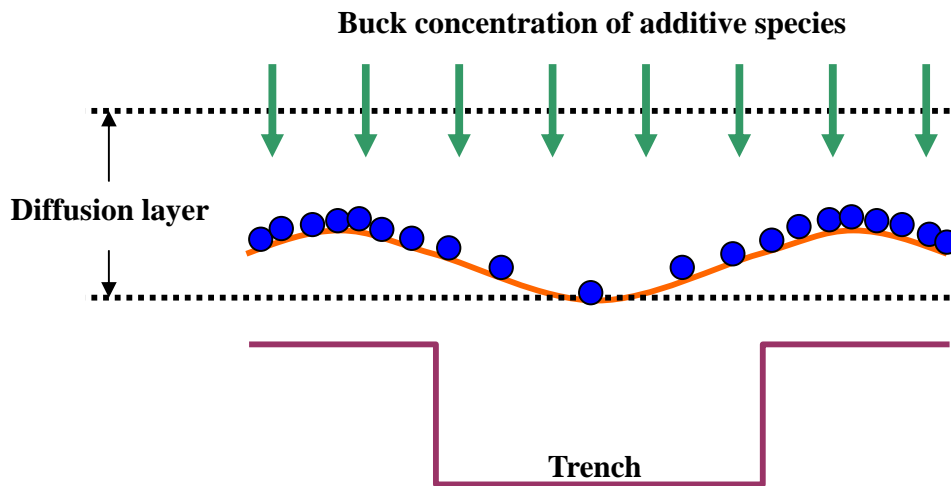


Fig. 4-4. Proposed model of step-reduction mechanism by adding organic acid into H_3PO_4 electrolyte in Cu-EP. ²

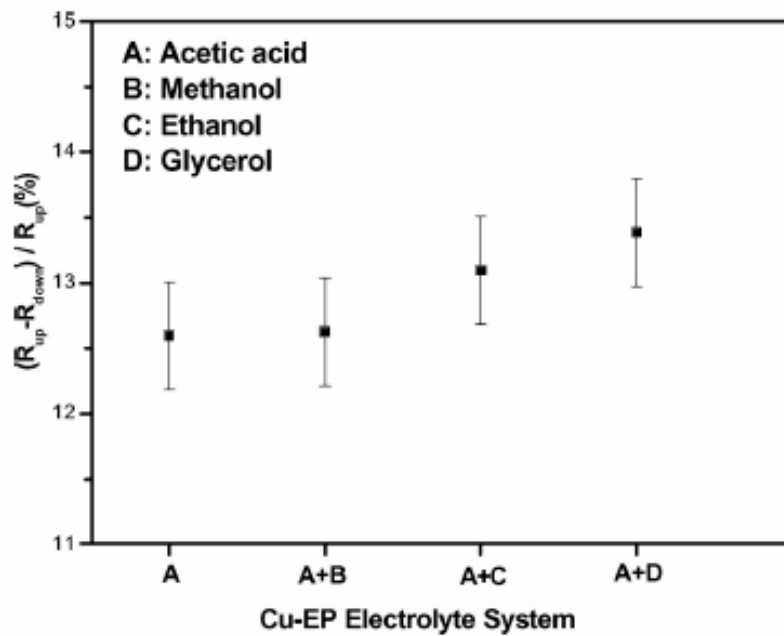
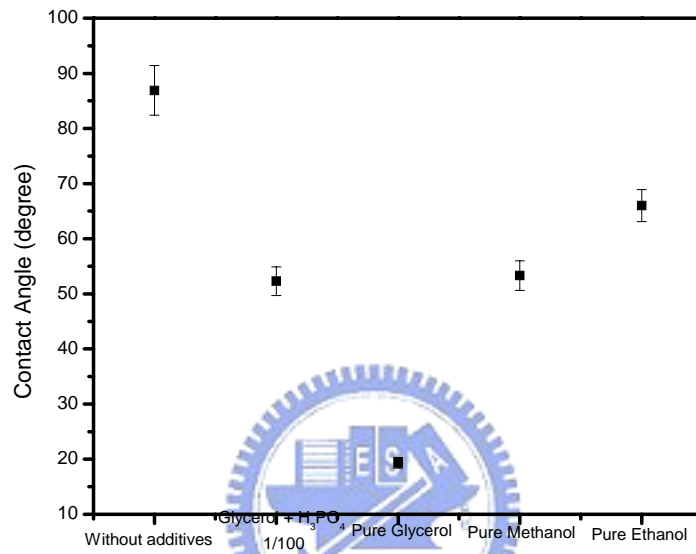


Fig.4-5. The extracted Cu removal rate gradient for two-additive (alcohols + acetic acid), and one-additive (acetic acid) EP electrolytes. EP was conducted at 1.75 V.

(a)



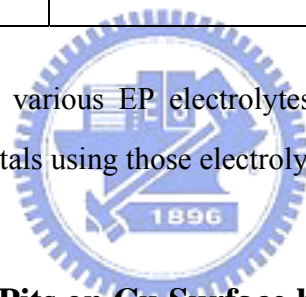
(b)

	H ₃ PO ₄ (additive-free)	H ₃ PO ₄ + Glycerol	Pure glycerol	Pure Methanol	Pure Ethanol
Average contact angle (degree)	86.9	52.3	19.3	53.3	66
OM image					

Fig.4-6. (a) Measured contact angle for pure phosphoric acid, phosphoric acid electrolytes containing pure glycerol, pure glycerol, pure methanol and pure ethanol on Cu substrate. (b) OM image capture form in-situ measurement.

	Without additive	One-additive	Two-additive
Effective concentration range for improvement PE	H₃PO₄: 85%	Acetic acid: 10000~12000ppm Citric acid: 500~1000ppm	Glycerol/H₃PO₄: 1/100~1/500 Methanol/ H₃PO₄: 1/100~1/150 Ethanol/ H₃PO₄: 1/100~1/150 Acetic acid: 10000~12000ppm Citric acid: 500~1000ppm
Optimum resistivity (μΩ-cm)	2.60	2.72	2.76
Optimum mean roughness (nm)	2.20 (initial roughness: 5.3nm)	2.35	0.75

Table II. Optimal recipes for various EP electrolytes with best PE and fundamental performance of polished Cu metals using those electrolytes.



4.2 Reduction of Etching Pits on Cu Surface by Additives

Pitting is a kind of metallic corrosive attack on surface. Once a pit is formed on metal surface, rapid dissolution occurs within this pit while oxygen reduction take place on adjacent surfaces.⁷⁻⁸ The high energy may be involved in the surface defect, which can lead to more serious corrosive reaction. Therefore during Cu EP, oxygen formation causes serious etched pits and uniform etching on the Cu surface. However, the oxygen bubbling is an additional and unavoidable electrochemical reaction of Cu-EP on anodic surface.^{7,9} The pits may degrade the electrical reliability for the subsequent processes.¹⁴⁻¹⁶ Many investigators added several kinds of additives into H₃PO₄-based electrolyte to reduce the effect of surface defect after Cu-EP such as Polyethylene glycol (PEG) and sulfuric acid.^{2,10} In general, the adsorption of PEG on Cu surface can block the oxygen attack during Cu-EP and addition of sulfuric acid can increase the over-potential of oxygen formation. However, PEG and sulfuric additives can not achieve high

planarization efficiency and low defects on polished Cu interconnect concurrently. Figure 4-7 shows AFM images of Cu surfaces that have been polished by additive-free, one-additive (acetic acid), and two-additive electrolytes, respectively. A pit-free surface of polished Cu was observed using the two-additive EP electrolytes with alcohol/phosphoric acid volume ratios ranging from 0.1 to 1%. Moreover, we demonstrate a useful additive system that can enhance the planarization efficiency of Cu-EP and produce a pit-free surface finally.

Two possible mechanisms for reducing etching pits are proposed: (I) the added alcohols acting as inhibitors (or wetting agents) reduce the Cu removal rate or even form a passivation layer on the reacting surfaces. Both reactions alleviate the generation of crevices or pitting on the polished Cu surfaces. (II) Because alcohols are reducing agents in Cu surface treatments,³ the oxidation of alcohol accompanies the release of electrons in electrolytes during EP. Therefore, oxygen reduction on Cu surfaces can react with the electrons released from the alcohol oxidation reaction instead of from the Cu ionization reaction.⁸ Consequently, the dissolution rate of Cu metal in a local area is retarded.

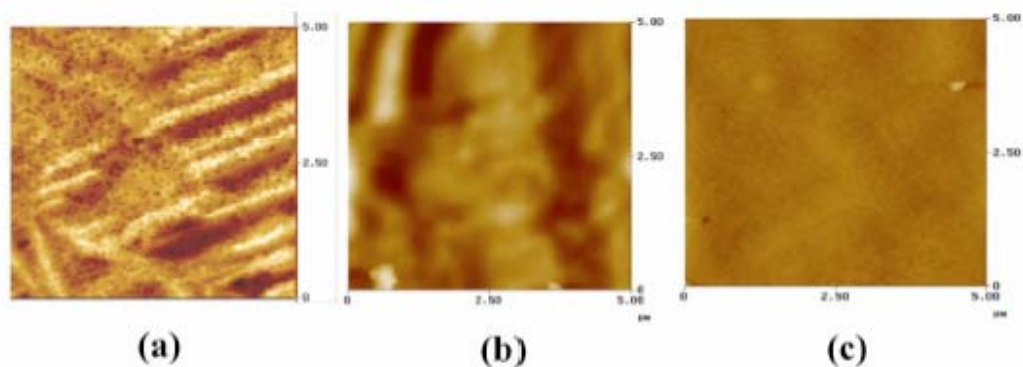


Fig.4-7. AFM images of Cu surfaces polished at 2.0 V using (a) additive-free, (b) one-additive (acetic acid), (c) and two-additive (glycerol + acetic acid) EP electrolytes. The recipes for the EP electrolytes are listed in Table II .

Chapter 5 Role of Organic Acids in Two-additive System for Cu Damascene Copper Electropolishing

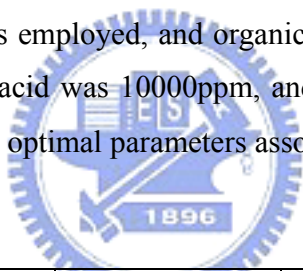
5.1 Introduction of Accelerator and Inhibitor in Cu Electropolishing

As mentioned previously, the electropolishing rate of Cu metals mainly depends on the acidity of the solution¹⁻², and the resistance of the viscous layer³⁻⁴. Accordingly, the introduction of additives, whose chemistries can modulate the properties of acidity of electrolyte and surface viscosity, has been demonstrated to enhance the rate of Cu removal within the damascene features¹. As shown in previous report, two additives can be utilized to promote the planarization-efficiency (PE) of damascene Cu metallization². One is an organic acid accelerator, which increase the acidity of the solution, and thus the EP rate¹. Another is an organic alcohol inhibitor, which increases the viscosity of the solution and thus inhibits the dissolution of Cu². Although an increase of electrolyte acidity typically enhances the dissolution of Cu, in some cases, it also enlarges the resistance of the passivation layers⁵, which change actually inhibits the removal of Cu. This conflict is consistent with the observation that the PE values of various one-additive (organic acids) EP electrolytes almost saturate at a similar levels, despite a difference of one order of magnitude among the concentrations of the optimal additives. Of course, the saturation of PE is attributable partially to the limitation of additive hydrolysis in phosphoric acids. Furthermore, for two-additive (alcohol + organic acid) EP electrolytes, an esterification⁶ reaction is likely to occur between alcohols and organic acids. This reaction not only changes the concentration of the additives but also generates new constituents within the polished interfaces. Accordingly, the additive-related EP mechanisms that are involved in the electropolishing of damascene features and the optimization of associated recipes are of considerable interest.

5.2 Results and Discussions

Cross-sectional SEM images in Fig. 5-1 (a-e) display patterns with widths of 50 μ m

before and after EP, using four glycerol-containing two-additive electrolytes, which contain different accelerators in the form of acetic, citric, citrazinic and benzoic acids. For comparison, additive-free electrolytes are also used. The results demonstrate that the acetic acid-containing electrolytes can more efficiently form a gradient in the Cu dissolution rate between the bottom and opening of damascene than can other acid-based electrolytes. A PE value^{1, 4, 7} index of the planarization capacity of electrolytes is calculated from the changes in the step-height of the morphologies. The PE value of those electrolytes for various feature sizes, as presented on Fig. 5-2, also reveal that acetic acid outperforms other organic acids in the planarization of damascene Cu metals. In the calculation of the PE values of 50 μ m-wide features, the measured residual Cu thicknesses outside the features and inside the feature at 5, 10 and 25 μ m away from the edges of the features, yielded the error bars on the PE values; the averages of these values were also shown. For the additive-containing electrolytes, a constant volume glycerol/H₃PO₄ ratio of 1/100 is employed, and organic acids are added to optimize PE; the concentration of the acetic acid was 10000ppm, and that of the other acid additives was 1000ppm. Table III lists the optimal parameters associated with those electrolytes.



Basic	H ₃ PO ₄ (85%)	H ₃ PO ₄ (85%)	H ₃ PO ₄ (85%)	H ₃ PO ₄ (85%)
Additive I : organic acids	Acetic acid 10000ppm	Citric acid 1000ppm	Citrazinic acid 1000ppm	Benzoic acid 1000ppm
Additive II : glycerol	1/100 (volume ratio to H ₃ PO ₄)	1/100	1/100	1/100

Table III: Optimal parameters associated with two-additive electrolytes in this study.

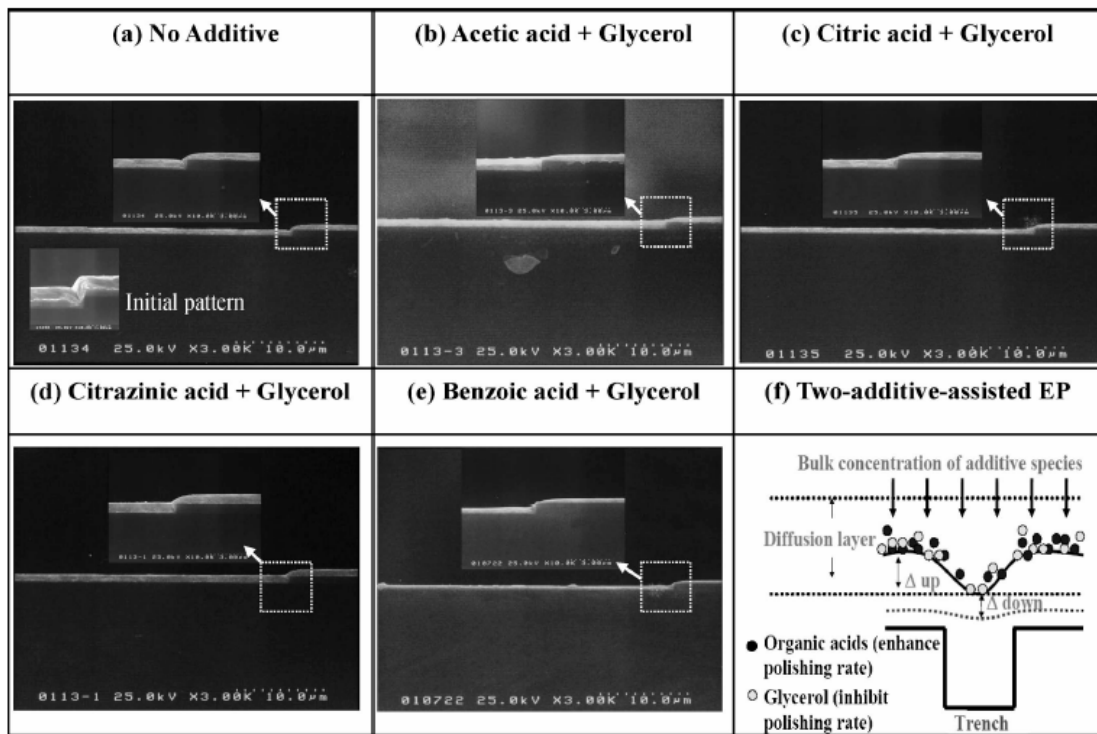


Fig.5-1. Cross-sectional SEM images for 50 μm damascene patterns filled with electroplating Cu metals before and after electropolishing at 1.75 V using (a) additive-free and (b)–(e) four two-additive (various organic acids + glycerol) EP electrolytes. (f) A schematic illustration of two-additive-assisted EP within damascene features shown.

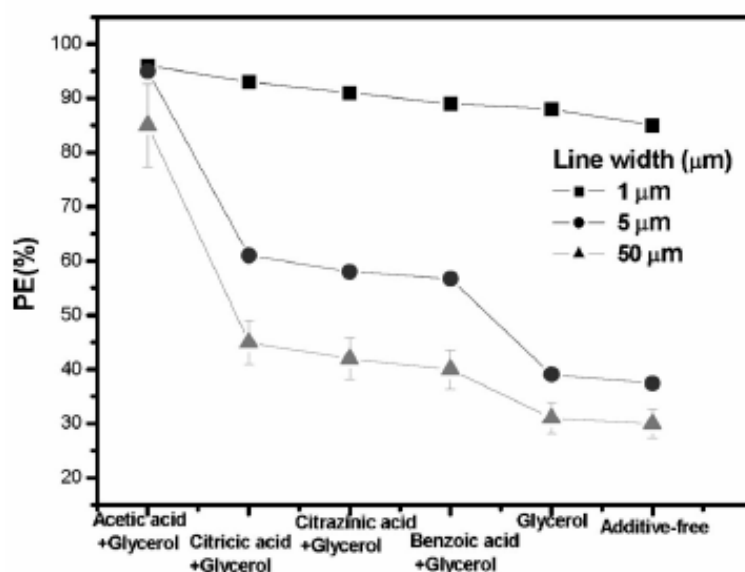


Fig.5-2. PE for additive-free, one-additive (glycerol), and four two-additive (glycerol + various organic acids) EP electrolytes as a function of feature size. EP was conducted at 1.75 V.

Comparing the Cu removal rates associated with four two-additive electrolytes at the bottom and opening of the feature for 1 and 50μm-wide patterns, shows that the EP rate at the damascene bottom (in the middle of the feature) depends on the organic acid species and changes by 1.5 to 5 times of magnitude; at the feature opening, the rate varies by only 20 %, as shown in Figs. 5-3 (a) and (b). With reference to the glycerol-containing one-additive electrolyte¹, all organic acids, except acetic acids, considerably reduced the glycerol-induced inhibition of the removal of Cu at the damascene bottom. Therefore, the difference between the PE of these two-additive electrolytes is closely related to the change in the alcohol-related inhibition of Cu removal rate at the feature bottom in the presence of various organic acids.

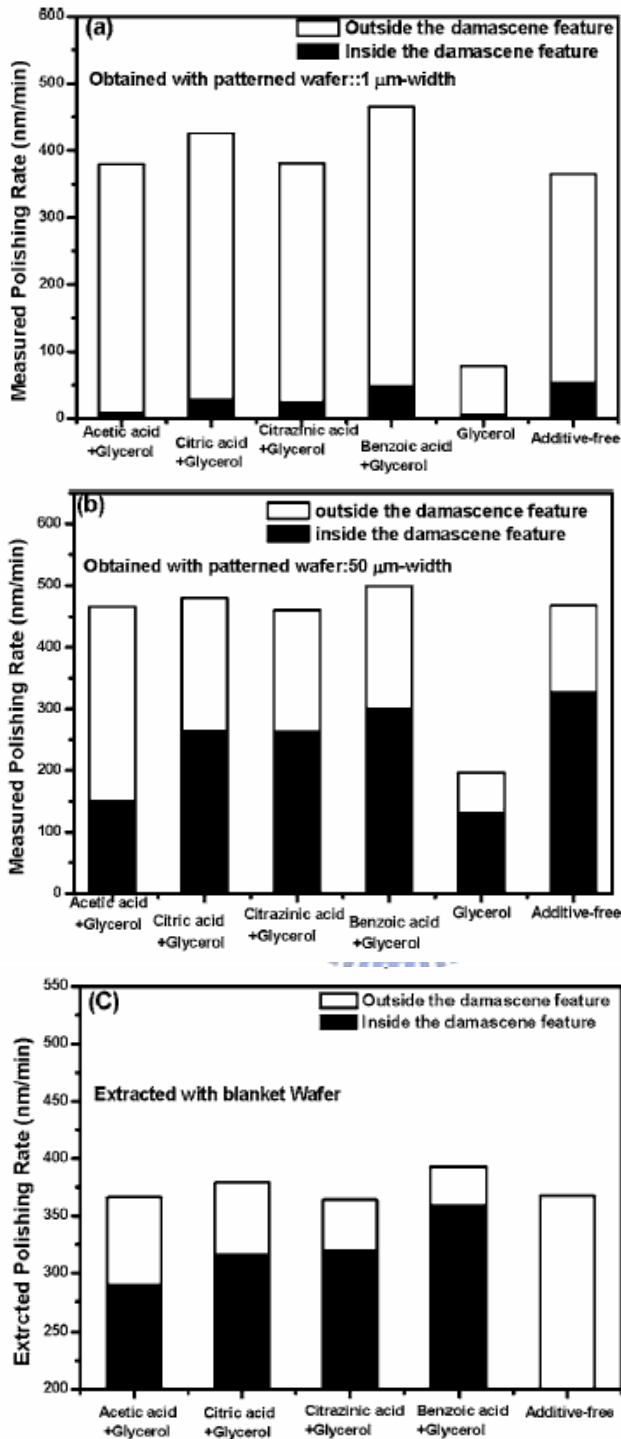


Fig.5-3. Polishing rates outside and inside the features for four two-additive, glycerol-containing one-additive and additive-free. EP electrolytes: (a) obtained with 1 μm width patterned substrates; (b) obtained with 50 μm width patterned substrates; and (c) extracted with blanket substrates. EP was conducted at 1.75 V.

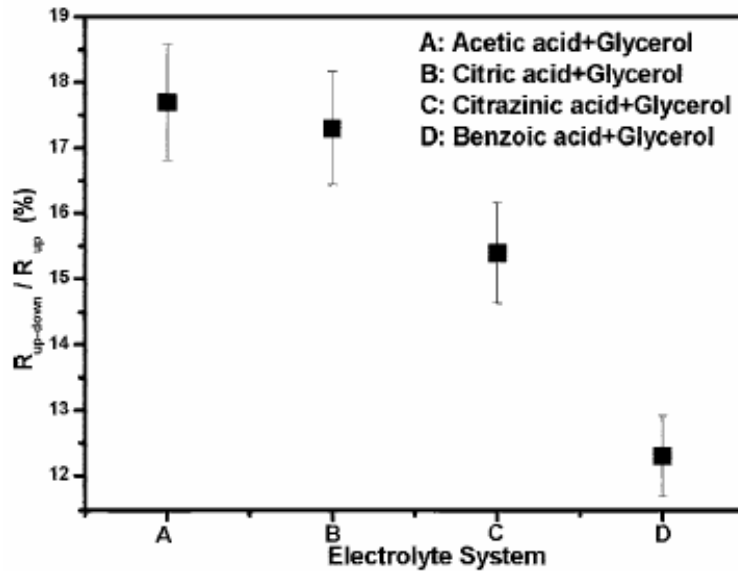


Fig.5-4. The extracted Cu removal rate gradient for four two-additive EP electrolytes. EP was conducted at 1.75 V.

Alcohol inhibitors suppress the removal of Cu by increasing surface viscosity⁸ whereas organic acids promote the removal of Cu by increasing the acidity of solutions¹⁻². However, if an elemental esterification reaction occurs between these two additives during EP, then the concentration of the additives changes and the new constituents are formed in solution, and then in the interacting interfaces. Both factors probably influence Cu planarization. The selective Cu dissolution rate, the acidity, the resistance of the passivation layer and even the interfacial compositions within features cannot be easily determined experimentally, so alternative approaches should be developed. Our previous work stated that electrolytes with additives can be used at various concentrations to electropolish Cu metals, and the associated polishing rates are analyzed to determine the gradient of the Cu removal rate^{2,9}, $(R_{\text{up}}-R_{\text{down}})/R_{\text{up}}$. Herein, R_{up} represents the Cu removal rate at the damascene opening and is obtained using two-additive EP electrolytes with additives at optimal concentrations. R_{down} represents the Cu removal rate at the damascene bottom and is obtained using electrolytes with diluted additives. This method predicts Cu removal rates within the features and $(R_{\text{up}}-R_{\text{down}})/R_{\text{up}}$ for four organic

acid-containing two-additive electrolytes, as shown in Figs. 5-3 (c) and 5-4. The trend concluded from these extracted values agrees closely with those in Figs. 5-1-2 and 5-3 (a)-(b). Notably, the error bars displayed in Fig. 5-4 and later figures represent the data concerning electrolytes with variously diluted additives. Hence, within the damascene features, the chemistry of the electrolytes, the EP properties and the compositions of polished Cu surfaces could be evaluated.

In maximizing the PE of the two-additive electrolytes, the measured solution acidities around the damascene opening, as shown in Fig. 5-5 (a), appear to fluctuate around $\text{pH} \sim 0.62$. Basically, an insufficiency of additives results in the small modulation of the Cu removal rate within the features, whereas an excessive additive concentration^{1, 10} fails to form a mass-transport-controlled distribution of additives. Both conditions degrade the organic acid-enhanced PE, which fact explains the small observed change in optimal pH values in response to organic acid, as presented in Fig. 5-5 (a).

Another important EP parameter of these electrolytes, the resistance of the passivation layer within the reacting interfaces, is also measured by Nyquist plots, as displayed on Fig. 5-6 and summarized in Fig. 5-5 (b). An additive-free electrolyte with a higher acidity has a larger viscous resistance¹¹ just adding sulfuric acid to H_3PO_4 electrolytes increases the viscous resistance. Accordingly, on the feature opening, even though the acidity-related EP rate for the additive-free electrolyte is expected exceed that for the two-additive electrolytes, the fact that the real polishing rate of the former electrolyte is lower is reasonably attributed to the inhibition of the removal of Cu by viscous layers. The situation is different when four two-additive solutions are involved. The extracted viscous resistances around the feature opening, as shown in Fig. 5-5 (b), monotonically increase from 80 to 140 Ω , even though the two-additive solutions exhibit similar bulk acidities. The data displayed in Figs. 5-3 and 5-5 indicates that at the opening of the feature, the solution acidity is determined to dominate the removal of Cu, but the acidity of the solution and the removal rate of Cu differs slightly because of the modulation of viscous layers.

The EP properties at the feature bottom are investigated by diluting the additive. The extracted acidity for all two-additive electrolytes decreases from $\text{pH} \sim 0.62$ at the

feature opening to $\text{pH} \sim -0.5$ at the feature bottom, as presented in Fig. 5-5 (a). Moreover, different organic acid species correspond to a wide distribution of local acidities (pH of -0.5 to -0.35) at the feature bottom, rather than an almost constant value at the feature opening. A less acidic electrolyte results in greater viscous resistance for a passivation film, as determined in relation to four local two-additive electrolytes at the feature bottom. A similar observation is also made by comparing local electrolyte systems at the opening and bottom of the feature. This pH -dependent viscous resistance obviously differs from the increase in the viscous resistance due to acidity, exhibited by sulfuric acid-diluted electrolytes that contain no organic additives⁵. Both pH variance and such a pH -dependent viscous resistance within the features cannot be simply attributed to the additive distributions, based on the transport-limited law^{1, 8, 10}.

Before the real causes of the interesting organic additive-assisted EP properties can be examined, an attempt is made to correlate the acidity with the viscous resistance to the removal of Cu or the planarization efficiency. Outside the damascene feature, the measured acidity and the related EP rate is almost the same for all electrolytes. Inside the damascene feature, two additives in one electrolyte not only reduce the acidity of the solution but also increase the resistance of the interacting surfaces, both of which enhance the inhibition of Cu removal. At the bottom of the feature, the acetic acid-containing two-additive electrolyte has the lowest acidity but the highest viscous resistance of all of the electrolytes, so the corresponding EP rate is least. It therefore has the best PE.

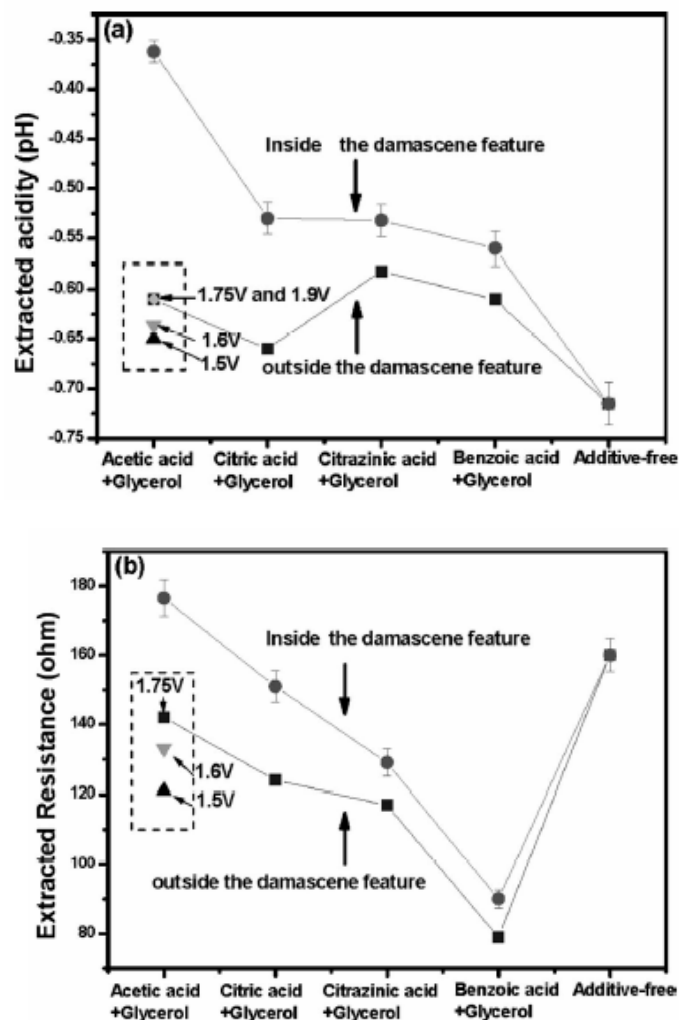


Fig.5-5. (a): Extracted acidity, and (b) extracted viscous layer resistance (calculated from Nyquist plots shown in Fig. 5-6) outside and inside the features for four two-additive, and additive-free EP electrolytes. EP was conducted at 1.75 V. For evaluating the impact of applied voltage on esterification, EP using acetic acid-containing two-additive electrolytes was also conducted at 1.5, 1.6, and 1.9 V, respectively.

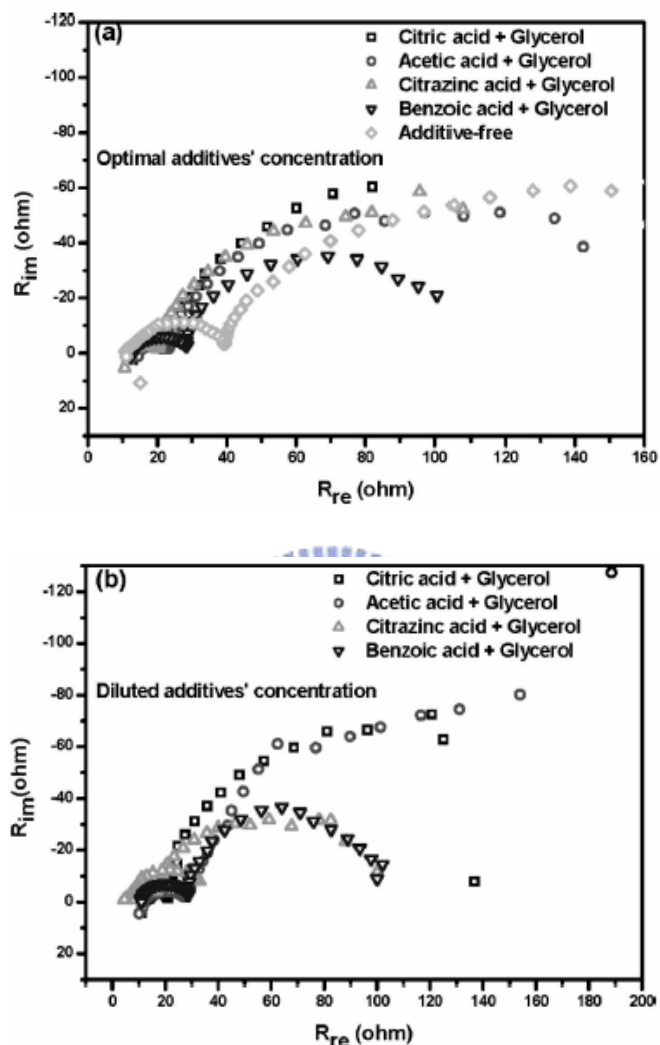


Fig.5-6. Nyquist plots for four two-additive EP electrolytes using (a) optimal, and (b) diluted additive concentrations. For comparison, the plot for additive-free electrolytes was also shown. EP was conducted at 1.75 V.

The esterification between alcohols and organic acids is an essential organic chemical reaction⁶. This reaction probably occurs in the two-additive-assisted EP experiments performed herein. It generates new species in solutions, interacting interfaces and even polished Cu surfaces, so surface material analyses are conducted to elucidate the

mechanisms. Figure 5-7 displays XPS spectra of carbon (1s) for Cu surfaces polished using these two-additive and additive-free electrolytes. Comparing all spectra reveals that the C-O peak is present only in spectra obtained using two-additive electrolytes, rather than using the additive-free electrolyte. Furthermore, a shift in the binding energy for the benzoic acid-containing two-additive electrolyte is observed. Such results suggest the adsorption of organic constituents (including ester-related by-products) on Cu metals polished with organic additive-containing solutions. High-resolution chemical composition analyses using Raman spectroscopy were performed to characterize the adsorbed species in polished Cu, as shown in Fig. 5-8. Later, EP electrolytes with diluted additives are adopted to explore esterification at the bottom of damascene.

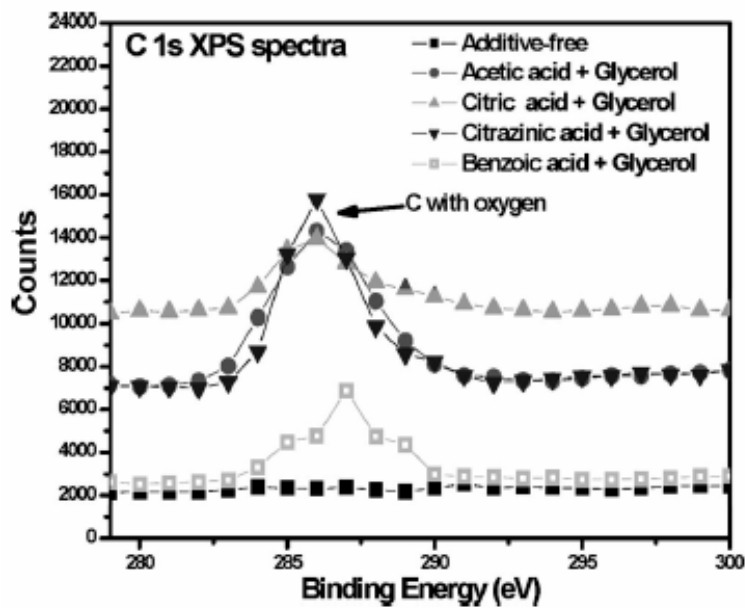


Fig.5-7. XPS spectra for Cu metals polished using four two-additive, and additive-free EP electrolytes.

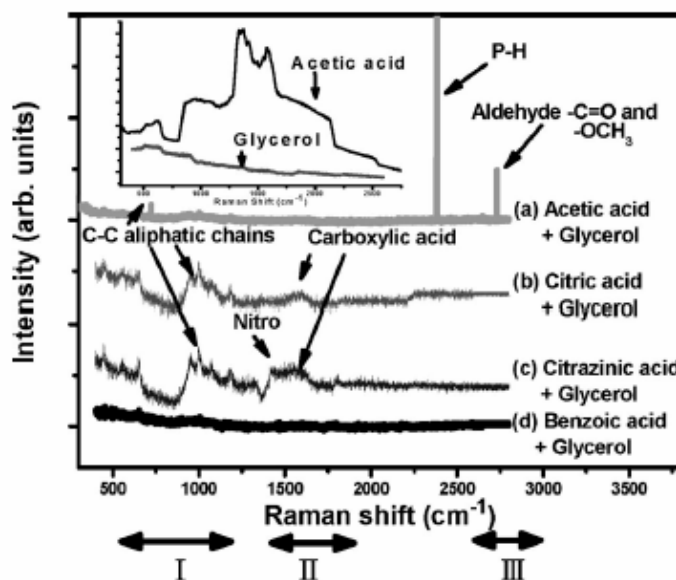


Fig.5-8. Raman spectra for Cu metals polished using four two-additive EP electrolytes that comprise diluted additives with concentrations that are 10 times less than the optimal additive concentrations. The inset shows the spectra associated with glycerol-containing, and acetic acid-containing one-additive EP electrolytes.

These Raman spectra are divided into three bands associated with the chemical compositions of carbon aliphatic chains ($500-1200\text{ cm}^{-1}$), carboxylic acids ($1500-1650\text{ cm}^{-1}$), aldehyde -C=O and -OCH_3 bonds ($2700-2850\text{ cm}^{-1}$)¹¹. In the inset in Fig. 5-8, the Raman spectrum of glycerol-containing one-additive electrolytes includes only the signal associated with the bonds of carbon aliphatic chains ($500-1200\text{ cm}^{-1}$) whereas that for acetic acid-containing one-additive electrolytes includes only the Raman signal associated with the bonds of the carboxylate salt and the carboxylic acids ($1300-1700\text{ cm}^{-1}$). Both cases indicate no aldehyde-related bonds. However, the Raman spectra for two-additive electrolytes reveal an aldehyde-related bond. Esterification⁶ between alcohols and organic acids is described by the following formula:



The symbol “R” represents the group of alkane such as -CH_3 .

Ester contains -C=O and a -OCH_3 bonds (aldehyde-related bonds), so esterification occurs during two-additive-assisted EP. The Raman signal strengths, related to

aldehyde-related bonds, exhibit a trend associated with viscous resistances¹¹⁻¹². Of four two-additive electrolytes, the acetic acid-containing two-additive electrolytes exhibit the greatest viscous resistance and strongest Raman intensity associated with aldehyde-related bonds. Therefore, the viscous resistance increases with the degree of esterification. The signal from the P-H bond (2400 cm^{-1}) in the spectrum from the acetic acid-containing two-additive electrolytes further shows that the strong ester-containing passivation film efficiently traps phosphoric acids, reducing electropolishing at the damascene bottom. Notably, for benzoic acid-containing two-additive electrolytes, the absence of a observable signal throughout the spectrum reveals negligible adsorption, indicating fast Cu removal throughout the features, as confirmed by the data presented in Figs. 5-3 (a) and (b).

During esterification, accompanying consumption of organic acids may reduce local acidity, which effect becomes evident when intense esterification occurs or when a few additives are present at the feature bottom. The most intense esterification and highest viscous resistance are observed when acetic acid is used as the additives, markedly reducing the related acidity at the damascene bottom. For the citrazinic acid-based solution, the Raman spectra show a nitrogen-related composition, presumably because of the chemistry of this organic acid. The nitrogen-related species slightly retards the dissolution of Cu throughout the feature, increasing the PE value to close to that obtained using the citric acid-based solution. The latter solution exhibits higher bulk acidity and a more intense esterification reaction than the former solution.

The proposed esterification successfully explains the two-additive-related EP characteristics. However, what causes the difference between the degree of esterification among the electrolytes that containing various organic acids? Among four two-additive electrolytes, the concentration of the weak acidic acetic acids is the highest, 10000 ppm, being one order of magnitude greater than that of other accelerators. Essentially, the number of acetic acid additives allows them to react more easily than other accelerators with alcohols. It thus fairly predicts the difference in PE values in response to organic acid species. Efforts must be made to evaluate more additive species to study the additive-assisted EP mechanisms and optimize multi-additive-containing EP electrolytes.

Cu electropolishing is normally carried out at an applied voltage of 1.3-2.0 V in the “plateau region”^{7, 13}, so the impact of the applied voltage on the determined acidity and viscous layer resistance was evaluated by EP at 1.5V, 1.6V, 1.75V and 1.9V (Figs. 5-5 (a-b)). As the applied voltage increases, for acetic acid-containing two-additive electrolytes, the acidity decreases moderately but the viscous resistance rises. Hence, esterification increases with the applied voltage in the plateau region. Additionally, increasing the applied voltage can overcome the heightened electropolishing barrier associated with esterification-induced viscous resistance. However, further increasing the applied voltage to ~1.9 V initiates oxygen evolution⁵, detrimentally affecting the passivation of the viscous layer with quite low resistance. Therefore, an applied voltage of 1.75 V is favorable in additive-assisted electropolishing.

We speculate that the reduction of a local acidity may be due to the enhancement of esterification with higher applied voltage and more consumption of acetic acids in this reaction on Cu surface. Furthermore, during Cu-EP in plateau region, esterification may be assisted because the viscous resistance also increased with the rise of applied voltage on Cu surface, as shown in Fig.5-5 (b). Once an ester-containing dense passivation film was formed on Cu anode/electrolyte interface, it needed more voltage to overcome the barrier height of Cu-EP. We assumed that more esterification needed more voltage to carry out polishing, but more voltage enhanced more esterification on Cu surface during Cu EP. On the other hand, if the applied voltage was closed to breakdown voltage (about 1.9 V), the oxygen evolution may be occurred and damaged the passivation of viscous layer and esterification, so that the viscous resistance can not be easily measured by electrochemical method (the second semi-circle of Nyquist-plot could not be formed).

Chapter 6: Integration of Electroplating and Electropolishing of Cu Damascene Process: Dual-mode Cu Plating

6.1 Motivation of Dual-Mode Cu plating

An effective technology containing two functions of Cu film depositing and polishing in one-step electrochemical process in one tank has been developed, and it will save many risks and cost at the back end of the interconnect fabrication. Integration of electroplating and electropolishing in sub-millimeter dimension has attracted many attentions recently for its unique processing characteristics. It is thus highly expected to find applications in areas other than semiconductor manufacturing. For example, the deposition and planarization of metal is critical in fabricating metallic photonic crystals. The metallic photonic crystal is an artificial structure composed of metallic components arranged in periodic three-dimensional array in which certain frequencies of electromagnetic waves are forbidden to transverse through the structure. Currently, it is prepared using well-established VLSI technologies in which interpenetrating layers of metal are assembled by precise patterning, deposition, and etching. It is understood that the homogeneity and surface roughness of the metal layers determine its photonic bandgap characteristics¹. Therefore, by employing electroplating and electroplating simultaneously, it is likely to achieve highly uniform metallic structure for improved photonic frequency response. We plan to follow the methodology of Shawn Lin and Jim Fleming to fabricate desirable metallodielectric structure.¹ In addition, by adjusting the structural arrangement, we are able to tune the photonic stopband to tailored end application. Our ultimate goal is to build a highly efficient solar cell for commercial application.

In particular, it is interested in the deposition capability and film uniformity for high aspect ratio trench by using Dual-Mode plating. For long term, after further development of electrode materials and chemical formulations, we hope to prepare metallic photonic crystal or highly-planarization metal surface on silicon wafer with specific structure.

6.2 Experimental set up of Dual-Mode plating

This promising method, which can be called Cu dual-mode electroplating, integrates the process of electroplating and electropolishing in one tank by alternating the program of controlled computer and exchanging the electrode during electrochemical process. All the equipment of dual-mode process is similar to Cu ECD process, but only one different point is the controlling program in computer. Figure 6-1 shows schematic diagram of experimental set up of dual-mode plating. The Cu deposition was occurred when the sliced wafer was set for cathode during that period of time. When the wafer electrode was switched to anode by computer, the Cu dissolution similar to electropolishing was also occurred. The whole dual-mode plating process consisted of the alternative switching these two electrodes. The testing conditions of dual-mode plating should be pulse-time and cycles, various concentrations and types of organic additives, phosphoric acid. Therefore, the concentration of H_3PO_4 in dual-mode electrolyte can affect the removal rate of Cu in Dual-mode dramatically.

6.3 Results and Discussions

Dual-mode Plating entails switching of current polarity in copper electroplating bath to achieve smooth and uniform deposition of copper for integrated circuit manufacturing. With precise control of each polarity, it is possible to achieve both electroplating and electropolishing in a single electrochemical bath. Figure 6-2 depicts a typical in-situ record of potential and current as a function of processing time during dual-mode plating. The electrochemical information near electrode may be speculated in the form of current densities and voltage on wafer surface. In order to prepare copper solution for both electroplating and electropolishing functionalities, phosphate acid is added to typical electroplating solution to promote Cu planarization. So far, in limited time we have produced impressive results in this area. However, the novel electrolyte in this study consists of phosphoric acid and other organic additives with appropriate concentration and standard Cu electroplating solutions.

For example, we have identified chemical additives and processing parameters in dual-mode plating. By mixing inhibitors, leveler, and phosphoric acid with standard copper electroplating solution, we are able to obtain similar planarization and pore-filling

performance in narrow trenches (350nm) to those of standard electroplating solution with identical processing time. Figure 6-3 illustrates preliminary result of phosphate acid amount on the conductivity of the resultant copper film. As shown in the figure, the electrical conductivity of copper increases gradually with the increment in phosphate acid concentration. It is reasonable, because the phosphorous in electrolyte can be adsorbed on Cu surface during dual-mode plating.

The concentration of H_3PO_4 in electrolyte for Cu dual-mode plating is a critical value for achieving smoother surface. In Fig.6-4, at the same pulse condition after dual-mode plating, the surface morphology will be very different in electrolytes containing different amount of H_3PO_4 . If the amount of H_3PO_4 in electrolyte excess one threshold value, Cu will be etch away very fast after dual-mode plating. The optimum volume ratio range of H_3PO_4 in dual-mode plating electrolytes should be 1/30~1/50.

Figure 6-5 displays the filling capability of dual-mode plating as a function of various benefit organic additives with their optimized concentration and pulse-frequency. Apparently, the step-height reduction and surface smoothing can be achieved for small feature size after dual-mode by tuning the optimized chemical additive concentration with the suitable pulse-frequency. On the other hand, it is crucial to investigate the optimization of pulse-frequency and plating time. Figure 6-6 shows the filling capability of dual-mode plating as a function of various tuning pulse-time and frequency with the optimized chemical conditions.

However, for wide trenches (greater than $10\ \mu\text{m}$), it needs enhancing the step-height reduction, with proprietary processing parameters, we are able to achieve 10% of step-height reduction with yield over 60% in 50 and $100\ \mu\text{m}$ trenches, as shown in Fig.6-7. We select the optimized chemical parameters with various pulse-time conditions to obtain step-height reduction after dual-mode plating.

Finally, a high planar Cu surface and profile, Cu films with high filling capability in small trench width and step-height reduction in various pattern sizes ($1\text{-}50\ \mu\text{m}$) were obtained after Cu Dual-Mode plating. These benefit functions of Cu dual-mode plating depend on the precise collocation of various conditions as discussed above. However, the detail electrochemical mechanisms of Cu dual-mode plating which can obtain smooth surface, superior filling capability for high-aspect ratio trench and step-height reduction

for wide trench needs further studies.

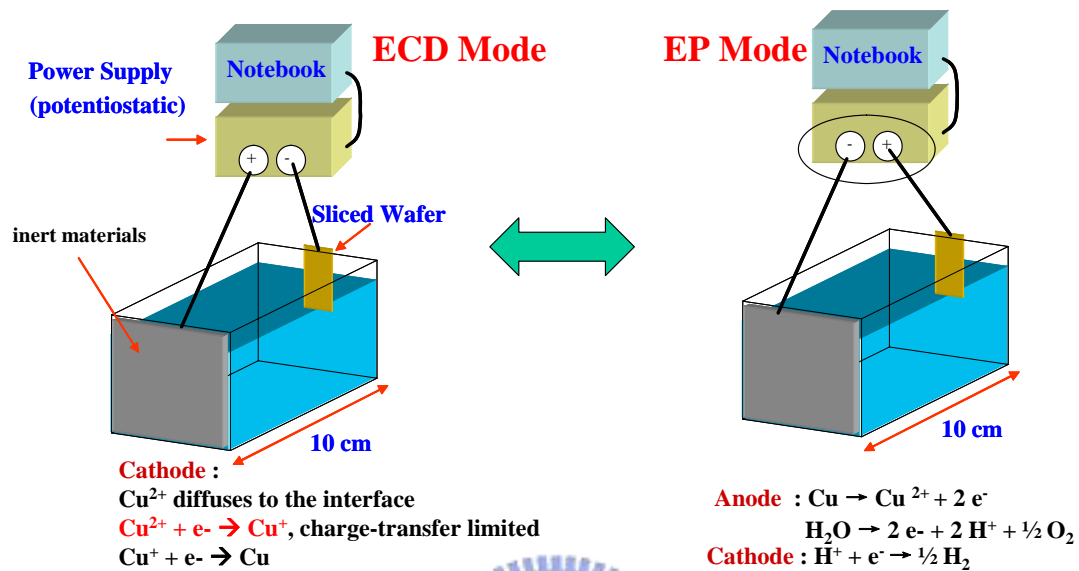


Fig.6-1. Schematic diagram of Cu dual mode plating

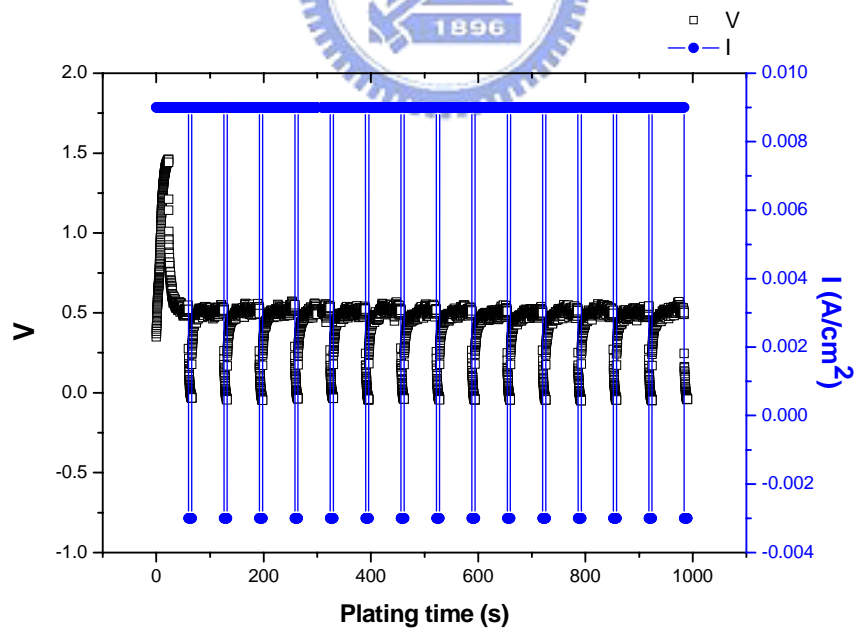


Fig.6-2. In-situ typical recorded current and voltage on electrode surface during Cu dual-mode plating

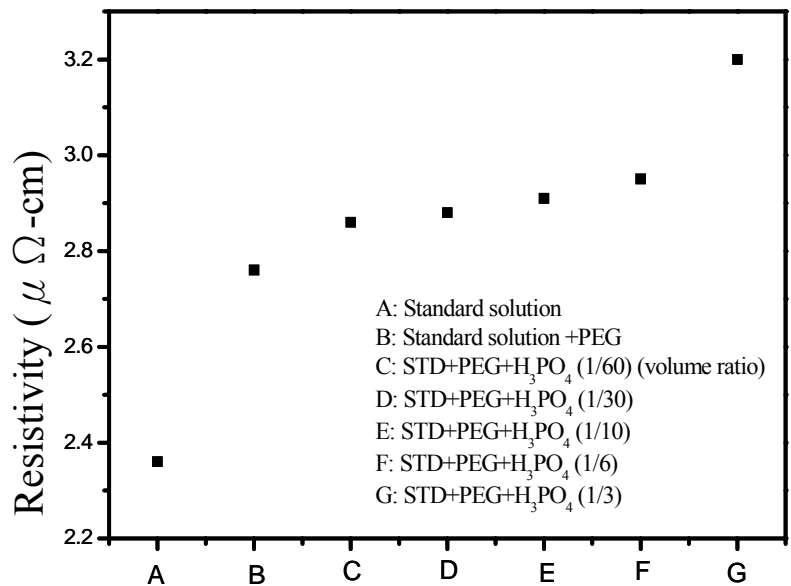


Fig.6-3. The dependence of electric conductivity with the amount of phosphate acid in various dual-mode electroplating solution.

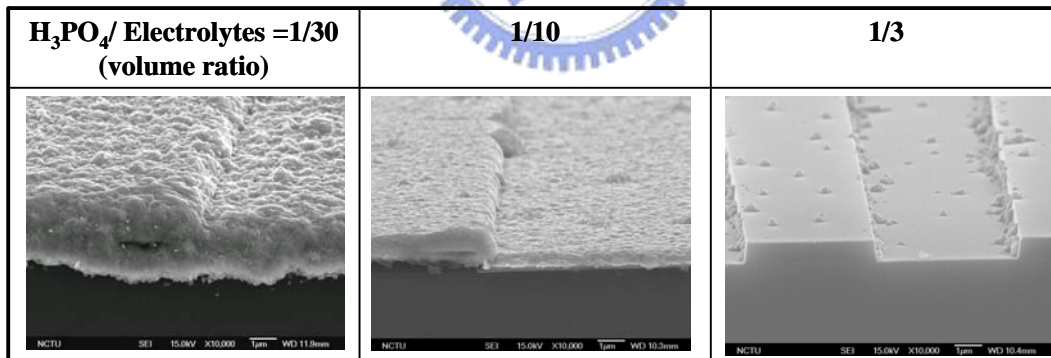


Fig.6-4. Surface morphology of Cu film after dual-mode electroplating in H₃PO₄/electrolytes = 1/30, 1/10 and 1/3 volume ratio trench at the same pulse-frequency. Pulse condition: ECD 30sec + EP 6sec, 30 cycles

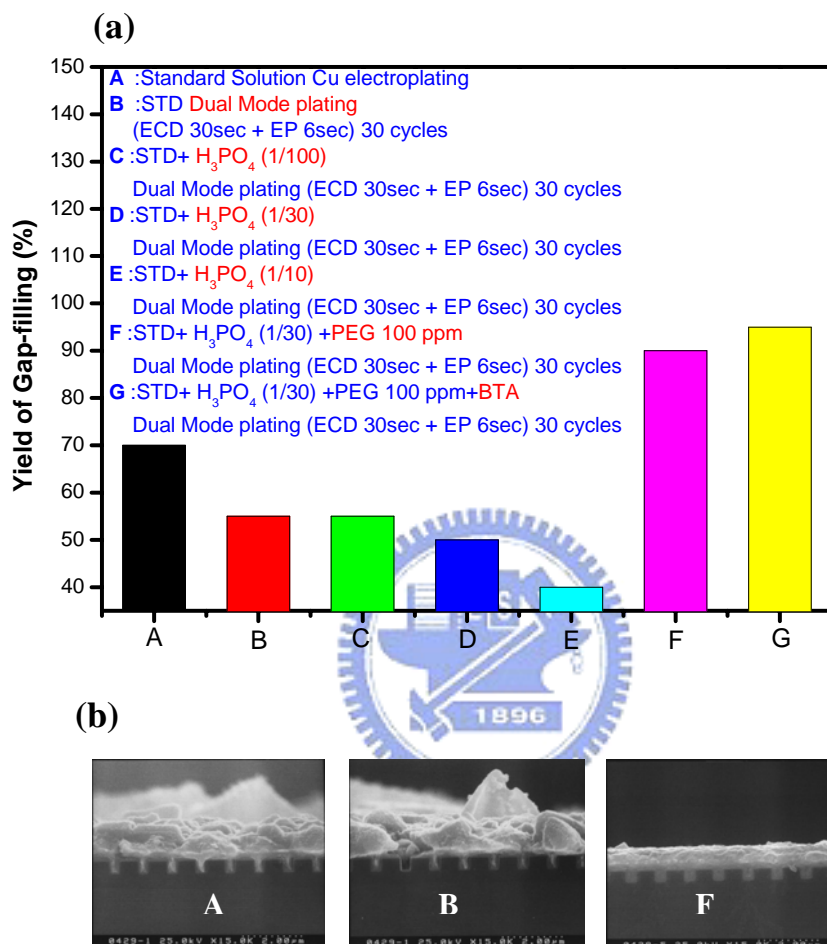


Fig. 6-5 (a) Comparison diagram showing pore filling capability with different chemical condition processing parameters at the same pulse-frequency of narrow trenches (trench width: 350nm) (b) SEM image of A, B and F are corresponded to the data in (a).

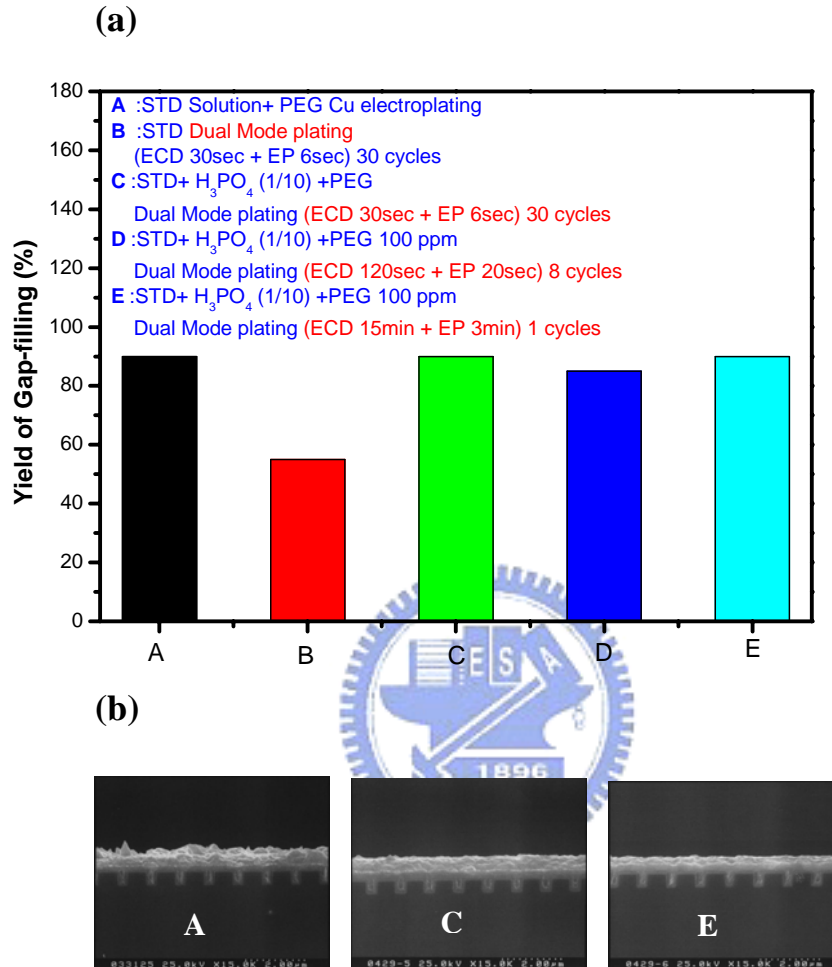


Fig.6-6. (a) Comparison diagram showing pore filling capability with different pulse-time processing parameters at optimized chemical condition of narrow trenches (trench width: 350nm) (b) SEM image of A, C and E are corresponded to the data in (a)

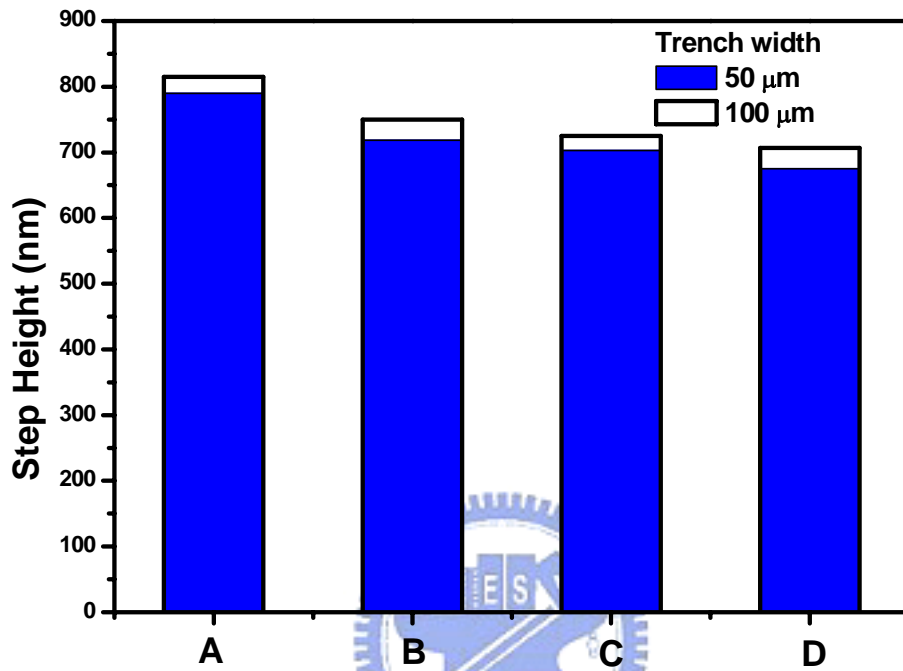


Fig.6-7. Step height of wide trench after Cu plating and under various dual-mode conditions. A: Standard plating for 15min, B: (ECD 10sec + EP 3sec) 90 cycles, C: (ECD 20sec + EP 3sec) 45 cycles, D: dual-mode at (ECD 30sec + EP 6sec) 30 cycles. Additives are H_3PO_4 (volume ratio 1/30) + PEG 100 ppm.

Chapter 7 Conclusions and Future Works

7.1 Conclusions

This dissertation reports the electrochemical aging influence of organic additives for Cu ECD and additive-assisted planarization of Cu-EP.

Super filling or bottom-up filling can be obtained when the Cu deposition rate on the feature bottom is higher than that on the bottom sidewalls. Therefore, an effective additive which can form a selectively deposition rate within a feature and produce a low-resistivity Cu film is required. However, the degradation behavior of electrolyte's effectiveness after plating a period of cycles is insufficient presently. For one-additive system in Cu ECD, the influences of aging poly PEG-Cl-containing electrolytes on Cu's gap-filling ability are studied. Originally, the adsorbed PEG competes for adsorption site with cupric ions on the cathode if chloride ions are present, then a monolayer of PEG-Cl can be formed and inhibit the deposition current on metal surface.

Undergoing a sequence of galvanostatic plating, PEGs cracked continuously in electrolytes, as confirmed by in-situ cells voltage-time measurements and electrochemical analyses, form numerous PEG-based complexes outside the double layer but fewer high-MW PEGs absorbed on the reacting surface. This is regarded as the predominant mechanism causing reduced polarization effects (or low inhibition effects) and the subsequent decay in gap-filling ability for aged electrolytes.

Meanwhile, the aging behavior of SPS combined with PEG after electroplating was also studied. A review of the behavior of SPS in ECD process was presented followed by a proof of the "slow adsorption / desorption mechanism." The depletion of SPS comes from: SPS is cleaved into MPS and S-product and then loss the accelerator ability. Ultimately, we clarified the issue of the degradation in (PEG, SPS)-containing bath by the AC impedance scan, that is, the SPS is easily to be decomposed by driven current and oxidation during ECD process.

Cu electropolishing technology is recently explored as a replacement of Cu-CMP. Electric field could be adopted to substitute for the mechanical force in CMP to remove overburden Cu layers. In particular, this stress-free characteristic of Cu EP can handle

low-k dielectrics. Moreover, Cu EP has been investigated for its electrochemical mechanism on electrode/electrolyte interface, tuning various parameters for planarization effect of Cu damascene structure, end point detection. Effective Cu EP usually takes place in the mass-transfer-limited plateau region and in useful acid solutions. Therefore, Cu electropolishing may be the one adopted of Cu planarization in damascene or other industrial application for the next generation. However, many challenges of Cu EP should be solved, such as precisely end-point detection and uniform distribution of current on whole 12 inch wafer.

In this study, the two-additive Cu EP electrolyte developed demonstrates the feasibility of locally modulating the Cu dissolution rate within damascene features and, therefore, exhibits a capability of completely planarizing Cu metallization with the size ranging from 1 to 50 μm . The role of alcohols in two-additive EP electrolytes is thus as an polishing inhibitor and is expected to passivate the damascene bottom from EP or to inhibit Cu dissolution at that area, leading to the improvement of the superpolishing functionality generated by only organic acids. Remarkably inhibited Cu dissolution at the damascene bottom, generated by alcohol additives, is considered as a dominant mechanism of forming the superplanarization phenomenon. This glycerol-containing two-additive EP electrolyte also solves the etch-pits problem.

Furthermore, electropolishing mechanisms for two-additive electrolytes that contain glycerol and various organic acid additives are investigated. Experimental results demonstrate that an esterification reaction modulates the acidity of solutions and the viscous resistance of passivation layers at the reacting interfaces. This reaction becomes dominant at the feature bottom, where a few additives are present. We suggest that the use of weak acidic organic acids at high concentration, such as acetic acids used as accelerators, enables numerous accelerators to participate in esterification, resulting in not only the formation of highly resistive layers but also a significant decrease in local acidity. Therefore, the acetic acid-containing two-additive EP electrolyte outperforms other electrolytes that contain accelerators at low concentration.

One developed electrochemical method which can achieve the integration of ECD and EP process in one electrolyte are demonstrated. It can be called Dual-mode plating. The advantage of dual-mode plating is Cu surface planarization can be obtained by

one-step electrochemical process. Presently, the crucial issues of dual-mode plating is maintaining high filling capability for small-width trench and enhancing step-height reduction for wide trench. More conditions including proper pulse-frequency, chemical parameters and plating time needs to be optimized in the future.

7.2 Future Work and Pulse Cu-Electropolishing

At present, planarization of the small aspect-ratio (large width) features by conventional or additive-assisted electropolishing is fundamentally limited by the minimum mass transport boundary layer (BL) thickness.¹⁻³ The precisely end-point detection will be a real challenge at next generation. Furthermore, how to enhance planarization uniformity on whole 300-mm wafer is another topic to research.

The electrochemical mechanical planarization (ECMP) process may be a revolutionary technology uniquely combining Cu dissolution controlled by charge with superior PE near Cu surface.⁴ Accordingly, requirement of equipments are important for Cu planarization on a 300-mm wafer.

In addition, by applying a pulse-electropolishing technique, the undesirable patterning effect on the silicon wafer might be completely eliminated at optimized current condition. The pulse method is performed by alternating the electrode potential on the substrate during electropolishing to obtain highly planarized Cu surface after several cycles. The underlying rationale is based on uneven distribution of electric fields during electropolishing in which depositing surface with convex interface experiences larger electric field than concave one does. As a result, the convex interface would suffer from higher rate for electropolishing while concave one receives electropolishing at reduced rate. This variation of polishing rate serves particularly nicely to effect uniform copper overcoat on patterned silicon surface. From our experience, addition of specific chemical compounds in electropolishing solution could enhance the ununiform distribution of electric field. However, the polishing rate would decrease substantially if the organic residue of the additive is attached to the copper surface and thus blocking the reaction close to the end of the electropolishing process. To minimize this negative

effect, we expect to alternate the potential on the copper electrode to promote the desorption of organic residue. In this way, it is likely to obtain better distribution of chemical additives and maintain the stability of desirable electric field unevenness. In this regard, so far we have identified specific processing parameters that achieve excellent selectivity in 1, 5 and 50 μm trench after pulse electropolishing, as shown in Fig.7-1. At the optimized duty cycle (75%), very high planarization efficiency (PE) for various width of trench was obtained when pulse-frequency is 0.033 Hz. Although in additive-free phosphoric acid, the pulse polishing method enhances higher PE than that after constant voltage polishing, as shown in Fig. 7-2.

Although the high planarization efficiency can be obtained by using Cu pulse-EP, the detail mechanism is not so clear at present. The further studies of chemical behavior on electrolyte/electrode interface during pulse Cu-EP are necessary in damascene processing.



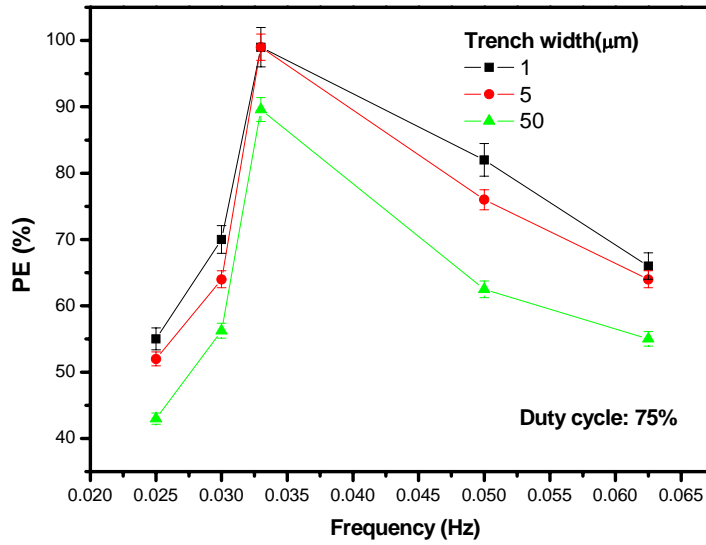


Fig.7-1. PE of pulse-polishing as a function of frequency for various of trenches widths. The positive voltage is 1.75V, and the negative voltage is 1.3V.

The chemical recipe is $H_3PO_4 + CH_3COOH$ 10000ppm + Glycerol1/100.

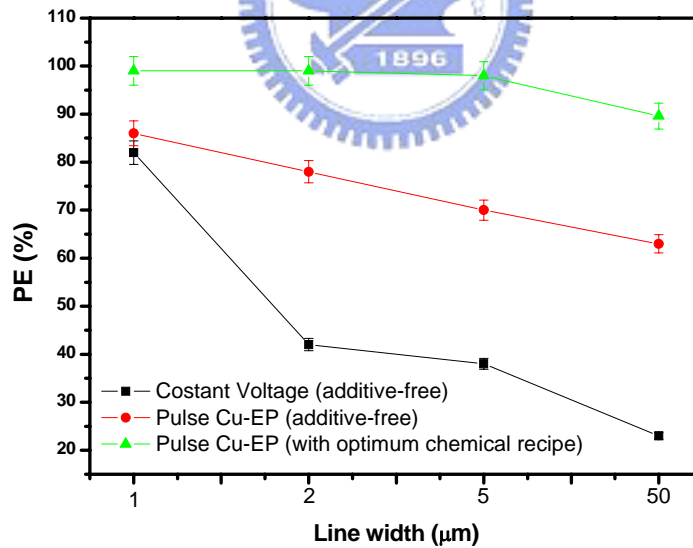


Fig.7-2. PE of constant voltage polishing and Pulse Cu-EP as function of line width

The pulse frequency is 0.033 and duty cycle is 75%.

Reference

Chapter 1

1. Changsup Ryu, Ph. D dissertation, Department of materials science and engineering of Stanford university (1998)
2. C. K. Hu, B. Luther, F. B. Kaufman, J. Hummel, C. Uzoh, and D.J. Pearson, *Thin Solid Films*, 262, pp. 84 (1995)
3. P. Taephaisitphongse, Y. Cao, and Alan C. West, *J. Electrochem. Soc.*, 148, C492 (2001).
4. K. Kondo, K. Hayashi, Z. Tanaka, and N. Yamakawa, *J. Electroanal. Chem.*, 559, 137 (2003).
5. J. G. Fleming, S. Y. Lin, I. El-Kady, R. Biswas and K. M. Ho, *Nature*, 417, 52-55 (2002).
6. S. C. Chang, Ph. D dissertation, Department of materials science and engineering of National Chao-Tung University (2003)
7. J. D. Reid and A.P. David, *Plat. Surf. Finish*, 74, 66 (1987).
8. M. Tan and J. Harb, *J. Electrochem. Soc.*, 150, C420 (2003).
9. T. O. Drews, J.C. Ganley, and R.C. Alkire, *J. Electrochem. Soc.*, 150, C325 (2003)
10. V. M. Dubin, R.R. Brewer, H. Simka, S. Shankar, *Future Fab*, 13 (2002)
11. J. D. Reid, S. Mayer, E. Broadbent, *Solid State Technology*, 86 (2000)
12. K.H. Dietz, *CIRCUITREE*, 22 (2000).
13. J. J. Kelly and A.C. West, *J. Electrochem. Soc.*, 145, 3472 (1998).
14. J. J. Kelly and A.C. West, *J. Electrochem. Soc.*, 145, 3477 (1998).
15. S. C. Chang, J. M. Shieh, K. C. Lin, B. T. Dai, T. C. Wang, C. F. Chen, M. S. Feng, Y. H. Li, and C. P. Lu, *J. Vac. Sci. Technol. B* 20(4), 1311 (2002).
16. J. M. Shieh, S. C. Chang, B. T. Dai, and M. S. Feng, *Jpn. J. Appl. Phys., Part1*, 41, 6347 (2002).
17. Tsung-Cheng Li, Master Thesis, Department of materials science and engineering of National Chao-Tung University (2003)
18. J. P. Healy and D. Pletcher and M. Goodenough, *J. Electroanal. Chem.*, 338, 155 (1992).

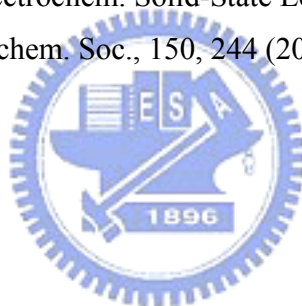
19. T. P. Moffat, B. Baker, D. Wheeler, D. Jossell, "Accelerator Aging Effects During Copper Electrodeposition," *Electrochem. Solid-State Lett.* 6, 59 (2003).
20. T. P. Moffat, D. Wheeler, W.H. Huber, D. Jossell, "Superconformal Electrodeposition of Copper," *Electrochem. Solid-State Lett.*, 4, C26 (2001)
21. T. P. Moffat, J.E. Bonevich, W.H. Huber, A. Stanisevsky, D.R. Kelly, *J. Electrochem. Soc.*, 147, 4524 (2000)
22. N. Kovarsky, Z. Sun, to be submitted to *Journal of the Electrochemical Society*.
23. E. E. Fardon, F.C. Walsh, S.A. Campbell, *J. Appl. Electrochem.*, 25, 574 (1995).
24. D. Jossell, D. Wheeler, W.H. Huber, T.P. Moffat, *Phys. Rev. Letter*, 87 16102-1 (2001).
25. L. T. Koh, G. Z. Tou, and S.Y. Lim, C.Y. Li, P.D. Foo, *Microelectronics J.*, 32 973 (2001).
26. A. Frank, J. Bard, *J. Electrochem. Soc.*, 150, 244 (2003).
27. S. K. Kim and J. J. Kim, *Electrochem. Solid-State Lett.*, 7, C98 (2004).

Chapter 2

1. J. J. Kelly and A.C. West, *J. Electrochem. Soc.*, 145, 3472 (1998).
2. J. J. Kelly and A.C. West, *J. Electrochem. Soc.*, 145, 3477 (1998).
3. K. Doblhofer, S. Wasle, D. M. Soares, K. G. Weil, and G. Ertl, *J. Electrochem. Soc.* 150, C657 (2003).
4. M. Hayase, M. Taketani, K. Aizawa, T. Hatsuzawa, K. Hayabusa, *Electrochem. Solid State Letters*, 5, C98 (2002)
5. Y. Jin, K. Kondo, Y. Suzuki, T. Matsumoto, and D. P. Barkey, *Electrochem. Solid State Lett.*, 8, C6-C8 (2005).
6. M. Hayase, M. Taketani, K. Aizawa, T. Hatsuzawa, and K. Hayabusa, *Electrochem. Solid State Lett.*, 5, C98 (2002).
7. Z. V. Feng, X. Li, and A. A. Gewirth, *J. Phys. Chem. B* 107, 9415, (2003).
8. D. Stoychev and C. Tsvetanov, *J. Appl. Electrochem.*, 26, 741 (1996).
9. S. C. Chang, J. M. Shieh, K. C. Lin, B. T. Dai, T. C. Wang, C. F. Chen, M. S. Feng, Y. H. Li, and C. P. Lu, *J. Vac. Sci. Technol. B* 20(4), 1311 (2002).
10. J. M. Shieh, S. C. Chang, B. T. Dai, and M. S. Feng, *Jpn. J. Appl. Phys., Part 1*, 41,

6347 (2002).

11. J. D. Reid and A.P. David, *Plat. Surf. Finish*, 74, 66 (1987).
12. P. Taephaisitphongse, Y. Cao, and Alan C. West, *J. Electrochem. Soc.*, 148, C492 (2001).
13. M. Tan and J. Harb, *J. Electrochem. Soc.*, 150, C420 (2003).
14. K.H. Dietz, , *CIRCUITREE*, 22 (2000).
15. C. Gabrielli, P. Mocoteguy, H. Perrot, A. Zdunek, P. Bouard, and M. Haddix, *Electrochem. Solid State Lett.*, 7, C31 (2004).
16. L. T. Koh, G. Z. Tou, and S.Y. Lim, C.Y. Li, P.D. Foo, *Microelectronics J.*, 32 973 (2001).
17. J. P. Healy and D. Pletcher and M. Goodenough, *J. Electroanal. Chem.*, 338, 155 (1992).
18. S. K. Kim and J. J. Kim, *Electrochem. Solid-State Lett.*, 7, C98 (2004).
19. A. Frank, J. Bard, *J. Electrochem. Soc.*, 150, 244 (2003).



Chapter 3

1. S. Kondo, N. Sakuma, Y. Homma, Y. Goto, N. Ohashi, H. Yamaguchi, and N. Owada, *J. Electrochem. Soc.* 147, 3907 (2000).
2. Y. Li and S. V. Babu, *Electrochem. Solid-State Lett.* 4, G20 (2001).
3. Q. Luo and S. V. Babu, *J. Electrochem. Soc.* 147, 4639 (2000).
4. S. C. Chang, Ph. D dissertation, Department of materials science and engineering of National Chao-Tung University (2003).
5. Buřlent M. Basol, *J. Electrochem. Soc.*, 151 (12) C765 (2004).
6. Feng Q Liu, T Du, A. Duboust, S. Tsai and W. Y. Hsu, *J. Electrochem. Soc.*, 153 C377 (2006).
7. J.-Y. Fang, M. S. Tsai, B. T. Dai, Y. S. Wu, and M. S. Feng, *Electrochem. Solid-State Lett.*, 8 (5) G128 (2005).

8. J.-Y. Fang , Ph. D dissertation, Department of materials science and engineering of National Chao-Tung University (2005)
9. H. Yamaguchi, N. Ohashi, T. Imai, K. Torii, J. Noguchi, T. Fujiwara, T. Saito, N. Owada, Y. Homma, S. Kondo, and K. Hinode, Proc. of the Int. Interconnect Technology Conf., San Francisco, CA, pp. 264 (2000).
10. D. Padhi, J. Yahalom, S. Gandikota, and G. Dixit, J. Electrochem. Soc. 150, G10 (2003).
11. S. C. Chang, J. M. Shieh, C. C. Huang, B. T. Dai, Y. H. Li, and M. S. Feng, J. Vac. Sci. Technol. B 20, 2149 (2002).
12. S. C. Chang, J. M. Shieh, C. C. Huang, B. T. Dai, and M. S. Feng, Jpn. J. Appl. Phys. 41, 7332 (2002).
13. S. C. Chang, J. M. Shieh, B. T. Dai, M. S. Feng, Y. H. Li, C. H. Shih, M. H. Tsai, S. L. Shue, R. S. Liang, and Y. L. Wang, Electrochem. Solid-State Lett. 6, G72 (2003).
14. B. Du, and I. Suni, J. Electrochem. Soc., 151, C375 (2004).
15. J. Huo, R. Solanki and J. McAndrew, J. Appl. Electrochem., 34, 305 (2004).
16. Ivar Suni and Bing Du, IEEE Transactions on Semiconductor Manufacturing, 18, 341, (2005).
17. G. B. Mohamed and A. M. Ahmed, B. Electrochem 4, 951 (1988).
18. R. J. Contolini, A. F. Bernhardt, and S. T. Mayer, J. Electrochem. Soc. 141, 2503 (1994).
19. R. J. Contolini, S. T. Mayer, R. T. Graff, and L. Tarte, Solid State Technol. 40, 155 (1997).
20. M. H. Tsai, S. W. Chou, C. L. Chang, C. H. Hsieha, M. W. Lin, C. M. Wu, Winston S. Shue, Douglas C. Yu, and M. S. Liang, IEDM, Washington, DC, Dec. 2-5, pp. 80 (2001).
21. S. Sato, Z. Yasuda, M. Ishihara, N. Komai, H. Ohtorii, A. Yoshio, Y. Segawa, H. Horikoshi, Y. Ohoka, K. Tai, S. Takahashi, and T. Nogami, IEDM, Washington, DC, Dec. 2-5, pp. 84 (2001).

22. S. C. Chang and Y. L. Wang, *J. Vac. Sci. Technol. B*, 22, 2754 (2004).
23. J. M. Shieh, S. C. Chang, Y. L. Wang, B. T. Dai, S. S. Cheng, and J. Ting, *J. Electrochem. Soc.*, 151, C459 (2004).
24. S. Soukane, S. Sen, and T. S. Cale, *J. Electrochem. Soc.*, 149, C74 (2002).
25. Yang Cao, Premratn Taephaisitphongse, Radek Chalupa, and Alan C. West, *J. Electrochem. Soc.*, 148, C466 (2001).
26. A. Satta, D. Shamiryan, M. R. Baklanov, C. M. Whelan, Q. T. Le, G. P. Beyer, A. Vantomme and K. Maex, *J. Electrochem. Soc.*, 150, 300 (2003).
27. Ch. Ammon, A. Bayer, G. Held, B. Richter, Th. Schmidt, H.-P. Steinruck, *Surf. Sci.*, 507, 845 (2002).

Chapter 4

1. S. C. Chang, J. M. Shieh, C. C. Huang, B. T. Dai, and M. S. Feng, *Jpn. J. Appl. Phys.* 41, 7332 (2002).
2. S. C. Chang, J. M. Shieh, B. T. Dai, M. S. Feng, Y. H. Li, C. H. Shih, M. H. Tsai, S. L. Shue, R. S. Liang, and Y. L. Wang, *Electrochem. Solid-State Lett.* 6, G72 (2003).
3. A. Satta, D. Shamiryan, M. R. Baklanov, C. M. Whelan, Q. T. Le, G. P. Beyer, A. Vantomme and K. Maex, *J. Electrochem. Soc.*, 150, 300 (2003).
4. T. C. Hu, S. Y. Chiu, B. T. Dai, M. S. Tsai, I.-C. Tung, and M. S. Feng, *Mater. Chem. Phys.* 61, 169 (1999).
5. S. Soukane, S. Sen, and T. S. Cale, *J. Electrochem. Soc.*, 149, C74 (2002).
6. Yang Cao, Premratn Taephaisitphongse, Radek Chalupa, and Alan C. West, *J. Electrochem. Soc.*, 148, C466 (2001).
7. J. M. Shieh, S. C. Chang, Y. L. Wang, B. T. Dai, S. S. Cheng, and J. Ting, *J. Electrochem. Soc.*, 151, C459 (2004).
8. M. G. Fontana, *Corrosion Engineering*, p.66, McGraw-Hill, Inc., New York (1987)
9. T. N. Andryushchenko, A. E. Miller and P. B. Fischer, to be published in *Electrochem. Solid-State Letters*.

10. S. Sato, Z. Yasuda, M. Ishihara, N. Komai, H. Ohtorii, A. Yoshio, Y. Segawa, H. Horikoshi, Y. Ohoka, K. Tai, S. Takahashi, and T. Nogami, IEDM, Washington, DC, Dec. 2-5, pp. 84 (2001).

Chapter 5

1. S. C. Chang, J. M. Shieh, B. T. Dai, M. S. Feng, Y. H. Li, C. H. Shih, M. H. Tsai, S. L. Shue, R. S. Liang, and Y. L. Wang, *Electrochem. Solid-State Lett.* 6, G72 (2003).
2. S. H. Liu, J. M. Shieh, Chih Chen, B. T. Dai, Karl Hensen, and S. S. Cheng, *Electrochem. Solid-State Lett.*, 8 (3) C47 (2005).
3. S. C. Chang, J. M. Shieh, C. C. Huang, B. T. Dai, Y. H. Li, and M. S. Feng, *J. Vac. Sci. Technol. B*, 20, 2149 (2002).
4. S. C. Chang and Y. L. Wang, *J. Vac. Sci. Technol. B*, 22, 2754 (2004).
5. J. M. Shieh, S. C. Chang, Y. L. Wang, B. T. Dai, S. S. Cheng, and J. Ting, *J. Electrochem. Soc.*, 151, C459 (2004).
6. F. A. Carey, "Organic Chemistry" pp.785, McGraw-Hill, Inc., New York (1996).
7. S. C. Chang, J. M. Shieh, C. C. Huang, B. T. Dai, and M. S. Feng, *Jpn. J. Appl. Phys.* 41, 7332 (2002).
8. B. Du, and I. Suni, *J. Electrochem. Soc.*, 151, C375 (2004).
9. S. Soukane, S. Sen, and T. S. Cale, *J. Electrochem. Soc.*, 149, C74 (2002).
10. J. Huo, R. Solanki and J. Mcandrew, *J. Appl. Electrochem.*, 34, 305 (2004).
11. E. Smith and G. Dent, "Modern Raman Spectroscopy: a practical approach", pp.15-18, John Wiley and Sons, Ltd, England (2005)
12. B. Schrader, "Raman/Infrared Atlas of Organic Compounds", pp. B4-07-20, VCH publishers, New York, NY, USA, (1989).
13. S. C. Chang, J. M. Shieh, C. C. Huang, B. T. Dai, Y. H. Li, and M. S. Feng, *J. Vac. Sci. Technol. B* 20, 2149 (2002).

Chapter 6

1. J. G. Fleming, S. Y. Lin, I. El-Kady, R. Biswas and K. M. Ho, *Nature*, 417, 52-55 (2002).

Chapter 7

1. A. C. West, I. Shao, H. Delegianni, J. Electrochem. Soc. 152, C652 (2005).
2. T. N. Andryushchenko, A. E. Miller and P. B. Fischer, to be published in Electrochem. Solid-State Letters.
3. D. Padhi, J. Yahalom, S. Gandikota, and G. Dixit, J. Electrochem. Soc. 150, G10 (2003).
4. Feng Q Liu, T Du, A. Duboust, S. Tsai and W. Y. Hsu, J. Electrochem. Soc., 153, C377 (2006).



List of Publications

A. Journal Papers:

1. **Tin whisker growth driven by electrical currents**
S. H. Liu, Chih Chen, P. C. Liu, and T. Chou , Journal of Applied Physics, **95**, 7742 (2004)
2. **Two-additive electrolytes for superplanarizing damascene Cu metals**
Sue-Hong Liu, Jia-Min Shieh, Chih Chen, Bau-Tong Dai, Karl Hensen and Shih-Song Cheng, Electrochemical and Solid-State Letters, **8** (3) C47-C50 (2005)
3. **Study of electromigration in thin tin film using edge displacement method**
H. C. Yu, S. H. Liu, and Chih Chen, Journal of Applied Physics, **98**, 1354 (2005)
4. **Aging influence of PEG suppressors of Cu electrolytes on gap-filling**
Sue-Hong Liu, Tsung-Cheng Li, Chih Chen , Jia-Min Shieh , Bau-Tong Dai, Karl Hensen, and Shih-Song Cheng, Japanese Journal of Applied Physics, **45**, 3976, (2006).
5. **Roles of additives in damascene Copper electropolishing**
Sue-Hong Liu, Jia-Min Shieh, Chih Chen, Karl Hensen, and Shih-Song Cheng, Journal of the Electrochemical Society, **153**, C428 (2006).
6. **Investigation of PEG and SPS-containing bath degradation during Cu electrodeposition**
Sue-Hong Liu, Tsung-Cheng Li, Jia-Min Shieh, Chih Chen, Pu-Wei Wu, Karl Hensen and Shih-Song Cheng, to be submitted to Journal of the Electrochemical Society.

B. Conference Papers:

1. Sue-Hong Liu, Jia-Ming Shieh, Bau-Tong Dai, and Chih Chen, “Electropolishing of Copper with High Planarization Efficiency and Low Surface Defect “, Material Research Society, April 12-16, 2004, San Francisco, USA.
2. Sue-Hong Liu, Jia-Ming Shieh, Bau-Tong Dai, and Chih Chen, “Electropolishing of Copper with High Planarization Efficiency and Low Surface Defect “, poster P73, Symposium on Nano Device Technology 2004, May 12-13, 2004, Hsinchu, Taiwan,

ROC (SNDT 2004).

3. Sue-Hong Liu, Jia-Ming Shieh, Bau-Tong Dai, and Chih Chen, “Two-Additive Electrolytes for superplanarizing Damascene” Symposium on Nano Device Technology 2004, May 7-8, 2005, Hsinchu, Taiwan, ROC (SNDT 2005).
4. 劉書宏，陳智，謝嘉民，戴寶通 “Planarization of Damascene Copper by Electropolishing Technology” Invited Talk, 2005年中華民國材料科學年會，淡江大學，台北.
5. Sue-Hong Liu, Chih Chen, Jia-Min Shieh, Bau-Tong Dai, Karl Hensen, and Shih-Song Cheng, “Integration of Electroplating and Electropolishing of Cu Damascene Process” The Minerals, Metals, Materials Society, pp.74, March 12-16, 2006, San Antonio, USA.

C. Patent:

1. “電解拋光液及其平坦化金屬層之方法”，中華民國專利，公開號：200611998。
2. “ELECTROPOLISHING ELECTROLYTE AND METHOD FOR PLANARIZING A METAL LAYER” 美國專利申請中。

